uOttawa

L'Université canadienne
Canada's university

FACULTÉ DES ÉTUDES SUPÉRIEURES ET POSTOCTORALES

uOttawa

L'Université canadienne
Canada's university

FACULTY OF GRADUATE AND POSDOCTORAL STUDIES

Ahsan Ahmed
AUTEUR DE LA THÈSE / AUTHOR OF THESIS

Ph.D. (Mechanical Engineering)
GRADE / DEGREE

Department of Mechanical Engineering
FACULTÉ, ÉCOLE, DÉPARTEMENT / FACULTY, SCHOOL, DEPARTMENT

Design, Fabrication, and Analysis of Foam Composite Structures with Metal Inserts
TITRE DE LA THÈSE / TITLE OF THESIS

Atef Fahim
DIRECTEUR (DIRECTRICE) DE LA THÈSE / THESIS SUPERVISOR

Hani Naguib
CO-DIRECTEUR (CO-DIRECTRICE) DE LA THÈSE / THESIS CO-SUPERVISOR

Paul Straznicky

Michel Nganeb

Micheal Munro

Xiaodong Wang
University of Alberta

Gary W. Slater
Le Doyen de la Faculté des études supérieures et postdoctorales / Dean of the Faculty of Graduate and Postdoctoral Studies

DESIGN, FABRICATION, AND ANALYSIS OF FOAM COMPOSITE STRUCTURES WITH METAL INSERTS

by

Ahsan Faraz Ahmed

A thesis submitted to the Faculty of Graduate and Postdoctoral Studies in partial fulfilment of the requirements for the degree of

DOCTOR OF PHILOSOPHY

in Mechanical Engineering

Ottawa-Carleton Institute of Mechanical and Aerospace Engineering
University of Ottawa
Ottawa, Canada

September 2009

Your file Votre référence
ISBN: 978-0-494-69103-8
Our file Notre référence
ISBN: 978-0-494-69103-8

Abstract

Metal or solid polymer anchors are employed as the load transfer components for foams and foam composites structures, when they are used as the structural element in design. The traditional method of fixation of these components is gluing and fastening, typically to the surface of the foam or composite. In this work, the anchors are in the form of inserts and are imbedded in the foam during the foaming process. Flexural testing was conducted on different metal foam configurations to establish typical interaction trends. The load-deflection response, mode of failure and fracture stresses of the structures are elucidated. Tests were conducted on the foam and foam composites with rectangular, cylindrical, and taper insert geometries with different lengths. Leaf inserts were designed and manufactured. Flexure testing was done on foam and sandwich composite structures with leaf inserts. A linear elastic fracture model was studied, and fracture toughness for the foam beam with inserts was calculated. Finite element analysis (FE) of the interactions between the inserts and the foam structures under different loads were carried out. The FE modeling results coincided with the experimental ones hence validating the model. FE simulations were also run with foams, and sandwich composite structures with close-outs.

Acknowledgments

I would like to thank and express my gratitude to my supervisors, **Dr. Atef Fahim** and also **Dr. Hani E. Naguib**, for their guidance, encouragement and help in completing this thesis. I would also like to thank my family for their prayers, especially my parents, **Mr. Amjad & Mrs. Samina**, my wife **Javaria**, and my kids, **Arham, Rahma** and **Muaz**.

Table of Contents

List of Figures

List of Tables

List of Symbols

E	Modulus of elasticity (MPa)
G	Shear modulus (MPa)
D	Flexural rigidity (MPa)
E_f	Flexural modulus of foam (MPa)
E_C	Flexural modulus of the core (MPa)
f	Facing thickness (mm)
c	Core thickness (mm)
b	Width of the beam (mm)
s	Distance between the neutral axis of the faces (mm)
V	Shear force (N)
G_{12}	In plane shear modulus of the lamina (MPa)
G_{23}	Out of plane shear moduli of the lamina (MPa)
P	Force on the specimen (N)
W	Width of the specimen (mm)
a	Crack length (mm)
S	Span length of foam beam (mm)
h_1	Longitudinal layer of laminate (mm)
h_2	Transverse layers of laminate (mm)
r	Crack tip radius (mm)
K_I	Stress concentration factor (MPa $\sqrt{}$m)
K_{Ic}	Fracture toughness (MPa $\sqrt{}$m)
y	Distance from N.A. (mm)
I_f	Moment of inertia of facing (mm^4)
I_c	Moment of inertia of the core (mm^4)
E_X	Initial modulus of laminate (MPa)
E_X'	Reduced modulus of laminate (MPa)
θ	Angle of crack from the axis (degree)
α	Normal stress (MPa)

r	Crack tip radius (mm)
τ	Shear stress (MPa)
σ_f	Flexural stress (MPa)
ε_f	Flexural strain (MPa)
γ_f	Shear strain (mm/mm)
σ_x	Axial stress in x direction (MPa)
σ_y	Stress in the y direction (MPa)
τ_{xy}	Shear stress in x-y direction (MPa)
γ_{xy}	Shear strain in x-y direction (mm/mm)
σ_r	Residual stress (MPa)

CHAPTER 1

INTRODUCTION

1.1 Preamble

Cellular foam usage as a structural element has been steadily increasing over the past decade primarily due to its favorable mechanical properties such as impact strength, toughness, stiffness to weight ratio, fatigue life, and reduced material weight. These distinctive properties have enabled foams to gain increasing acceptance in applications in industries like aerospace, automotive, and marine structures and vessels.

The application of sandwich composites in load-bearing constructions is rapidly increasing. Sandwich structures usually employ two thin, stiff and high performance laminate face sheets, bonded to a relatively thick low-density foam core. The structure through its increased moment of inertia transforms a bending load to tension and compression loads in the face sheets. The core keeps together the face sheets and resists shear loads. This arrangement combines high bending stiffness and strength with lightness.

Research has been conducted on the mechanical properties of foams, and sandwich composite structures, but not extensively on the adhesion properties of the polymer foams with metal. Although work was done on metallic foams interaction with inserts using pre-drilled holes with and without glues, but not on polymers with metals.

The main drawback of polymer-based composites is their inability to withstand concentrated loads. Joints, hinges and anchors used in polymer structures invariably are made of non-foamed materials, primarily metals, and the interface between the two materials become the weakest link of the foam structures. The foam structures, and sandwich composite structures containing various metal inserts are characterized in the present study. Flexural tests were conducted on the polymer foam and the sandwich composite beams and load-bearing properties are elucidated. The leaf insert concept is also introduced. Finite element analysis using ANSYS version 11 was also done on the foam, and sandwich composites. Results from the foam and sandwich composites with inserts and close out were also compared.

1.2 Cellular Foams

A cellular solid is one made-up of an interconnected network of solid struts or plates which form the edges and faces of cells. The simplest is a two-dimensional array of polygons which pack to fill a plane area like the hexagon cells of the bee similar to the beehive. For this reason it is known as two dimensional cellular material honey combs. More commonly, the cell polyhedra which pack in three dimensions to fill space are called three dimensional cellular materials foams [1]. Almost any material can be foamed. Polymers are the most common, but metals, ceramic glasses and even composites can be fabricated into cells.

Foam is a material, and foaming is a phenomenon. Production of foamed polymers include three stages within the polymer, injection of gas, expansion of gas and stabilization of the polymer. Different techniques are used for foaming different types of solids. Polymers are foamed by introducing gas bubbles into the liquid monomer, or hot polymer allowing the bubbles to grow and stabilize, and then solidifying by cross linking or cooling. The gas is introduced by mechanical stirring or mixing a blowing agent into a polymer. Physical blowing agents are inert gases such as carbon dioxide or nitrogen; they are forced into the polymer at high pressure and expanded into the bubble by reducing the pressure. Alternatively, low melting point liquid such as methylene chloride is mixed into the polymer and evaporates on heating to form vapor bubbles. Molecular foams with cell sizes of 10μ can be made by saturating a polymer with an inert gas under pressure and at room temperatures and then relieving the pressure and heating the supersaturated polymer to the glass transition temperature causing cell nucleation and growth to occur.

Chemical blowing agents are additives which either decomposes on heating, or combine together when mixed to release gas. Each process can produce open and close celled foams; the final structure depends on the rheology and surface tension of the fluids in the melt. Close-cell foams then sometimes undergoes a further process known as reticulation, in which the faces of the cells are ruptured to give open cells foams.

If the solid of which the foam is made is contained in the cell edges only (so the cells connect through open faces), foam is said to be open-celled. If the faces are solid, so that each cell is sealed off from its neighbors, it is said to be a closed-cell. The open celled and closed celled foams are shown in the Figure 1.1.

Polymeric foams are eminently suitable for a wide range of applications. Man made foams manufactured on a large scale are used for absorbing the energy of impact (in packaging and crash protection) and in light weight structures (the core of the sandwich structure). Even if their primary use is not insulation, foam can also be used for thermal insulation.

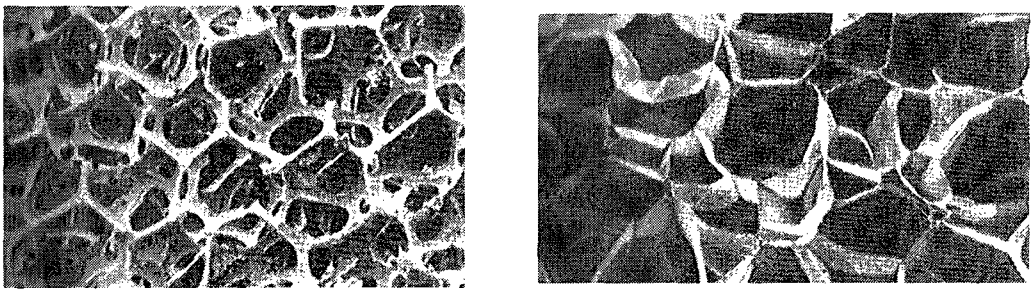

Figure 1.1: Open and close cell foams

1.3 Structural Composites

A structural composite is composed of both homogeneous and composite materials, the properties of which depend not only on the properties of the constituent's materials but also on the geometrical design of the various structural elements. The laminated composites and sandwich panels are two of the most common structural composites [2].

A laminate composite is made out of two-dimensional sheets or panels that have a preferred high strength direction. The layers are stacked and bonded together such that the orientation of the high strength direction varies with each successive layer. Depending on the combination of the constituent materials, sandwich beams may have high strength and stiffness combined with low weight, and good dimensional stability, corrosion resistance, and fatigue properties.

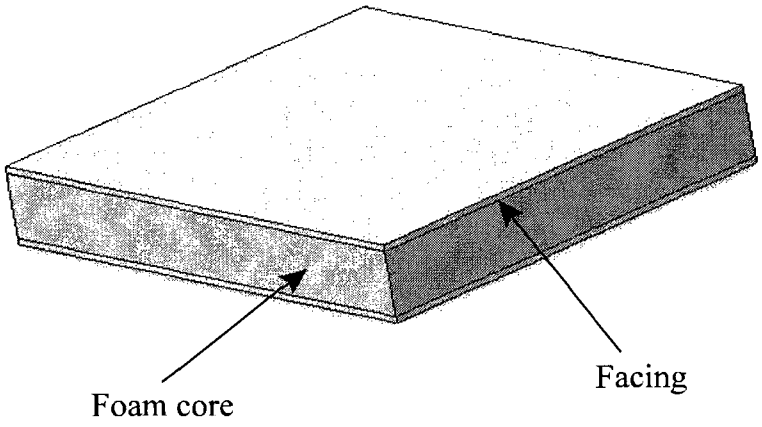

Figure 1.2: Sandwich composite with facing and core

The sandwich panels, consists of two strong outer sheets, or faces, separated by a layer of less dense material or core, such as foam, which has lower stiffness and lower strength as shown in the Figure 1.2. The structure through its increased moment of inertia transforms a bending load to tension and compression in the face sheets. The faces bear most of the in-plane loading, and also any bending stresses. Typical face materials include aluminum alloys, and fiber reinforced plastics and steel.

The core serves two functions. Firstly, it separates the faces and resists deformations perpendicular to the face plane. Secondly, it carries the shear load. The core is made of materials such as foamed polymers and rubbers. Honey comb sheets are also used in aerospace application. Sandwich panels are found in applications that include roofs and walls of buildings, aircraft wings, fuselages, . . . etc. [2].

1.4 Motivation and Objectives

Sandwich panels revolutionized the aerospace industry more than 40 years ago, making aircraft lighter, stronger and faster and allowing them to carry more weight and improve fuel efficiency. Today, panels are used from aerospace to recreation, in transportation vehicles on land and sea, in architecture and many other applications and areas as well. Principal among foam sandwich panels many advantages are their very high strength-to-weight ratio and their resistance to flexure and

fatigue. Some of the important applications of sandwich composites in aircraft and aerospace are floor panels, interior walls, capsule nose cones, bulkhead panels, satellites and for recreation: snow boards and motorcycles.

Engineers worldwide have integrated these panels into a myriad of applications. The most common problem hindering an even wider use of such panels has been deciding how to attach them to each other or to other components of the structure. With the advent and improvement of adhesives and epoxy as an adhesive, many designers have simply glued the panels together. Others have chosen to use metal or solid polymeric fasteners, which are typically glued into place to provide threads into the panel, or act as a grommet through which a bolt can be fastened.

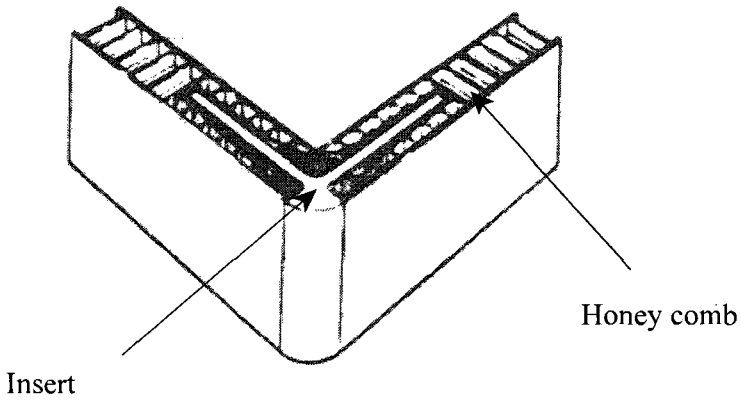

Figure 1.3: Honey comb with inserts

Until now, these have been the only methods available for attaching panels and both of these methods have serious drawbacks. Gluing panels together can work, but it is difficult and time consuming, as special fixtures and tools must be made in order to hold the components in place while the glue sets, especially for honey comb components as shown in the Figure 1.3. Inserts glued into the panels has been the preferred method, but they present a different set of problems as they are applicable to the metallic foams. Therefore, there is a need to redesign the metallic insertion inside foam sandwich composites based on the panel attachment.

The main drawback of the foam structures is their inability to withstand concentrated loads. Joints, hinges and anchors used in foam structures invariably are made of non-foamed material,

primarily metals and solid polymers, and the interface between the two materials becomes the weakest link of such structure.

This study investigated this issue, by focusing exclusively on characterizing metal-foam interaction in the form of metal inserts inside foam structures as well as in the sandwich composite. Furthermore, a sandwich composite manufacturing methodology is reported for bonding facing with the core without using any adhesive. An optimal insert geometry design was suggested for forming the metal joints with foam and sandwich structure.

1.5 Thesis Organization

This thesis consists of seven chapters. The general idea of foam and sandwich composite is presented in this chapter. The objective and motivation of the proposed research are also included.

A literature review dealing with the fabrication of foam and composite is presented in Chapter 2. Different manufacturing techniques for foam and sandwich composites are cited. The chapter also includes a literature survey on mechanical and adhesion properties of foams with emphasis on the bending properties. Mechanical and adhesion properties of sandwich composites are also investigated. Finite element analysis results using commercial software ANSYS-11 is also presented in this chapter.

Chapter 3 presents a novel methodology for the manufacture of foams with metallic inserts of different geometries. The chapter starts by discussing the design and manufacturing techniques of foam-metal structures. An experimental set-up is discussed and testing procedures are elaborated. The test data is presented in detail and discussed. Finite element analysis results using ANSYS are presented and compared with the experimental results.

A new approach for fabrication and design of the sandwich composite with metallic inserts is presented in Chapter 4. The chapter starts by explaining the fabrication techniques of sandwich composite with inserts. The testing set-up and experimental results are discussed. Stiffness reduction model for sandwich composite is also discussed. Finite element analysis results using ANSYS are presented and compared with the experimental results.

Chapter 5 starts by introducing a design of a new type of inserts: leaf inserts. Design and manufacturing techniques of leaf inserts inside foam beams and sandwich composites is presented.

Test results for leaf inserts inside foam and sandwich composites are compared with other existing geometries. Fracture toughness results are also presented in the chapter. Finally, FE results using ANSYS are presented and compared with the experimental results.

Chapter 6 discusses attachment of the foam and sandwich composites with close-outs. The close-outs are the replacement of inserts and are used as an attachment device with which the foam and sandwich composite structure panels can be attached to another structure. Simulation results for the foam and sandwich composite with inserts and close-out were compared.

Chapter 7 concludes with a summary and general discussion of the results and main contributions of this work. Recommendations for future research are also presented.

CHAPTER 2

BACKGROUND AND LITERATURE SURVEY

2.1 Introduction

Polymeric foams has been used to manufacture lighter, stiffer, and stronger structure in different sectors including marine and aerospace for almost half a century. Other foams based on other polymers were developed afterwards. Polyurethane foams are used nowadays to provide a compromise between properties like better loading bearing, good moisture resistance, high strength, and damping properties. Polyvinyl (PVC) was the first foam which was formulated for a marine environment.

This chapter includes a detailed description of the previous work done on the properties of foam polymers and their composites. Manufacturing and fabrication methods of these materials are highlighted. A literature review of the mechanical and adhesion properties of foams and their sandwich composite was conducted. Furthermore, FE analysis results on foam and their sandwich composites reported in the open literature were also studied. It is noted that extensive work was done on the mechanical properties of foam and sandwich composites, but not much research was carried out on the adhesion properties of polymeric foam and sandwich composite structures with metals or the interaction between them across the bond. Work was done, however, on metallic foam interactions with inserts using pre-drilled holes and with glues. Research on the foam and sandwich composite structures were primarily done in the last decade. Consequently the literature search carried out in this thesis will focus on foam-based composites from the year 2000 onwards.

2.2 Manufacturing and Fabrication of the Foams and Composites

Studies have been conducted on the fabrication of foams and composite structures. Mahfuz et al. [3] studied the fabrication, synthesis and mechanical characterization of nano particles infused polyurethane foams. Polyurethane foams were fabricated by doping of liquid polymers with 5-8 % nano-particles and then casting the polymer into a rectangular mold. Flexural tests were conducted on the fabricated samples and it was revealed that nano-particles enhanced the mechanical properties

of the polymer by almost 30-40%. Gain in strength is attributed to the delay in formation of cracks during loading which resulted due to the surrounding of cell walls and edges by particles.

Hawkins et al. [4] manufactured the polyurethane foams using different mold sizes and investigated the relationship between cell morphology, density, and compressive properties of polyurethane foams. It was shown that the polyurethane foams formed in smaller molds had higher density and less elongated cells, and hence better compressive properties. Xiong et al. [5] fabricated the polyurethane foam tubes and studied the effect of distribution of carbon particles on tubes under compression. Foaming materials and carbon particles were mixed together, poured into molds and cured under compression. The micro structural analysis results revealed that the orientation of the carbon particles was more uniform in the direction of compressive force as compared to other directions where they are mostly scattered.

Ilie and Park [6] investigated the feasibility of applying the single charge rotational foam molding processing for the manufacturing of an integral skin polymer foams comprising of a solid skin and foamed cores. Such configurations were obtained by creating both the core and skin in the concurrent manner by using the same foam material but different basic polymeric resins as shown schematically in the Figure 2.1.

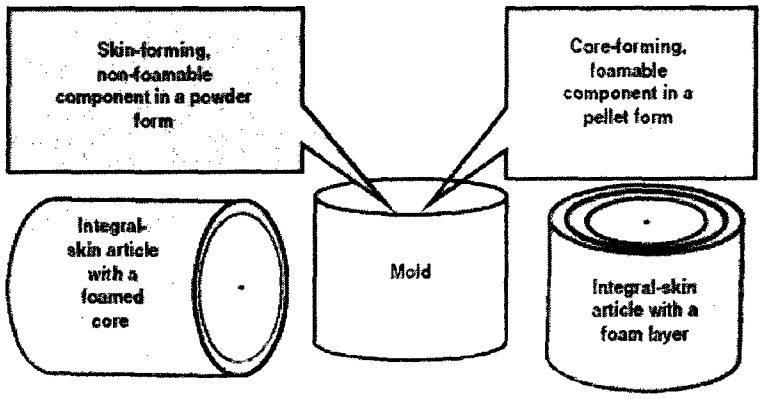

Figure 2.1: Schematic for the manufacture of cellular materials [6]

Houser et al. [7] fabricated a polyurethane core sandwich in which glass and carbon sheets were used separately as well as together as facing surfaces. Impact tests were conducted on the sandwich composite with single and multiple sheets to compare damage resistance. Results showed that the provision of additional sheets considerably enhances the damage resistance of sandwich composites.

Lee et al. [8] manufactured the foam cored sandwich beam inside a mold using the co-curing method; using the large difference in coefficient of thermal expansion between the foam core and the steel mold. In this method, pressure was generated due to the difference in expansion rate of the foam and steel mold. This process resulted in the co-cure bonding of the composite faces and foam core. Sihn and Rice [9] fabricated and studied the flexural properties of the foam core sandwich beams with the laminated face sheets under static and fatigue loading. The beams under the static loading showed nearly linear elastic behavior until the maximum failure loads, and then failed either yield or brittle mode. Failure in the core was due to shear. Both the moduli and strength of the sandwich structure with carbon cores remained unchanged after a few hundred cycles of loading.

Bezazi and Scapra [10] presented a comparative analysis between the cyclic loading compressive behavior of conventional, iso-density non-auxetic, and auxetic thermoplastic polyurethane foams. While the three types of foams share the same base material (open cell rigid PU), one batch is transformed into auxetic, using a special manufacturing process involving molding and exposure to particular temperature profiles to stabilize the micro structure transformation. The specimens were loaded in cyclic compression with a sinusoidal waveform in displacement control. The static tests show the specific stress–strain compressive mechanical behavior of these auxetic thermoplastics foams that are contrary to conventional ones and other similar data on the auxetics available in the open literature. The effect of the load loss, stiffness degradation, the evolutions of dynamic rigidity and accumulation of energy dissipation versus the number of cycles are discussed for different load levels. The energy dissipated by the auxetic foams is significantly higher than that of the conventional foams and iso-density foams at each number of cycles and load levels.

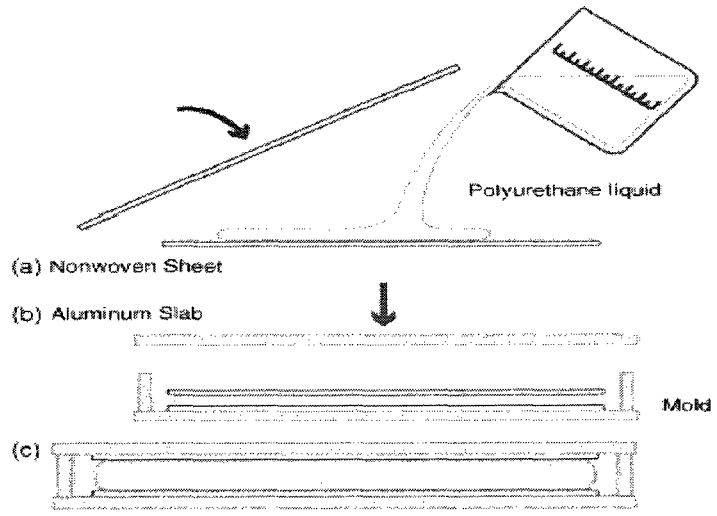

Figure 2.2: Manufacture of Polyurethane foams process [11]

Tsai et al. [11] manufactured polyurethane foams of different thicknesses. The expanding polyurethane was mixed with two-part liquid, and the combination resulted into a rigid, closed cell polyurethane foam as shown in the Figure 2.2. Before the urethane was foamed, the sample was placed in a mold with the two facing sheets to form a composite structure. Foam with varying thicknesses was manufactured by using four fixed height washers in the corner of the mold, until the polyurethane foaming was complete. Once the sample was fully cured, it was then removed from the mold. In the manufacturing process of the composite board, the polyurethane foam thickness was controlled to 7 mm, 10 mm and 15 mm to evaluate its effect on the thermal conductivity. The Thicker PU foams were found to have the better thermal conductivity properties.

2.3 Mechanical and Adhesion Properties of the Foams

Studies that were conducted previously have focused primarily on various properties of the polymer, metallic and ceramic foam using standard testing techniques such as shear, compression, fatigue and flexure, but not extensively on the adhesion properties of the polymer foams to metals.

Olurin et al. [12] explained the joining principle of aluminum foams using fasteners with and without adhesives. Four types of mechanical fasteners were used, wooden screw, nails, threaded inserts and studs. Two sets of investigation were carried out. In the first case, the dry fasteners were directly driven into the foam, and in the second case, fasteners were embedded in epoxy adhesives in pre-drilled holes in the foam giving a combination of mechanical and adhesives attachment as shown in the Figure 2.3. The mechanical characteristics were determined using the tensile, bending and pull-out loads. The effects of the fasteners geometry on the load-bearing characteristics was studied. It was reported that epoxy adhesive joints were better than the foam itself in all modes of loading.

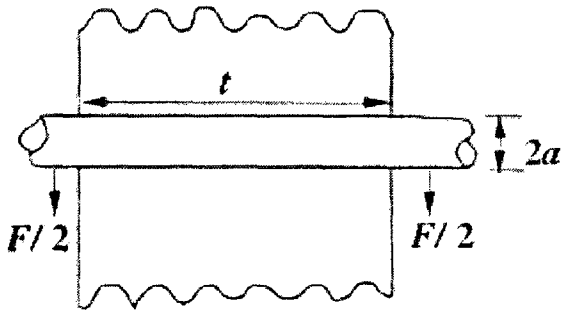

Figure 2.3: Insert inside foam [12]

Bernard et al. [13] reviewed various conventional joining techniques, like gluing and riveting, which can be applied to the foam-sheet sandwich structures. Flexural as well as torsional tests were conducted on the structures. The combined application of riveting and gluing was presented. It was reported that the structure was weakened due to the drilled holes that were necessary for introducing rivets, and resulted in failure of the foam core. The flexural tests also indicated that increasing the joint area between the foam and cover sheets result in a rise in the failure load value. Furthermore, it was reported that compared to riveted samples, welded compound structures have a larger joining area which results in higher maximum loads. For these structures, torsion tests revealed that it was neither the foam core nor the applied joining technique which was responsible for the failure of the structure, but the sheet metal itself. The research provides deep insight into the various types of cellular materials and explains the foam loading properties as well as the failure mechanism (elastic buckling, plastic yielding, etc . . .).

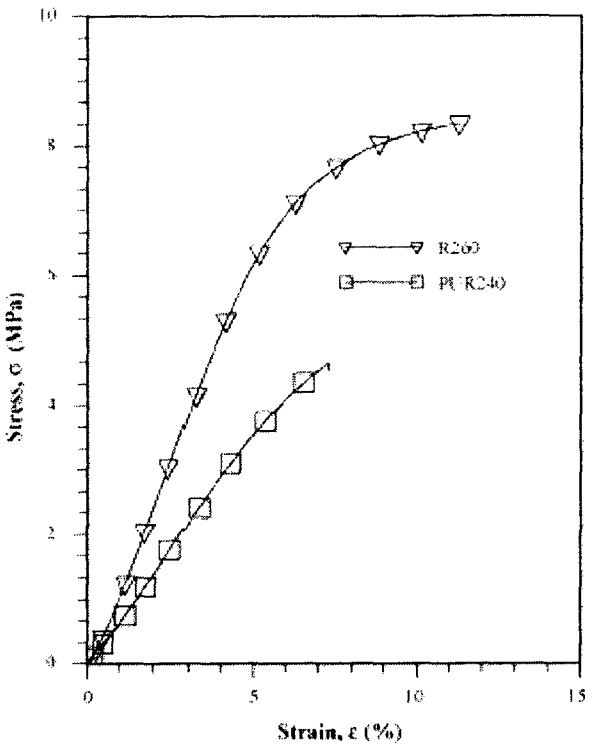

Figure 2.4: Tensile behavior of foams [14]

Kabir et al. [14] conducted the tensile and fracture tests on polyurethane and other polymer foams. Various parameters such as specimen size, foam density and crack length were studied. Tensile and fracture behavior was found to be non- linear up to the failure load as shown in the Figure 2.4. Both the tensile strength and modulus were found to be strongly dependent on the foam density. Fracture toughness of foam specimens with different crack lengths was also examined under flexural loading. It was demonstrated that the fracture toughness is a function of crack length. It remained constant to a certain length and then decreased beyond that point.

McIntyre et al. [15] compared the tensile and fracture properties of high and low density polyurethane foams. Fracture properties were characterized in terms of the fracture toughness and critical strain energy release rate. It was reported that the fracture toughness and the critical energy release rate were increased at high density. Furthermore, the fracture behavior of low density foams was ductile whereas that of the high density foams was brittle.

Huang [16] developed a theoretical criterion for evaluating the failure of the cellular foams under multi-axial loading and compared the predicted results with the published experimental data.

Experimental results reported in the research literature show that foam could fail in several modes; elastic buckling, plastic yielding, brittle crushing or brittle fractures. It was concluded that only the shear, tensile and compression tests were sufficient to completely describe failure behavior of foams. Studies were also done on the compressive, tensile and flexural properties of different structural polymers foams under various testing scenarios [17 -19]. It was reported that epoxy-based structural polymeric foams exhibited increased modulus and higher ultimate stress and strain to failure with the increased density under quasi static loading. The failure behavior of the low density foams under compressive loads is dominated by the collapse of porous cells which in turn triggers macroscopic fracture, whereas high density foams exhibited more uniform failure. In the case of the bending, failure occurred on the surface of the beam that is under tensile stress. At high strain rates, low-density foams exhibit random macroscopic fracture, indicating that the failure behavior is not shear dominated, whereas high-density foams fracture at 45°, thus indicating shear-dominated failure. Under high strain rate loading, foams exhibited increased yield stress and failure strength. In the range of the strain rates investigated, the strain to failure of high-density foams decreased at high strain rates.

Research was conducted on the bending properties of light weight epoxies based syntactic foams [20-21]. Foams are made by mixing the micro balloons (filler) with the resin material (binder). The foam material can serve as the core in the sandwich composite with fiber reinforced polymeric facing. It was reported that the addition of the elastomer increased the flexural strength of the composite. Failure in the syntactic foams occurred due to crack propagation through the filler resulting in failure of the entire composite. Based on the results presented, it was concluded that the dispersion of glass micro spheres in an epoxy resin increased the fracture toughness compared to the unfilled epoxy resin.

Kanny et al. [22] studied the shear and dynamic property of two different closed cell polymer PVC foams, namely HD 130 (linear) and H130 (cross linked). Shear tests revealed that HD130 foams were more ductile, had almost twice the energy absorption capability, and better crack propagation resistance. For the foam, shear deformation occurred without volume change and the material failed due to shear in the vicinity of the centerline along the longitudinal axis. In both cases, 45^0 shear cracks formed along the length and across the width of the specimen immediately prior to the final failure event.

Kreter [23] studied the effect of varying density on the mechanical and physical properties of polyurethane foams. 26 polyurethane commercial samples were obtained from five different manufacturers with densities varying from 20 to 138 kg/m^3. Samples were subjected to fatigue, compression and shear tests. Test results show that an optimum density value of 80 kg/m^3 of polyurethane foams is required in order to maximize the fatigue properties.

Davy et al. [24] studied the critical stress-intensity factor for crack initiation using different test geometries for rubber-toughened epoxy polymers. A main difference between the test geometries was that some employed a through-thickness crack whilst others contained an embedded surface crack. Fracture toughness was calculated using the 5% offset method. A detailed study of the applicability of linear-elastic fracture-mechanics (LEFM) was conducted, and only valid LEFM results were considered, it was shown that the values of stress intensity factors were independent of the geometry. Furthermore, the results from a through-thickness crack were the same as those obtained from a surface crack. The particular aspect of slow crack growth on the determination of the stress intensity factor was considered in detail.

2.4 Mechanical and Adhesion Properties of the Composites

Studies were also done on the mechanical properties of sandwich composites [25]. Bakos and Papinocolou [26] studied the bending behavior of sandwich beams with polyester resins as core and a glass fiber and aluminum as facing sheets. Testing was done in accordance with ASTM D70 which outlines the flexural behavior of plastics. Four different skin treatments and three different core materials were applied in order to study the effect of these parameters on the overall bending behavior. Stresses in the x-direction of the facing were calculated as shown in the Figure 2.5 and the experimental results were compared with the theoretical model. Delamination between the core and the skin was reported as a mode of failure.

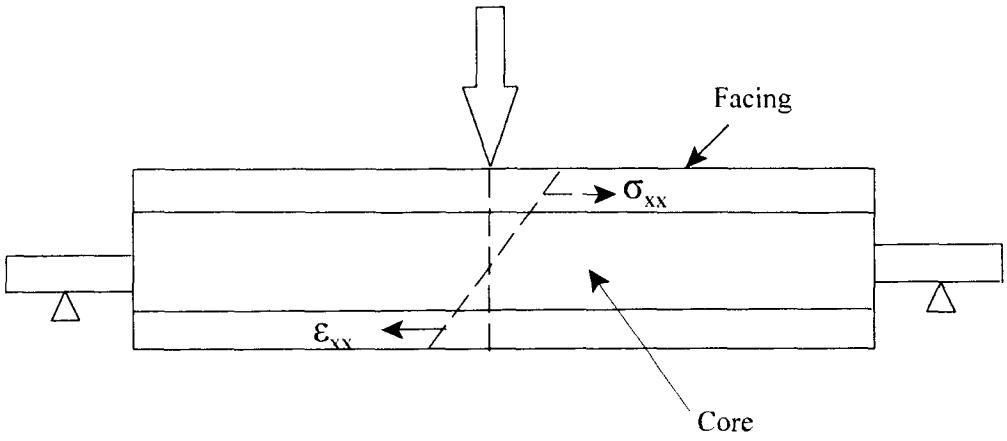

Figure 2.5: Bending set-up [25]

An experimental study was conducted on the behavior of composite sandwich beams under flexural loading [27]. Sandwich beams were fabricated by bonding unidirectional carbon/epoxy face sheets (laminates) to aluminum honeycomb cores with an adhesive film. It was reported that bending behavior of the beams, whether loaded under four-point or three-point bending, was governed by the face sheets. Furthermore, as the core stiffness was much smaller when compared to the facing layers, hence no failure in the facing was observed. Furthermore, stress strain plots revealed that failure occurred at a stress value much lower than the yield strength of the facing. Experimental results were in good agreement with the predictions of the simple models assuming that the face sheets behaved like membranes and neglecting the contribution of the core.

Research was conducted on sandwich composite with inserts [28]. Inserts were used as the reinforcements in the composite. Inserts were made of metal, polymer and ply wood. The new design of the core inserts substantially diminished the level of local stress concentration effects in the faces. The suggested inserts were structurally graded by means of shaping insert boundaries to be inclined with respect to the sandwich faces, which provides smoothing of material discontinuities at the junction of different materials. The new design of the core insert was studied experimentally, and the design parameters of the core insert were studied using finite element modeling (FE).

Xia et al. [29] presented an exact solution based on the classical plated laminated theory for composite pipes under pure bending. Detailed stresses and deformation of the filament wound sandwich pipe subjected to bending loads were investigated and discussed. It was shown that the

stresses and strains depend strongly on the winding angle when the pipe has the filament-wound layers with highly anisotropic composite. The cross section of a pipe was no longer a circle after the pipe was subjected to bending loads.

Karthikeyan et al. [30] investigated the bending modulus of fiber-reinforced polymers and syntactic foams containing varying percentages of E-glass fiber for sandwich and structural applications. Polymer composite foams or syntactic foams containing 0.9, 1.76, 2.54, 3.54 and 4.5 % volumes of short E-glass fibers were processed and subjected to a three-point bending test. The results show that the flexural modulus increased with fiber content, with the exception of 1.76% and 3.5% of fibers. This deviation was due to a higher void content for 1.76% and a non-uniform distribution of fibers in the polymer composite foam system for 3.5%. However, in general, the incorporation of chopped strand fibers improved the flexural behavior of the syntactic foam system without much variation in density, thus making the reinforced syntactic foams act as improved core materials for sandwich and other structural applications. The results showed that for the polymer foams the flexural modulus increased as the percentage of fiber increased. Thelun and Sarzynski [31-32] studied the flexural behavior of sandwich composites. The minimum core -to- face weight ratios for bending stiffness and failure modes of sandwich structures were investigated. The primary damage mode that was observed took the form of cracks in the foam core. The optimum core-to-face weight ratio for bending stiffness was found to be two and for bending strength was found to be one. Finite element models were also developed to study and validate the experimental results.

Moutriz and Shafiq [33-34] reported the compressive, flexural and shear properties of sandwich composites containing defects. The properties were found to be reduced with increasing interfacial crack or impact damage, but only when the defects caused a change in the failure mode, which was dependent on the load state. The principal failure modes under the different load states were also compared. The properties were also dependent on the severity of impact damage with low energy damage to the skin having a small effect on the stiffness and strength than high energy impact which damaged both the skin and foam core.

Shafiq and Kulkarni [35-36] reported the failure properties of foam core sandwich composite with and without an end notch under flexural fatigue loading. Extensive fatigue data was generated and S-N curves were plotted. For the flexural results without an end notch, three distinct damage

events were found. The first was the core skin debond parallel to the beam axis. This debond propagated slowly along the tip interface and eventually kinked into the core as shear crack and then grew in an unstable manner resulting in total specimen collapse. For the notched beam, the core damage was found to be the predominant failure activity while fiber rupture served as a precursor to the complete failure. Multiple crack initiation sites were observed under the fatigue loading in the vicinity of the notch tip. Both mode I and II cracking was observed in the core and along the interface of the core and the face sheets. Flexural stiffness was also reduced by increasing the number of cycles to failure.

Lee and Tsotsis [37] studied the failure behavior of honeycomb sandwich panels subjected to the indentation loads. Two scenarios of loading were considered which are the point and distributed loads. It was revealed that indentations induced stresses in the core relevant to the onset of indentation failure, and were found to be dependent on the skin bending stiffness, core stiffness, and indenter size. The calculated maximum normal and shear stress value were studied. Comparison showed that core failure dominated the onset of the indentation failure.

Load carrying capacity of fiber reinforced plates were studied by Movsumov and Shamiev [38]. The plates were simply supported as well as clamped. It was reported that depending upon the ratio of ultimate radial and circumferential bending moments, in the plastic range, circular plates took the shape of a cone or frustum of a cone. The statically allowable fields of bending moments and corresponding deflections were calculated.

Kanny and Mahfuz [39] studied the effect of frequency on the behavior of reinforced sandwich composites with two different PVC cores. It was observed that fatigue strength increased with core density and that the number of cycles to failure increased with the increase in frequency. In all cases, failure was dominated by primary shear stress in the core, however, the crack path and crack propagation rates varied with the frequency. It was also reported that crack growth rate decreased with an increase in loading frequency.

Thomsen and Bunyawanichakul [40-41] studied the impact of inserts in sandwich structures for aerospace applications such as flaps and landing gear doors. In the case of landing gear doors, the junction is made through Nomex. Experimental investigations were presented and a related numerical model of quasi-static pull-out tests of potted inserts.

The different types of damage were identified and a failure mechanism was proposed. Initially, the cell walls of the core buckled under shear. This was followed by the appearance of damage in the potted insert under the head of the screw. Finally the head of the screw penetrated the skin because of the lack of resistance of the potted insert and the increase in shear stress in the skin. Following these experimental conclusions, a nonlinear finite element model was constructed. It included the nonlinear behavior law of the honeycomb which was identified by a simple three-point bending test. Other material characteristics were identified by the classic tests and the perfect plastic behavior of the potted insert was taken into account.

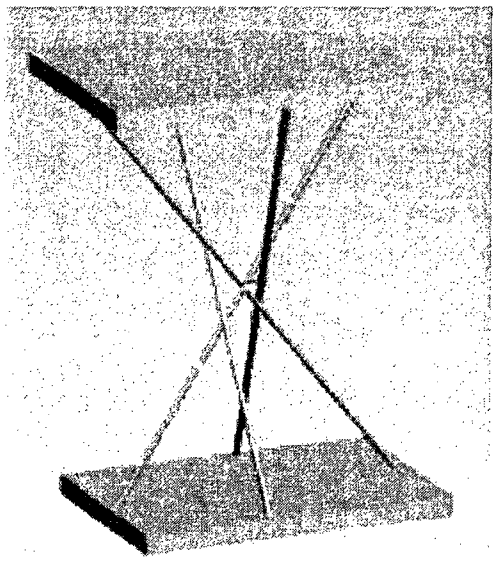

Figure 2.6: Insert inside foam core [41]

Rice et al. [42] studied the flexural properties of hybrid sandwich structures with carbon fibers or metallic pins that were inserted into the foam core in the out-of-plane direction and extended from face sheets as shown in the Figure 2.6. Experimental results revealed that under the correct geometric conditions, pins reinforced panels would still fail by indentation; however the predicted shear failure mode was not observed. Explicit experimental observations were used to calibrate the analytical energy balance models describing the panel collapse as a function of geometry and properties.

Steeves et al. [43] presented the analytical solution of the three-point bending collapse strength

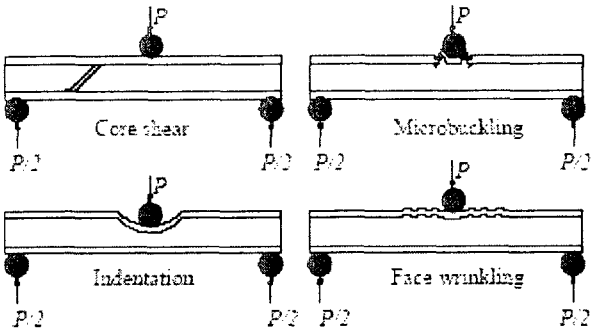

Figure 2.7: Modes of sandwich composite fracture [42]

of sandwich beams with composite faces and polymer foam cores. Failure was caused by the competing modes of face sheet micro buckling, and plastic shear of the core, and face sheet indentation beneath the loading rollers as shown in the Figure 2.7. Particular attention was paid to the development of a mathematical indentation model for elastic faces and an elastic–plastic core. Failure mechanism maps were constructed to reveal the operative collapse mode as a function of the geometry of the sandwich beam, and minimum weight designs were obtained as the function of an appropriate structural load index. It was shown that the optimal designs for composite–polymer foam sandwich beams were of comparable weight to sandwich beams with metallic faces and a foam core.

2.5 Finite Element Analysis Results on the Foams and Composites

Finite element analysis (FE) plays a vital role in predicting the linear and non-linear behavior of polymer and composite structures. Sandwich beams were modeled and studied by Vincent Manet [44] in ANSYS. He used various models to compute displacements and stresses of a simply supported beam. Eight-node quadrilateral elements (Plane 82) and multilayered 20-node cubic elements (Solid 46) were used. The influence of mesh refinement and of the ratio of Young's moduli of layers were studied. Simulation results were compared with the published data. It was observed that the Plane 82 element was the most accurate element based on comparison with published data for calculating the stresses and strains of sandwich facing and core.

Lin and Bull [45] developed a finite element simulation model using ANSYS for predicting the deformations and stresses of non-rigid materials (NRM) under the influence of a pinch gripper.

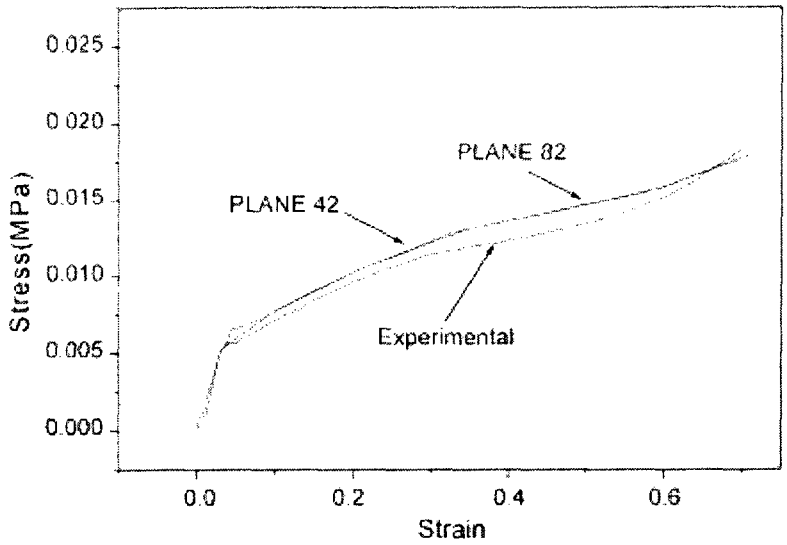

Figure 2.8: ANSYS comparison with experimental results [45]

Two dimensional plane element types 82 and 42 were used, and the results were compared with experimental results as shown in Figure 2.8. Specific attention was given to the differences in response of the NRMs to the shape (rectangular and cylindrical) of the gripper used. The influence of mesh refinement and aspect ratios of the elements has been studied. The non-linear behavior of NRM compression has been described in the materials model used by the FE program.

Queiroz et al. [46] investigation focused on the evaluation of full and partial shear connections in composite beams using the commercial finite element(FE) software ANSYS. The proposed FE model was able to simulate the overall flexural behavior of simply supported composite beams subjected to either concentrated or uniformly distributed loads. The reliability of the model was demonstrated by comparisons with experiments and with alternative numerical analyses. The nonlinear behavior of NRM compression was described in the materials model used by the FE program. Experiments were carried out to validate the FE modeling approach for a specific material sample (Polyurethane foams). It is concluded that there is a good comparison between the modeling and

experimental results and that the model can reasonably predict what could happen in real applications. The advantages of this model were ease of construction, fast solution times and good accuracy.

Kolakowski and Kubiak [47] presented basic ideas for an approach to assess stability, post buckling behavior, and load carrying capacity of thin-walled composite structures using ANSYS. Thin walled composite beam-columns with open and closed cross-sections (channel and square) were used as examples. In order to analyze the stability of the structure, and estimation of critical stress, ANSYS was used. Results obtained from ANSYS were compared with the theoretical model. Presented examples show that the sole application of the FEM cannot guarantee correct results of load carrying capacity and post buckling behavior.

Kramer et al. [48] investigated the experimental and numerical configurations of hollow and foam filled stringers under axial and bending moments. The use of stringer profiles has proven to be the most suitable method for stiffening thin shells, typically used as engine air inlet duct panels or engine cowling panels. Finite element analysis software ANSYS was used for the numerical purpose. Foam filled stringers demonstrated higher buckling loads as compared to hollow ones. The reliability of the model was demonstrated by comparisons with experiments results and with alternative numerical analyses.

2.6 Summary

Manufacturing and fabrication techniques of the foam and sandwich composite were studied. A detailed literature review on the mechanical and adhesion properties of foams and sandwich composite was also conducted. Furthermore, FE results on foam and their sandwich composites reported in the available literature were also studied. It was concluded that extensive work was done on the mechanical properties of foam and sandwich composite structures. However, it was also noted that these researches did not thoroughly examine the adhesive properties of foam-based sandwich structures with metals, especially in flexural loading. Work was done, however, on metallic foam interactions with inserts using pre-drilled holes and also with glues. Chapter 3 will presents a novel methodology for the manufacture of foams with metallic inserts of different geometries.

CHAPTER 3

DESIGN, FABRICATION, AND TESTING OF FOAM STRUCTURES WITH INSERTS [1]

3.1 Introduction

This chapter focuses exclusively on characterizing metal-foam interaction in the form of metal inserts in foam structures. Research conducted so far has focused primarily on the various properties of the polymer foams using standard testing techniques such as shear, compression, fatigue and flexure. These studies did not thoroughly examine the adhesive properties of foam with metallic inserts. Therefore, this chapter focuses on developing and examining an effective approach for introducing metal inserts for joining the foam structures together and provides anchor points. To that end, Polyurethane (PU) was foamed to partially engulf the metallic inserts of different shapes and sizes in order to study their effect on strength and adhesive properties. Once cured, flexure tests were conducted by supporting the structure through the inserts and loading the cured foam. The effects on modulus of elasticity and adhesive properties of embedded length and shape for these composite foam structures were studied and failure methods were analyzed. Results for the foam structures with different metallic inserts were compared. For design purposes, a finite element model was developed using commercial software, ANSYS 11. Models matching the experimentally tested dimensions and geometries were developed in ANSYS, analyzed, and the stress strain results compared to the experimentally obtained ones.

---

[1] Reproduced from: Ahmed, A, Fahim, A and Naguib, H., July 2008, " A Study on the Design and Mechanical Adhesion of Polymer Foam-Metal Joints". **ASME**-Journal of Engineering Materials and Technology, 130.No.3, pp.031011-1-7.

3.2 Experimental Procedure

3 .2.1 Fabrication of Foams with Inserts

Polyurethane foams, closed cells, of density, 25kg/m^3, and three times expansion capabilities were used in the experiments. Foaming was done inside a rectangular mold. Attachments for the inserts were designed and manufactured as shown in the Figure 3.1.

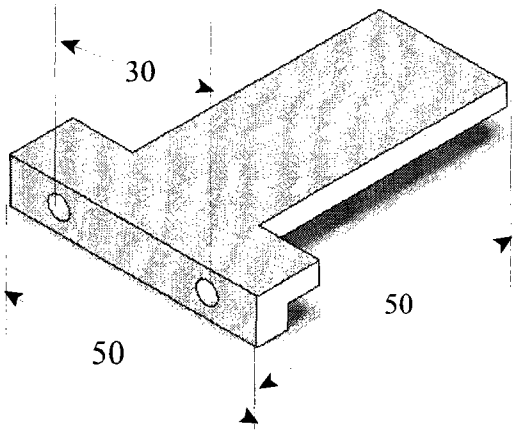

Figure 3.1: Attachment for holding inserts

The mold, attachments, and inserts were made of machined aluminum 6061 alloy. Proper surface treatment was given to all the aluminum components after machining and they were filed and cleaned with sand paper to remove any chips or burs. Two holes shown in Figure 3.1 are for holding rectangular and taper inserts with attachment, but for the cylindrical inserts, an additional hole was drilled in the middle of the attachment. Thickness of the attachment was 9 mm and the diameter of holes was 3 mm. Once foamed, each specimen was left in the mold for approximately 24-48 hours to ensure dimensional stability during curing. The dimensions of the rectangular foam beams produced are: 300 mm × 120 mm × 50 mm. The dimensions of the aluminum inserts are given in the Table 3(a). The photograph of foam with an imbedded insert is shown in the Figure 3.2.

Table 3(a): Insert geometries and dimensions

Insert Geometry	Dimensions (mm)			
	Diameter	Height	Width	Length
Rectangular	N/A	9	50	100, 75, 50
Cylindrical	12	N/A	N/A	100, 75, 50
Taper	N/A	9 to 1	50	100, 75, 50

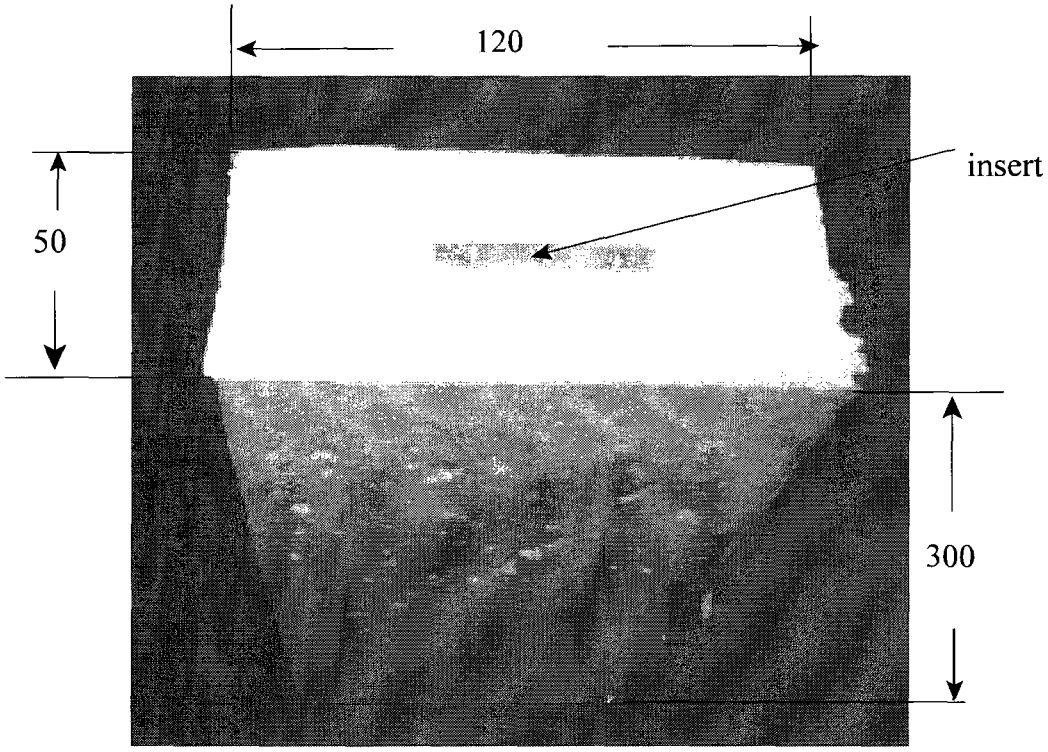

Figure 3.2: Experimental foam sample with insert (all dimensions in mm)

3.2.2 Flexural Tests

Flexure tests were conducted in accordance with the ASTM D790 which outlines the standard bending test procedure for plastics. Tests were conducted on an Instron 4482 machine with a 100 KN load cell at room temperature. The loads were applied at the center of the foam beam while the attachments screwed to the embedded inserts rested on two supports as shown schematically in the

Figure 3.3. The direction of the taper is shown in the Figure 3.4. The actual experimental set-up is shown in the Figure 3.5. A slow cross head speed of 5 mm/min was used for all the tests and the load-deflection data points were obtained using a PC. After the final failure, the maximum load was recorded and photographs were taken to document the final state of each specimen. Flexural tests were also conducted on foams without reinforcement and the results were analyzed and compared with foams with inserts. A total of five tests for each insert length was conducted as per the ASTM standard and the average values from the tests were plotted and are shown in the figures below. In order to avoid crushing of the foam beam, a line load along the width of the foam beam was applied.

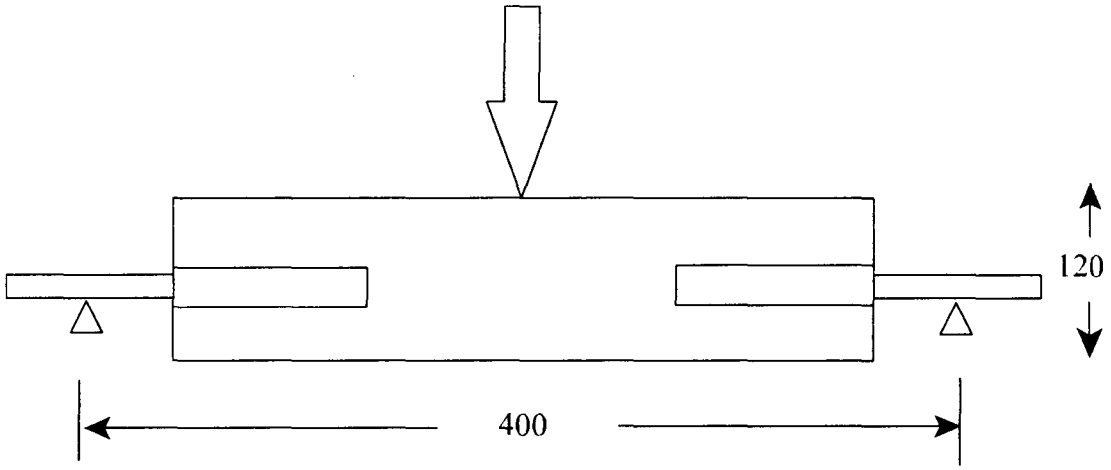

Figure 3.3: Schematic of the three point bend set-up (mm)

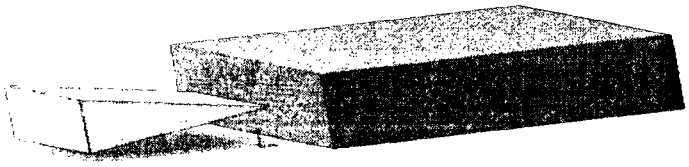

Figure 3.4: In plane direction of the taper insert

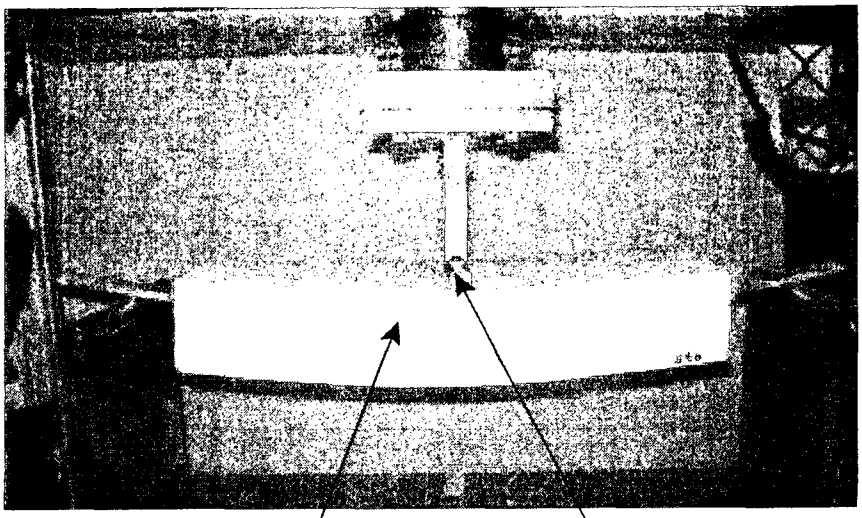

Figure 3.5: Experimental bending test set-up

Flexural stress- σ_f was calculated as follows:

$$\sigma_f = \frac{3PL}{2bd^2} \tag{3.1}$$

Where P is the applied load, L is the span length, b is the width of the tested beam and d is the depth of the tested beam.

Flexural Strain- ε_f was calculated using the equation:

$$\varepsilon_f = \frac{6Dd}{L^2} \tag{3.2}$$

Where D is the maximum deflection of the beam, L is the support span and d is the depth of the tested beam.

Shear Modulus- G was calculated using the equation:

$$E = 2G(1+\nu) \tag{3.3}$$

Where ν is the Poisson ratio.

3.3 Results and Discussions

Results obtained from the flexure tests with inserts that are rectangular, cylindrical, and the wedge (taper) in shape, and with lengths of 100 mm, 75 mm, and 50 mm are presented below.

3.3.1 Rectangular Inserts

Experimental results of the foam structures with three different lengths of the rectangular inserts were compared against those for foams with no inserts and are presented in the Table 3(b). Photographs of the failure modes for the cases of the 100 mm, 75 mm are shown in the Figure 3.4(a) and 50 mm inserts are shown in the Figure 3.4(b).

Table 3(b): Moduli of elasticity and shear of the composite structure with rectangular, cylindrical and taper inserts. (E & G for simple foams with no insert are 4.51 and 1.80 MPa respectively).

Insert	Modulus (MPa)	100 mm	75 mm	50 mm
Rectangular	E	5.12	5.02	4.86
	G	2.048	2.008	1.944
Cylindrical	E	5.04	4.91	4.73
	G	2.016	1.964	1.892
Taper	E	5.29	5.18	4.91
	G	2.116	2.072	1.964

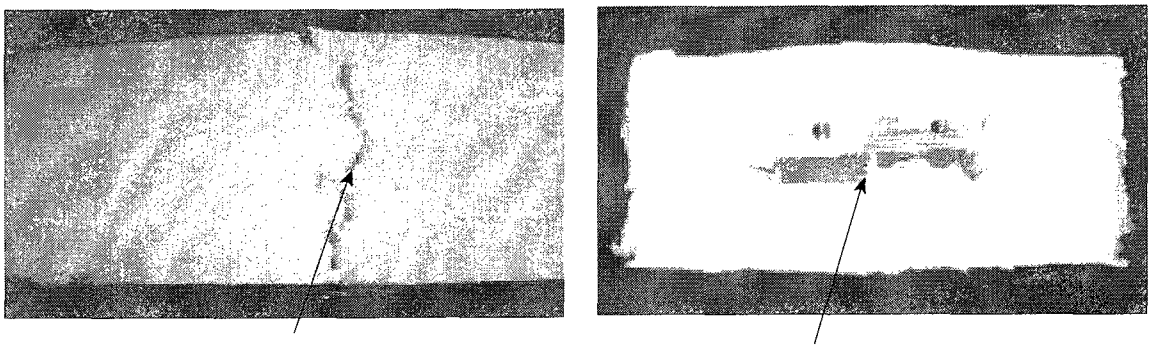

a) Foam fracture b) Adhesion failure

Figure 3.6: Photographs showing the nature of the fracture of the composite structure with rectangular inserts a) The foam fracture for long insert length b) adhesion failure for short insert length.

It was noted that for the two longer inserts (100 mm and 75 mm) strong bonding between the polymer and insert existed. The failure occurred due to fracture of the foam rather than debonding. The foam experience little plastic deformation and the nature of the fracture was ductile. Cracks were initiated in the tension side of the composite structure and propagated along the cross section of the foam, and finally resulted in complete fracture. This foam behavior in terms of yielding and ductile fracture is similar to that reported in McIntyre et al. [15] research where fracture properties of the low density foams were studied. However, for the smallest insert length, 50 mm, the adhesion failure occurred in the bond and resulted in the slip of the insert from the foam structure. The bond strength in the case of the 50 mm length inserts is less than the fracture strength of the foam, and consequently results in adhesion failure. Furthermore, it was observed that the foam-insert failure occurred in two steps; Firstly, due to bending, the inserts were pressed against the foam which resulted in higher concentration of compressive stresses in the foam under the insert surface, and the degradation of that foam. Secondly, due to its distance from the neutral axis the tensile stress on the surface of the rectangular insert, coupled with the higher stress concentration effect at its innermost corner, initiate de-bonding of the insert from foam. This eventually resulted in the rectangular insert pull-out failure as shown in the Figure 3.7.

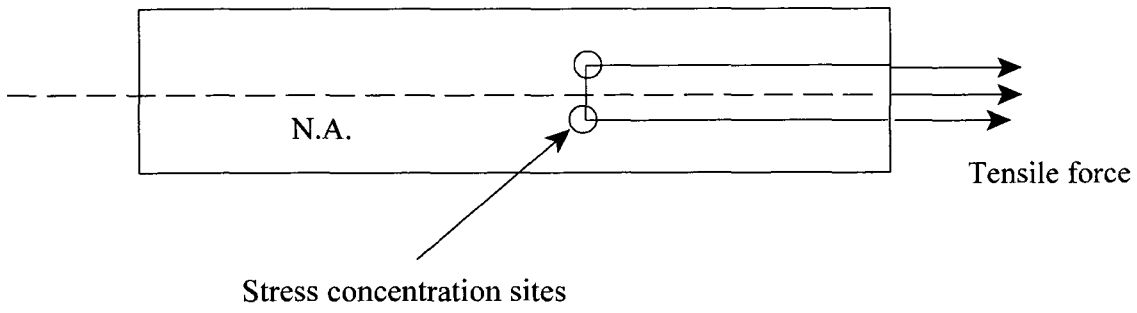

Figure 3.7: Stresses on the rectangular inserts

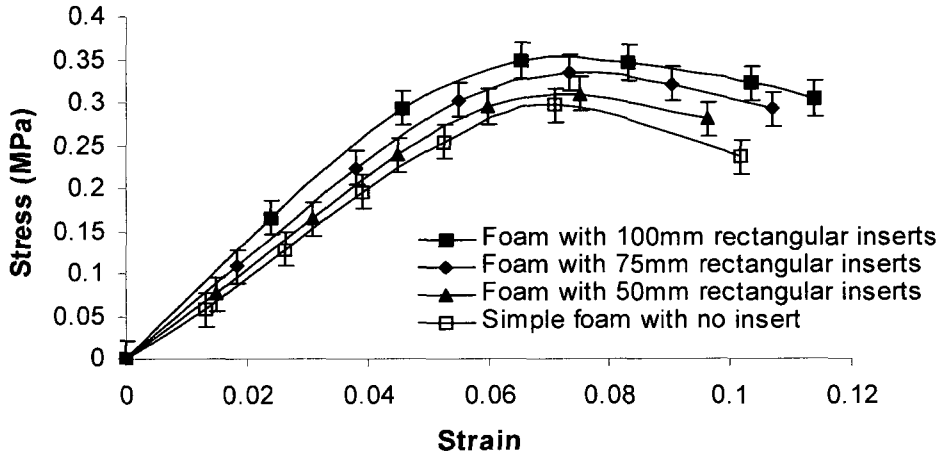

Figure 3.8: Bending stress and strain curves for foams with rectangular inserts

Typical bending stress-strain curves in the Figure 3.8 shows marked non- linearity for the low density foams similar to those reported in [15]. The peak of the graph represents the maximum stress value. Data for the three lengths of inserts are presented in the figures. The spread of the magnitude of the stress at selected strain values and the average of the stress values are indicated on the graphs. A smoothed curve is drawn to join the average stress values. Although two distinct failure modes (foam fracture and bonding failure) were observed in the tests, the pattern of stress strain curves was the same.

Since modulus of elasticity of foams was discussed in the ASTM D790 standard, therefore the

modulus of elasticity of foam structures were calculated from the test results. The modulus of elasticity, E, of the foam structure varied with the embedded length of the insert. As the insert length was increased so did the stiffness. Increasing the embedded length hindered the initial deformation of the composite structure under the load and resulted in a higher force being applied for the same bending displacement. In all cases the stiffness of the foam structure with inserts is larger than the stiffness of the simple foam (no insert) to some extent. As the shear modulus is directly proportional to the elastic modulus, therefore this coincided with the experimental results where the shear modulus of the foam structures increased with the increase in length of the inserts.

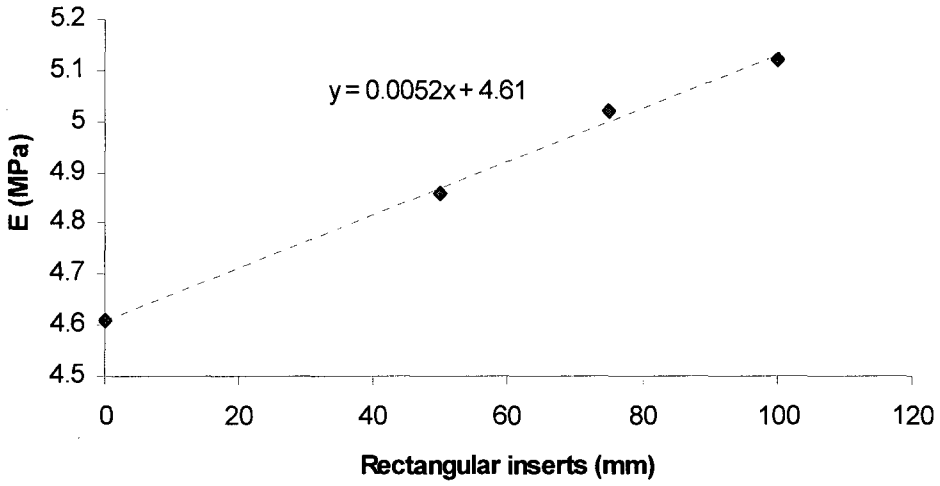

Figure 3.9: A trend line of the increase in modulus of elasticity due to the increase in rectangular insert length.

The Figure 3.9 shows the general trend of the increase in the modulus of elasticity due to the increase in the length of the insert in the foam structure. As can be seen from the figure, the trend is very close to being linear. Furthermore, the intercept of the trend line almost coincides with the value for the experimentally calculated modulus, 4.51 MPa, of the simple foam beam with no insert (zero insert length).

3.3.2 Cylindrical Inserts

The second set of tests was conducted with the cylindrical inserts, again with three different lengths. The experimental results were compared with those for the foam slab with no inserts, and are presented in the Table 3(b). Also, the photograph of the failure mode for the 50 mm inserts are shown in the Figure 3.10.

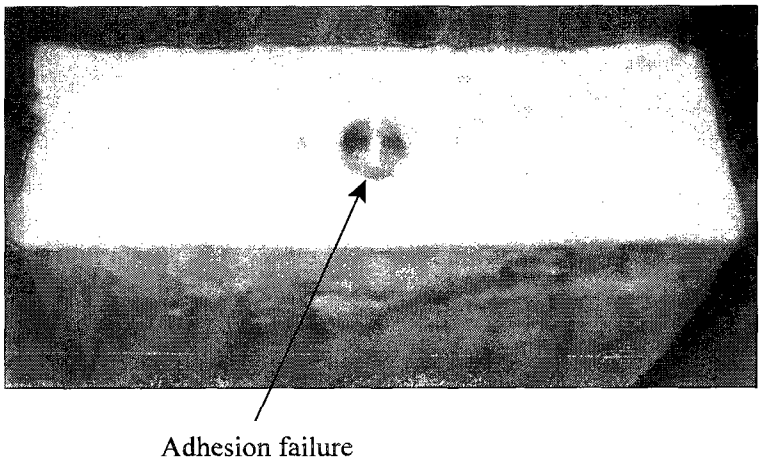

Figure 3.10: Adhesion failure for cylindrical inserts

It was observed that for the longer cylindrical inserts (100 mm and 75 mm) ductile foam fracture occurred with little evidence of yielding similar to the case of the long rectangular inserts. However, for the 50 mm length, slippage occurred between insert and foam.

The Figure 3.11 shows the plot of the stress strain curves obtained from these tests. As the load-bearing area for the cylindrical inserts is smaller than that for the rectangular inserts, the load magnitudes that resulted in de-bonding failure are smaller than those for the rectangular inserts. The plot in the Figure 3.8, was used to calculate the modulus of elasticity of the foam structure with cylindrical inserts.

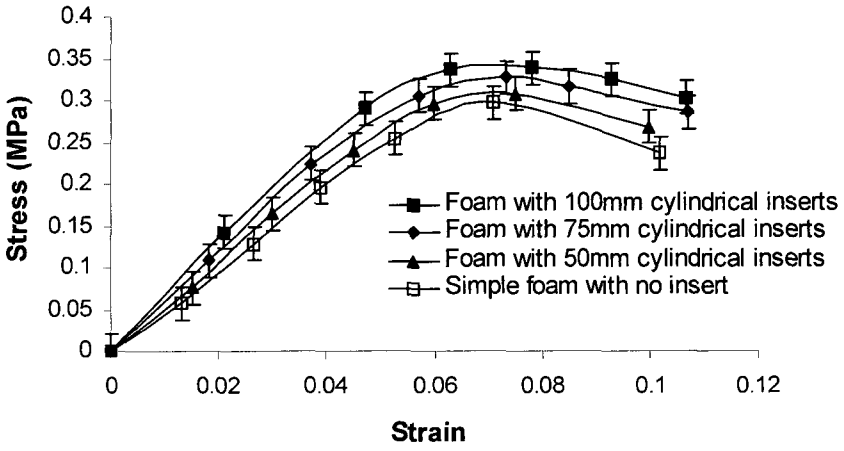

Figure 3.11:Bendingstress strain curves for foams with cylindrical inserts

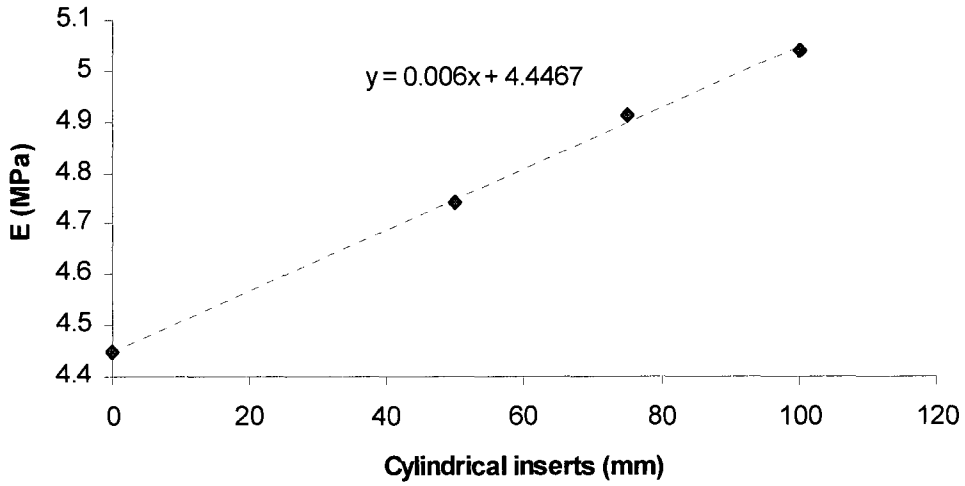

Figure 3.12: Trend line of the increase in modulus due to increase in cylindrical inserts length

The Figure 3.12 shows the linear regression line of the modulus of elasticity of the composite structure with increasing insert length. The intercept of the line again almost coincides with the *E* value of 4.51 MPa of simple foam slab without the insert.

3.3.3 Taper Inserts

Experimental results from the three different lengths of the taper inserts in foam structures were obtained and compared to those for foam slabs with no inserts and are tabulated in the Table 3(b).

For the case of the tapered inserts, again foam fracture was observed for the longer insert lengths, 100 mm and 75 mm. For the shorter insert length, 50 mm, it was observed that de-bonding

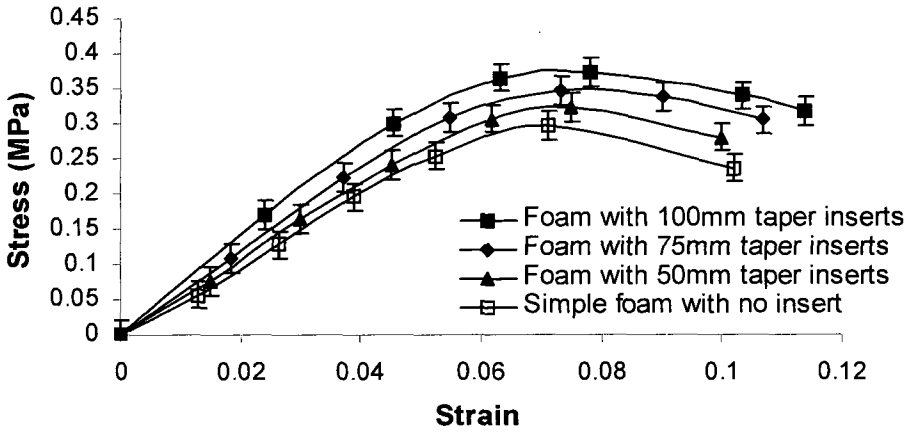

Figure 3.13: Bending stress strain curves for foams with taper inserts

failure occurred in both inserts. Compressive stresses on the foam and tensile stresses on the inserts resulted in the failure. The value of the maximum stresses calculated for the taper inserts were higher as compared to the rectangular and cylindrical inserts. This can be explained by the fact that the tensile (stretching loads) at the tip of the wedge are very low due to its close proximity to the neutral axis, and hence the effect of the stress concentration at the tip did not initiate too early failure. Furthermore, the taper inside the foam reduced the intensity of the force on the foam. The modulus of elasticity was calculated from the typical non-linear stress strain traces as shown in the Figure 3.13.

The Figure 3.14 shows the linear regression trend of the change in E versus the insert length. Again here the intercept of trend line is coinciding with the modulus of elasticity for a simple foam.

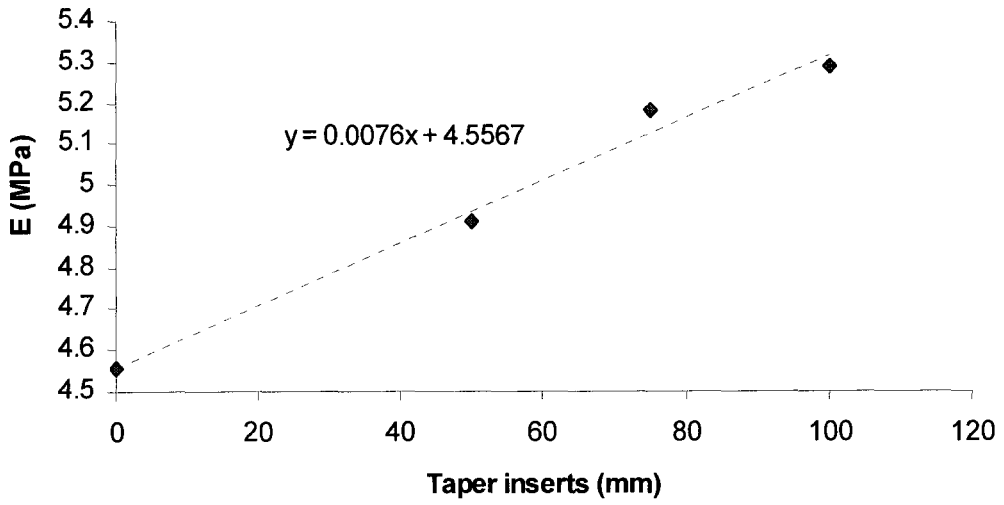

Figure 3.14: Trend line showing the increase in modulus with insert length

After analyzing all the different geometries separately, it was observed that the embedded length plays a significant role in estimating stiffness and adhesion properties. The larger the length, the better the results were for the stiffness and adhesion. Less bonded area for all the geometries resulted in the adhesion failure at lower loads compared to the bending failure for the longest inserts. Stress concentration also played a decisive role in initiating insert failure. The taper inserts were considered the best in terms of the geometry, stress concentration factors and placement with respect to the neutral axis.

3.4. Finite Element Analysis

Two dimensional finite element models were developed for the foam with inserts structures using the commercial finite element program, ANSYS 11. The purpose of the exercise was to validate the FE modeling technique, and use that later for the design of foam structure with inserts.

3.4.1 Model Parameters

Advances in computational features and software have brought the finite element method within reach of both academic research and engineers in practice by means of general-purpose non

linear finite element analysis packages, with one of the most used nowadays being ANSYS. The program offers a wide range of options regarding element types, material behavior and numerical solution controls, as well as graphic user interfaces (known as GUIs), auto-meshers, and sophisticated postprocessor and graphics to speed the analyses [51]. In this research, the structural modeling of foam was done on ANSYS version 11. The purpose of the exercise was to validate the FE modeling technique based on the stress strain response of the model.

An eight-node element (PLANE 82) was selected due to its proven better results in the open literature for foam structure modeling [44]. Plane 82 is a higher order 2D element. It provides more accurate results for mixed (quadrilateral-triangular) automatic meshes and can tolerate irregular shapes easily. The 8-node elements have compatible displacement shapes and are well suited to model curved boundaries. The 8-node element is defined by eight nodes having two degrees of freedom at each node: translations in the nodal x and y directions. The element has plasticity, creep, swelling, stresses stiffening, large deflection, and large strain capabilities which are required for contact analysis that are non-linear in nature.

3.4.2 Contact Modeling

Due to the large stiffness difference in properties between the foam and the aluminum, the interfaces between the two materials and the contact stresses resulting are generally highly nonlinear and cause convergence problems [51]. ANSYS contact features were used to designate proper values to the contact parameters to reduce the severity of the problem. Rigid-flexible contact scenarios were used. The contact surfaces of the foam were designated with CONTA 174 elements and the contact surface of the aluminum were designated with TARGET 170. During simulation, separation of the foam from aluminum frequently occurred. Any loss of contact between the surfaces resulted in simulation failure. ANSYS 'Automatic Adjustment' option was used to deal with such problems. Using this option instructed ANSYS to continuously monitor pending separation and ensure surface contact.

3.4.3 Loading and Convergence Conditions

A load representing the mid span loading was applied to the model. Because of the symmetry along the length, only half of the beam was modeled with the appropriate symmetry displacement

boundary conditions imposed. Nodes at each end of the beam were constrained to simulate a simply supported beam. The load was applied gradually using a short time step and a small load step to facilitate convergence. A number of convergence-enhancement and recovery features, such as line search, automatic load stepping, and bisection, were activated for some simulation cases where the convergence was slow in order to help in reducing convergence problems.

3.4.4 Analysis

In order to determine the non- linearity of the model, both the geometric and material non-linearities are considered. For material non- linearity, the large strain analysis option was used for running the simulation. This option accounts for stiffness changes that result from changes in an element's shape and orientation. It places no theoretical limit on the total rotation or strain experienced by the element. In order to account for the material non- linearity, automatic time stepping option was used. This option responded to plasticity, by reducing the load step after a load step in which a plastic strain increment greater than 15% was encountered. If too large a step was taken, the program will bisect and resolve to use a smaller step size. The loads were applied using a shorter time step and small load step to facilitate convergence.

3.5 Results and Discussions.

The Figure 3.15 showed the stress strain curves for the FE models of the foam structure with the rectangular, cylindrical, and tapered insert geometries obtained from ANSYS respectively. The figures show that for the different insert lengths the shape of the curves and the magnitudes coincide with those obtained experimentally. Simulations showed that for the foam with longer inserts, contours of higher stress were shown on the bottom end of the foam representing a foam fracture. For the foam with the shorter insert, contours of higher compressive stresses were visible on the foam area underneath the insert as well as tensile stress contours were visible on the inserts. Thus, the simulations validated the different experimental mode of failure. The Table 3(c) documents the maximum fracture load values for three inserts geometries obtained from the Figure 3.12.

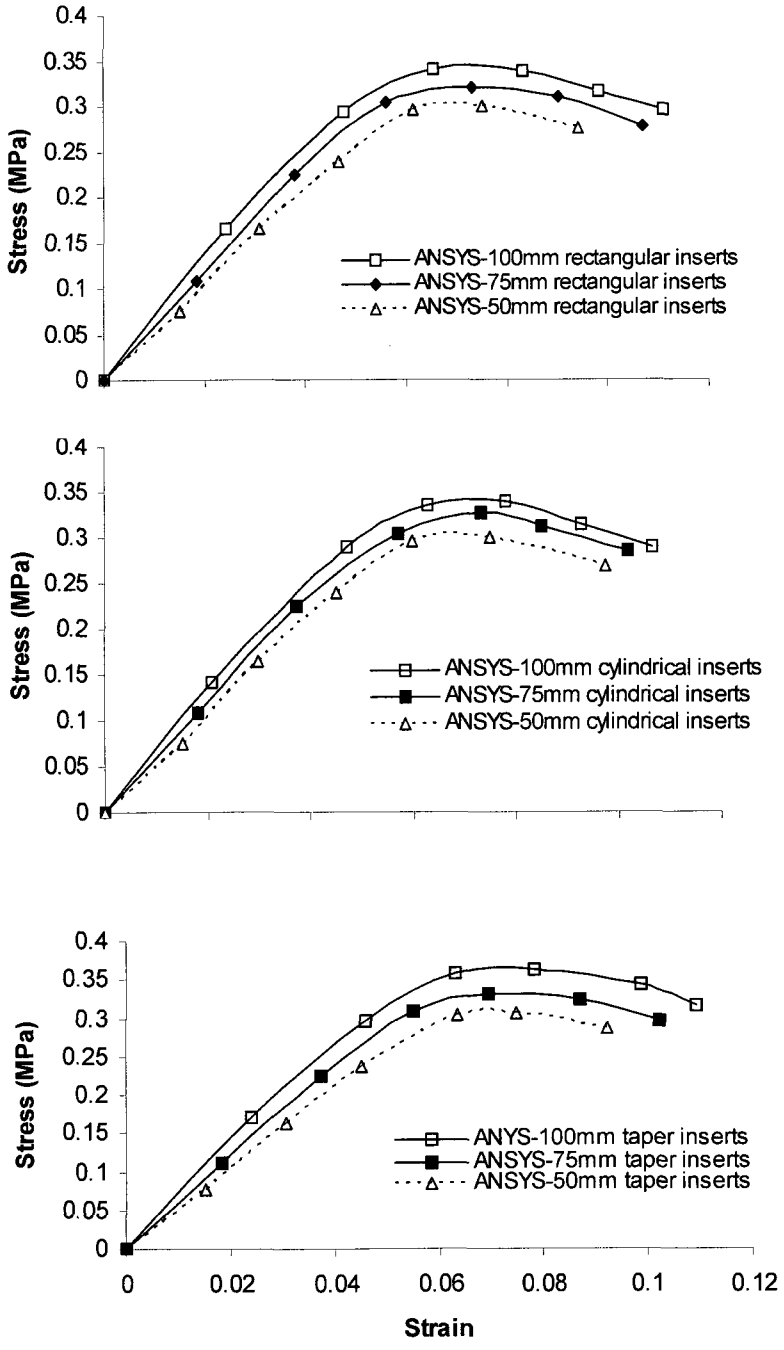

Figure 3.15: ANSYS stress strain curves for rectangular, cylindrical and taper geometries

Table 3(c): Failure stress comparison between Experimental and FE results for foam with different insert configurations

Insert	length (mm)	Failure Stress (M Pa)		Difference %
		Experimental	FE	
Rectangular	100	0.35	0.34	2.8
	75	0.33	0.32	3
	50	0.31	0.3	3.1
Cylindrical	100	0.34	0.33	2.9
	75	0.32	0.31	3.1
	50	0.29	0.3	3.4
Taper	100	0.38	0.37	2.6
	75	0.35	0.34	2.8
	50	0.33	0.32	3.0

The tabulated results show very good agreement with the loads leading to failure obtained experimentally. The maximum difference between the FE model results and the experimental ones is less than 4%, and provides a high level of confidence in the FE model approach developed. [45] has asserted that FE analysis can be used to reliably model the non-linear behavior of foam structures. In this work it is shown that FE can be also used reliably to model the highly non-linear behavior of the rigid-flexible interface between the foam and non-foam materials.

3.6 Effect of Changes in the Geometry on the Results

To study the effect of different specimen span length on the experimental and FE results, additional models were created in ANSYS. In the first foam model, the length of the original foam beam was reduced by 50 mm and in the second model, the height of the original foam beam was reduced by 20 mm. The dimensions of the new models were as follows: 350 mm × 120 mm × 50 mm and 400 mm × 120 mm×30 mm. The analyses were carried out for each of the insert length (100 mm, 75 mm, 50 mm) of the rectangular, cylindrical and taper geometries. The flexural stresses versus

strains were calculated for all cases and were plotted as shown in Figures (3.16, 3.17). It was found out from the FE analysis that for the reduced length model, the maximum fracture stress values were increased for all insert lengths as compared to the original model where as for the reduced height model, the fracture stresses were reduced as compared to the original model. This shows that the reduction in specimen length increases resistance to deformation of the foam structure and results in higher stress values, whereas the reduction in height of the foam beam causes the specimen to fail at lower stress as compared to the original model. Furthermore, for all the cases, taper inserts showed the higher values of failure stresses as compared to rectangular and cylindrical inserts. The Table 3(d) shows the comparison of results between the original model and the reduced span length and reduced height models.

Table 3(d): Comparison between the fracture load results from FE with different specimen dimensions.

Specimen dimensions L×W×H (mm^3)	Geometry	Failure Stress (MPa)		
		100 mm	75 mm	50 mm
400 × 120 × 50 (original)	Rectangular	0.34	0.32	0.3
	Cylindrical	0.32	0.31	0.28
	Taper	0.37	0.34	0.32
350 × 120 × 50	Rectangular	0.37	0.35	0.32
	Cylindrical	0.35	0.33	0.3
	Taper	0.4	0.36	0.33
400 × 120 × 30	Rectangular	0.32	0.3	0.28
	Cylindrical	0.29	0.27	0.25
	Taper	0.34	0.32	0.3

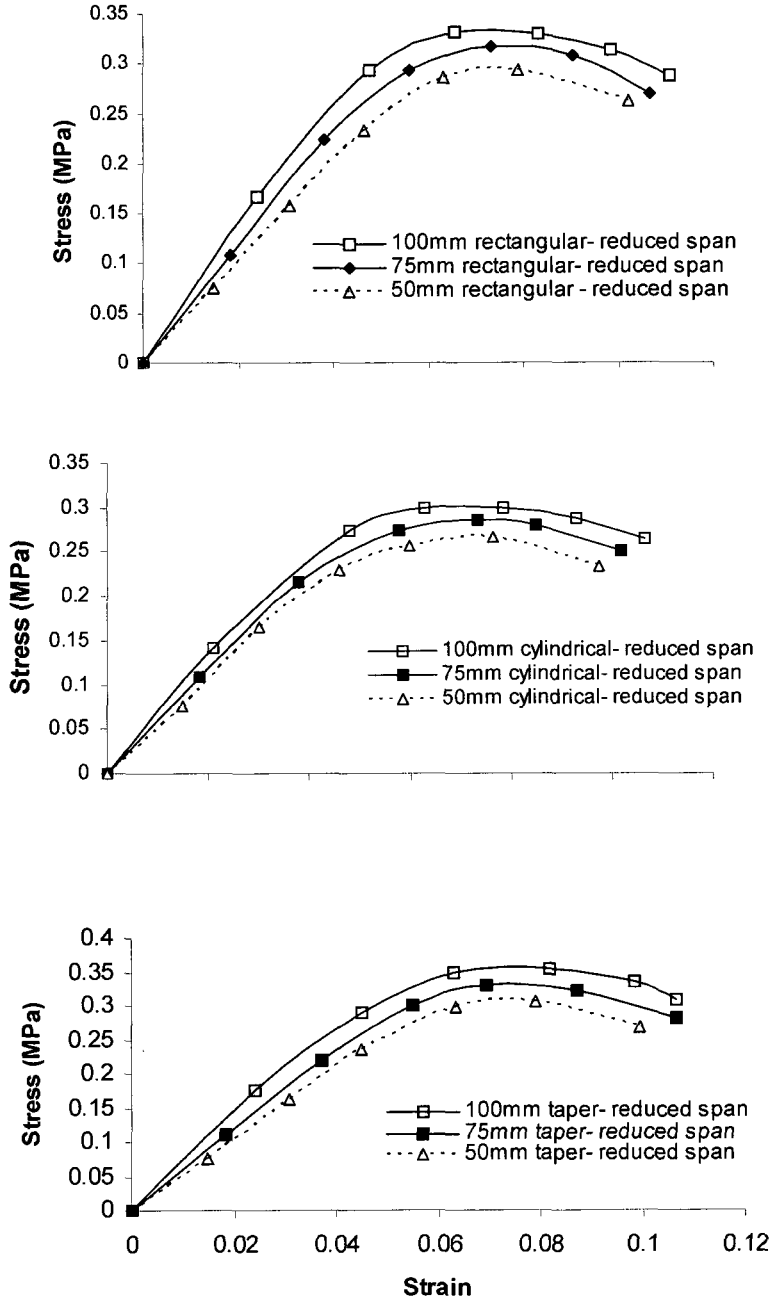

Figure 3.16: ANSYS stress strain curves for reduced span length

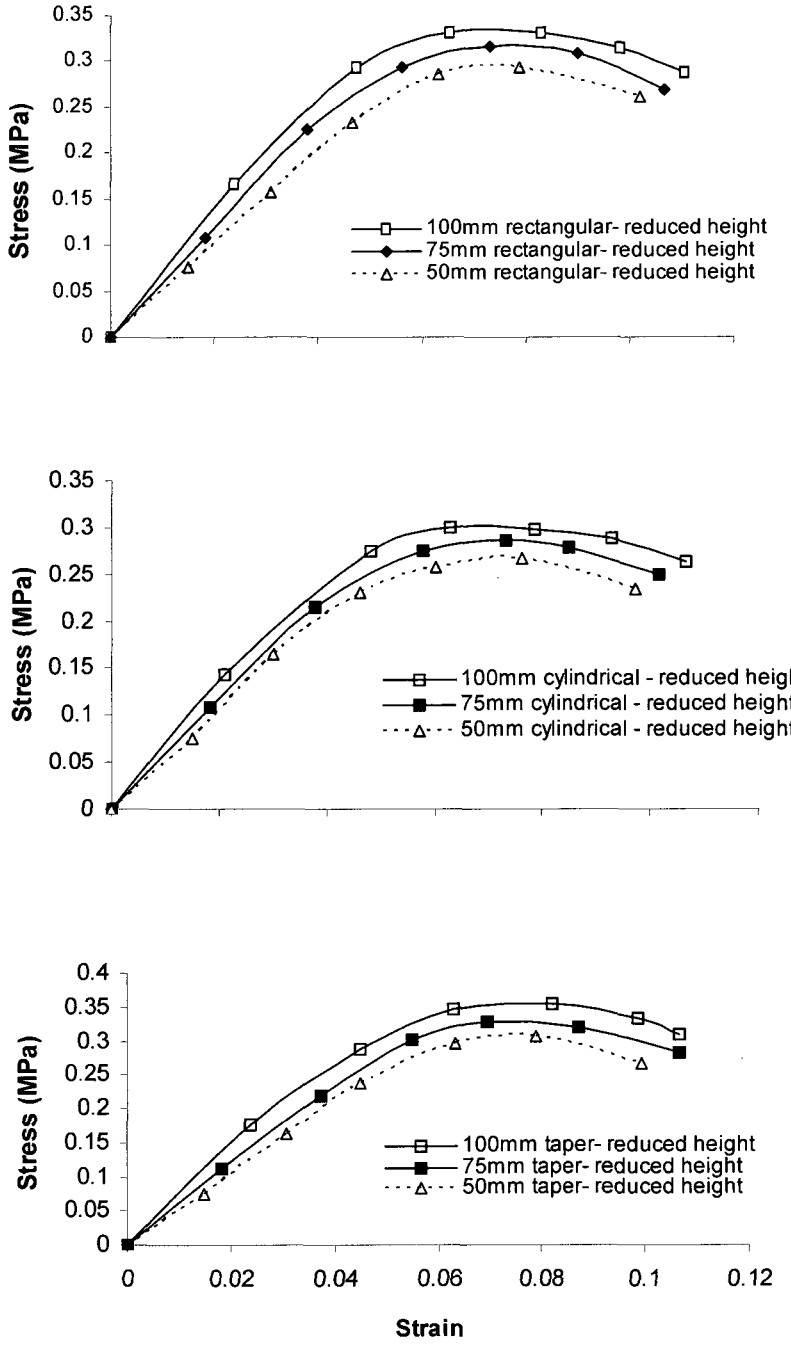

Figure 3.17: ANSYS stress strain curves for reduced height model

3.7 Summary

The modulus of elasticity and adhesion properties of foam structures in the form of slabs with inserts were studied under the flexural loading. Rectangular, cylindrical, and the wedge (tapered) inserts with different lengths were used. Experimental results were obtained and the load-deflection curves were plotted for the different combinations. The results showed that the stiffness, adhesion properties, and mode of failure were dependent on the insert embedded length. In general, longer inserts lead to higher elastic moduli. Two modes of failure were observed. For the cases of the long inserts, foam fracture was observed, while for the short inserts, de-bonding between the foam and metallic inserts occurred. Taper inserts had better load bearing properties. The study also showed the validity of the FE modeling approach used to simulate the interaction between the flexible foam slab and the rigid insert. This is of prime importance; as such a modeling technique can be used for the design of foam sandwich structures with inserts, which will be discussed in Chapter 4.

CHAPTER 4

DESIGN, FABRICATION AND TESTING OF SANDWICH COMPOSITE WITH INSERTS [2]

4.1 Introduction

This chapter focuses on characterizing the sandwich composite and metal interactions in the form of metal inserts in the composite structure. Previous research conducted focused primarily on various properties of sandwich composite using standard testing techniques such as shear, compression, fatigue and flexure, but not extensively on the adhesive properties of the sandwich metal joints. Therefore this chapter presents an effective approach for introducing metal inserts for joining the sandwich composite structures together and provides anchor points. To that end, Polyurethane (PU) was foamed to partially engulf metallic inserts of different shapes and sizes to study their effect on the adhesive properties. Once cured, flexure tests were conducted by supporting the structure through the inserts and loading the sandwich composite. The effects of adhesive properties on embedded length and shape for these composites were studied and the failure modes analyzed.

4.2 Experimental Set-up

4.2.1 Fabrication of Sandwich Composite with Inserts

In this study, the sandwich composites were manufactured by using a closed cell polyurethane foam as a core. Close cell, PU with a density of 25 kg/m^3, and threefold expansion capabilities were used. Layers of 1 mm thick plain weave S2-glass fiber matts with $[0/90/\pm45]_s$ orientation was used. Foaming was carried out inside a rectangular mold with proper provision to attach the inserts. Both mold and inserts were made of aluminum, and the mold was treated with an effective mold release compound with the help of a brush. Two fiberglass matts were affixed inside the mold before foaming.

---

[2] Reproduced from: Ahmed, A, Fahim, A and Naguib, H., July 2008, " Load Bearing Properties of Three Component Polymer Composite, ***Journal of Polymer Composites, Published online***, March 2010.

When foaming occurs, the matts were impregnated with the polyurethane to form the sandwich composite. After foaming, the specimen was left in the mold for approximately 24-48 hours to ensure dimensional stability during curing. The dimensions of the sandwich beams produced in all cases are 300 mm × 120 mm × 52 mm. Experimentally determined flexural modulus of the polyurethane core is found to be E_c = 4.5 MPa, and the manufacturer's given glass fiber modulus is E_f = 21GPa. The dimensions of the aluminum inserts are the same as given in the Table 3(a). The test specimen with rectangular and cylindrical inserts are shown in the Figure 4.1.

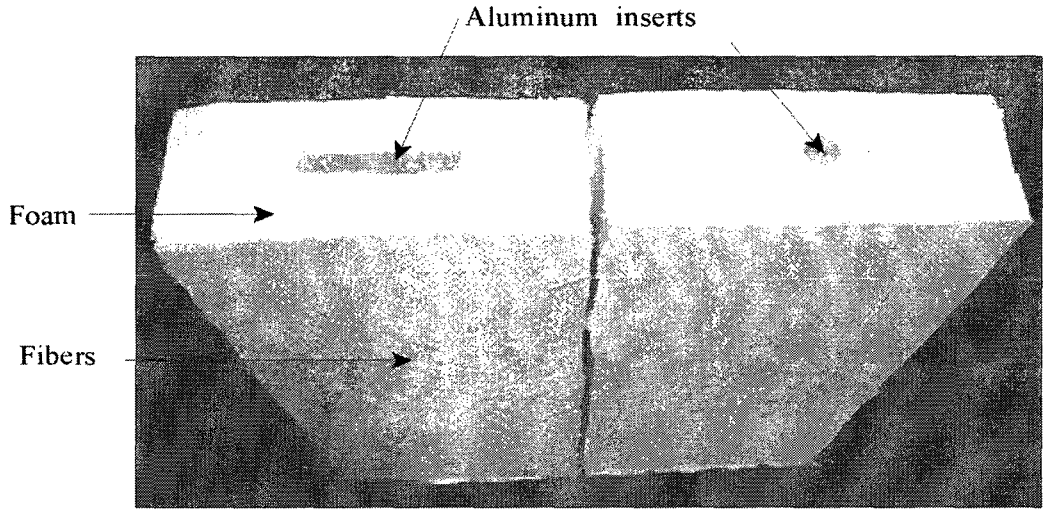

Figure 4.1: Sandwich composite with rectangular and cylindrical inserts.

4.2.2 Flexural Tests

Flexure tests on the sandwich composite were conducted in accordance with the relevant standard, the ASTM C393 (core shear properties) which outlines the bending procedure for sandwich constructions. Tests were conducted using an Instron 4482 machine with a 100 KN load cell. The load was applied at the center of the sandwich beam while being supported by the appropriate attachments screwed to the imbedded insert rested at both ends as shown schematically in the Figure 4.2. A span length of 400mm was used. All the tests were conducted at a rate of 5 mm/min, and the load deflection points calculated using a PC. A total of five tests per insert length was conducted as per the ASTM standard. Average data from the tests was used to plot the stress strain curves. After the final failure,

the maximum load was recorded and photographs were taken to document the final state of each specimen. In order to avoid crushing of the sandwich composite structure underneath the point of application of the load, the load was applied along the whole width of the sandwich structure.

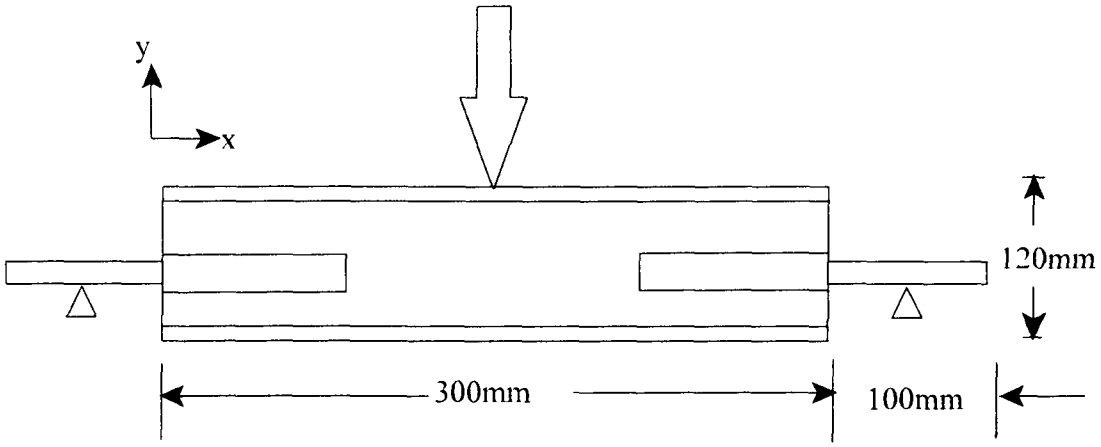

Figure 4.2: Bending set-up for the sandwich composite

For sandwich beams, the bending stress σ_f , in the face sheets [25]:

$$\sigma_f = \frac{M}{D} E_f \left(\frac{c+f}{2}\right) \tag{4.1}$$

$$D = E_f \frac{bf^3}{6} + E_f \frac{b f s^2}{2} + E_C \frac{b c^3}{12} \tag{4.2}$$

Where M is the bending moment, D is the flexural stiffness of facing, f is thickness of the facing, c is the core thickness, b is the width of the beam, and s is the distance between the centers of two faces.

The shear stress in core, τ_c is given by [25]:

$$\tau_c = \frac{V}{D}\left(E_f \frac{f s}{2} + E_C \frac{c^2}{8}\right) \tag{4.3}$$

Where V is the shear load, E_f and E_c are the flexural moduli of facing and core.

The axial strain ε_x in the facing is given by [57]:

$$\varepsilon_x = \frac{M}{E_f I_f + E_C I_C} y \tag{4.4}$$

Where M is the bending moment, I_c and I_f are the moments of inertia of the core and the facing, and y is the distance from the centroidal axis of the sandwich structure to the facing axis.

The shear strain γ_c in the core is given by [57]:

$$\gamma_c = \frac{V}{G_C b c} \tag{4.5}$$

Where G_C is the shear modulus of core.

4.3 Results and Discussion

4.3.1 Rectangular Inserts

Results obtained from the flexure tests with inserts that are rectangular, cylindrical, and the wedge (taper) in shape, and with lengths of 100 mm, 75 mm and 50 mm are presented below:

Experimental flexure test results of the sandwich composite with three different lengths of the rectangular inserts are presented in the Table 4(a).

Table 4(a): Fiber stress comparison between the experimental and FE results for the sandwich composite with different insert configurations.

Insert	length (mm)	Fiber Stress (M Pa)		Difference
		Experimental	FEA	%
Rectangular	100	1.82	1.8	1.1
	75	1.67	1.64	1.7
	50	1.53	1.51	1.3
Cylindrical	100	1.61	1.65	-2.4
	75	1.53	1.56	-2
	50	1.49	1.46	2
Taper	100	2.01	1.98	1.5
	75	1.83	1.8	1.6
	50	1.72	1.76	-2.3

Results from the bending test for the rectangular inserts with 100 mm, 75 mm and 50 mm length showed that the adhesion failure occurred in the foam core only. No failure in the facing was observed. Since the flexural modulus of the glass fiber facing was very high and its thickness very small as compared to the PU core, therefore the linear stress and strain variation through the facing thickness were documented with the neutral axis through the centroid of the cross section, similar to that reported in [27]. Typical sandwich composite facing stress and strain were calculated based on the Equations (4.1-2, 4.4) and plotted as shown in the Figure 4.3. The typical non-linear shear stress and strains were plotted for a sandwich composite structure with rectangular inserts and are shown in the Figure 4.4. The only acceptable mode of failure is the foam core shear as per the relevant test method ASTM C393, hence the facing stresses were calculated only as the reference values until maximum applied loads and did not represent the ultimate strength.

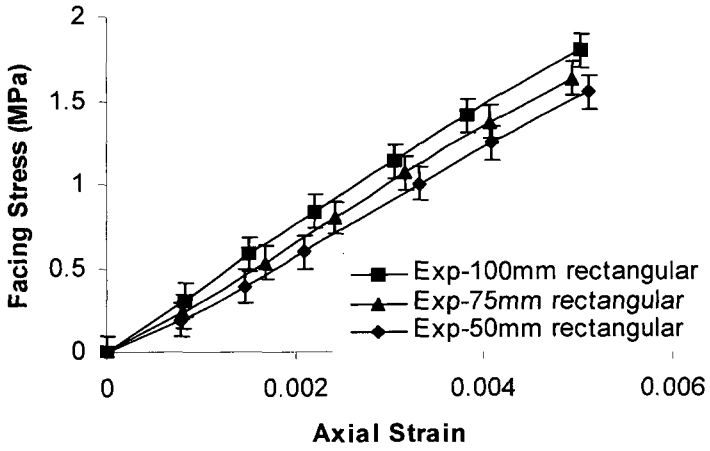

Figure 4.3: Axial stress strain curves for sandwich with rectangular inserts

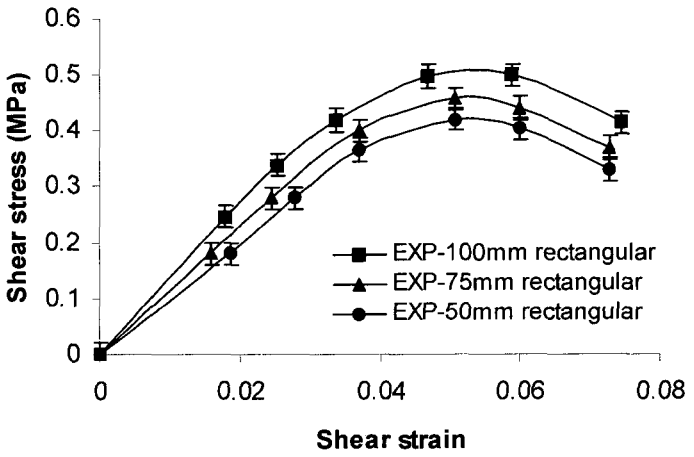

Figure 4.4: Shear stress strain for sandwich with rectangular inserts.

Since the sandwich core was in shear due to the flexural loading, adhesion failure occurred between the foam core and the insert resulting in the slip of the insert from the sandwich composite structure. This failure was also due to the core lower stiffness as compared to the fiber glass facing. It was also noted that the length of the insert is directly related to the failure load of the sandwich

composite structure. Typical shear stress strain values were calculated and are shown in the Figure 4.4. Shear (stretching loads) at the bottom surface of the rectangular insert due to its distance from the neutral axis and coupled with the higher stress concentration effect at the innermost corner of the rectangular insert initiated de-bonding failure. No failure in the facing was observed in any of the tests. This indicates that the bond between the impregnated fiber facings and the polymer core was sufficient for the application. The Figure 4.5 shows rectangular insert failure in the sandwich composite.

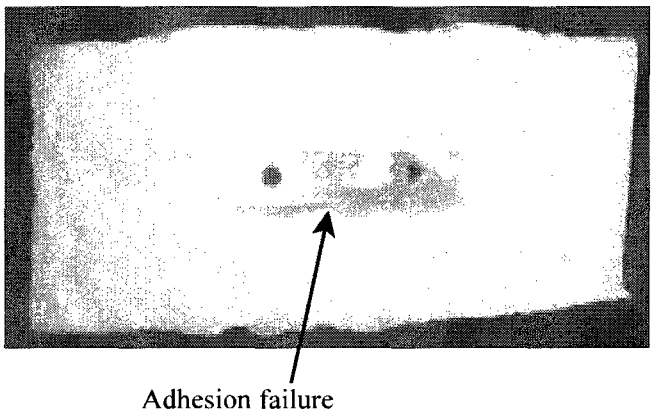

Figure 4.5: Adhesion failure for a rectangular insert.

4.3.2 Cylindrical Inserts

The second run of tests was conducted on the sandwich composite with the cylindrical inserts

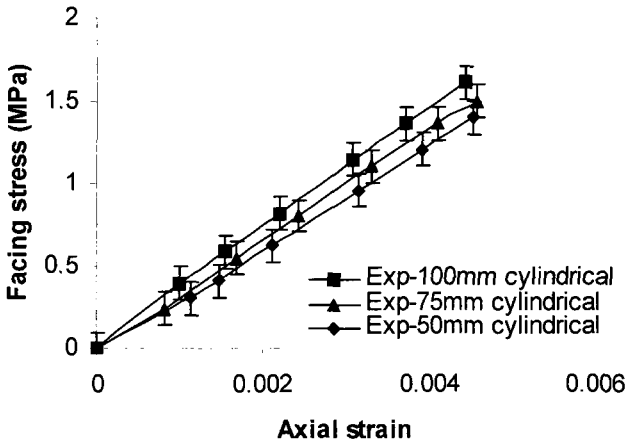

Figure 4.6: Axial stress strain curves for cylindrical inserts

and the same three different lengths (100 mm, 75 mm, 50 mm). No tensile or compressive failure occurred in the fiber facings and the structural integrity of the sandwich structure was preserved. The facing stress strain curves obtained from these tests are shown in the Figure 4.6. For the sandwich core, de-bonding and slippage occurred between the sandwich core and the insert. Representative shear stress strain curves are shown in the Figure 4.7. Again here, a direct relationship between the length of the insert and the load to failure was observed. Since the load-bearing area of the cylindrical inserts is smaller than that of the rectangular inserts, the load magnitudes that resulted in de-bonding failure are smaller than those for the rectangular inserts. The Figure 4.8 shows cylindrical insert failure in the sandwich core.

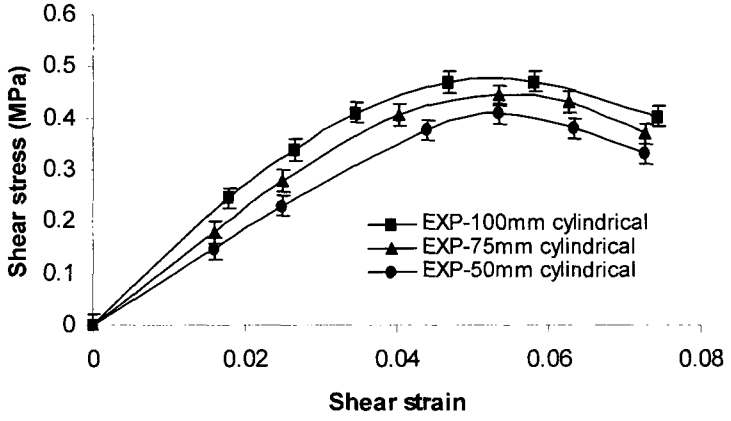

Figure 4.7: Shear stress strain for sandwich with cylindrical inserts

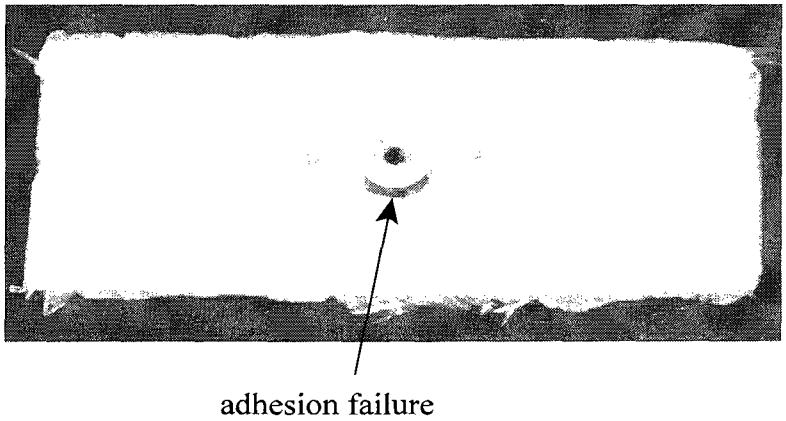

Figure 4.8: Adhesion failure in the sandwich composite

4.3.3 Taper Inserts

Experimental results of the sandwich composite with the three different lengths of taper inserts

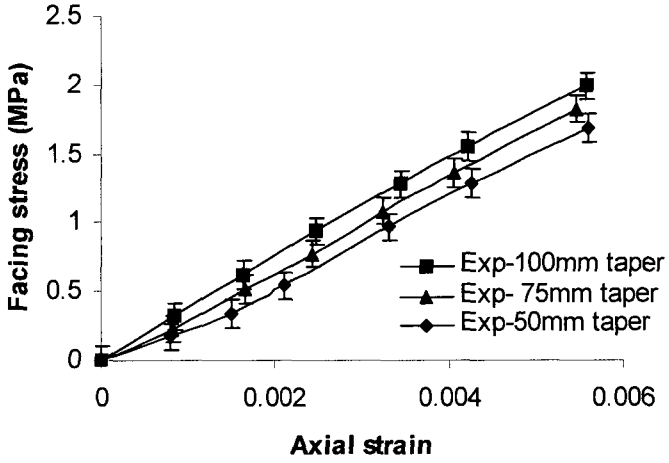

Figure 4.9: Facing stress strain for sandwich with taper inserts

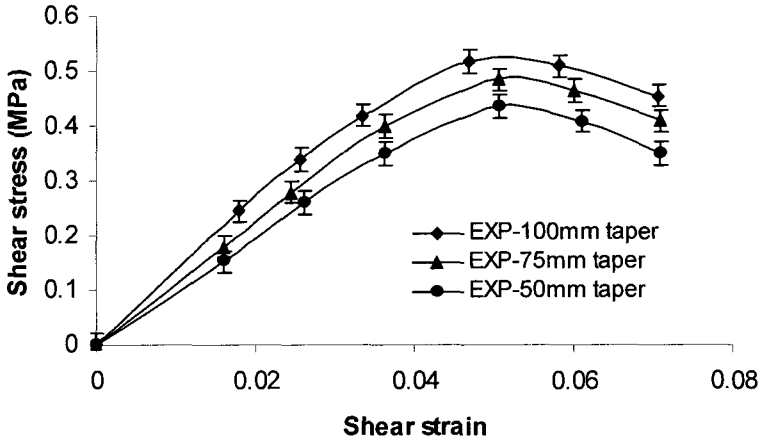

Figure 4.10: Shear stress strain curves for taper inserts in sandwich

were obtained. Again here, the integrity of the structure was preserved. Facing stress-strain traces obtained from these tests are shown in the Figure 4.9. Again, for the case of taper inserts, a direct relationship between the length of the insert and the load to failure was observed. The failure was again

due to the de-bonding between the core and insert. Typical shear stress strain curves for the sandwich cores are shown in the Figure 4.10. Furthermore, the failure stress values for the case of taper inserts were higher than those for the rectangular and the cylindrical geometries. This can be explained by the fact that the force at the tip of the wedge is very small due to its proximity to the neutral axis, and hence the effect of the stress concentration at the tip did not promote early de-bonding failure as in the case of the rectangular insert. The Table 4(b) shows comparison for different results.

Table 4(b): Shear stress comparison between the experimental and FE results for sandwich structure with different insert configurations.

Insert	length (mm)	Shear Stress (M Pa)		Difference %
		Experimental	FE	
Rectangular	100	0.49	0.48	2.0
	75	0.45	0.44	2.2
	50	0.42	0.41	2.3
Cylindrical	100	0.46	0.45	2.1
	75	0.43	0.44	-2.3
	50	0.4	0.41	-2.5
Taper	100	0.52	0.51	1.9
	75	0.48	0.47	2.0
	50	0.44	0.43	2.2

4.4 Stiffness Modeling of Sandwich Composite

In order to investigate the effect of the failure length on the stiffness of sandwich composite, a model was studied based on the laminate arrangement [49-50]. In the investigated model, a cross ply laminate was subjected to axial force to predict failure and reduction in stiffness in the layer. In this model, since the stiffness of the longitudinal 0^0 layers was greater as compared to the transverse 90^o layer, therefore the failure occurs in the transverse layer. As shown above experimentally, if the

sandwich composite with inserts is subjected to the bending loads, the weaker core fails in shear while the stiffer facing material remains intact. This indicates that in the studied model and the current experimental model, fracture occurs in the layer which has less resistance to deformation or lower stiffness. For the experimental model, the foam core represents the weak layer whereas the transverse layer of the studied model represented the weak layer.

In most cases, failure in the laminate is initiated in the layer with the highest stress perpendicular to the fibers. Failure initiation takes the form of distributed micro cracks which coalesce into macro cracks. This cracking results in the stiffness reduction of the ply as well as the laminate eventually causing failure of laminate.

An analytical method has been presented in [50] for predicting the stiffness degradation as a function of damage. In the method, solution for stress distribution, crack size and reduced stiffness for damaged layers and the entire laminate was expressed as a function of applied load stresses on the layers, properties of layers and residual stresses. The reduced axial modulus of a cross ply laminate in terms of modulus reduction ratio [50].

$$\rho_E = \frac{\overline{E'_X}}{\overline{E_X}} = \left[1 + \frac{2E_2 h_2}{\alpha l E_1 h_1} \tanh\frac{\alpha l}{2} + \frac{\sigma_{r1}}{\sigma_{r2}} \frac{\overline{E_X}}{E_1} \left(1 - \frac{2}{\alpha l} \tanh\frac{\alpha l}{2} \right) \right]^{-1} \tag{4.6}$$

Where $\overline{E_X}$, $\overline{E'_X}$ are the initial and reduced moduli of the laminate, l is the crack length, and σ_x, σ_r are the tensile and residual stresses of the cross ply laminate.

The factor α is given by:

$$\alpha^2 = \frac{3(h_1 + h_2)\overline{E_X}}{h_1 h_2 E_1 E_2} \times \frac{G_{12} G_{23}}{h_1 G_{23} + h_2 G_{12}} \tag{4.7}$$

Where h_1, h_2 are the heights for the longitudinal and transverse layers, and G_{12}, G_{23} are the in plane and out of plane shear moduli of the laminate.

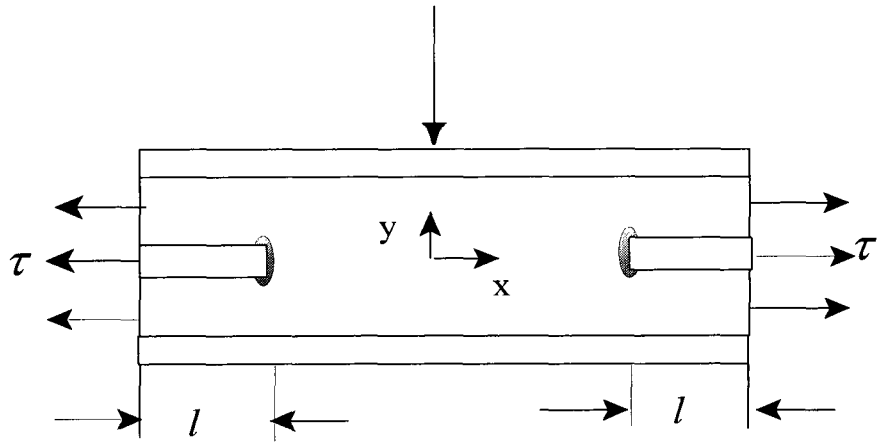

Figure 4.11: Estimation of stiffness reduction for sandwich

In order to establish an analogy between the failure mechanism of the experimental sandwich composites as shown in the Figure 4.11., and the laminate, the longitudinal layers of laminate were modeled as the facings of the sandwich structure and a transverse layer was considered as the sandwich core. As the foam core is considered to be isotropic, therefore: $E_1 = E_2 = E$ and $G_{12} = G_{23} = G$.

Rewriting the Equations 4.6 and 4.7 for the sandwich composite in terms of E and G, the modified factor α is given as:

$$\alpha = \sqrt{\frac{3(h_1 + h_2)\overline{E_X}}{h_1 h_2 E^2} \times \frac{G}{(h_1 + h_2)}} \tag{4.8}$$

Based on the core shear failure, the modified equation for the reduced modulus of the sandwich composite in terms of the modulus reduction ratio:

$$\rho_E = \frac{\overline{E'_X}}{\overline{E_X}} = \left[1 + \frac{2}{\alpha l} E \frac{h_2}{h_1} \tanh\frac{\alpha l}{2} + \frac{\sigma_{r1}}{\tau}\frac{\overline{E_X}}{E}\left(1 - \frac{2}{\alpha l}\tan\frac{\alpha l}{2}\right)\right]^{-1} \tag{4.9}$$

The Equations 4.8 and 4.9 were used to calculate the reduced modulus of the sandwich composite with inserts. Th experimental data for flexural and shear modulus were used. Insert failure length *l* was calculated from a sliced experimental fractured sample. It was observed as the damage of structure progressed, the stiffness of the sandwich core as well as that of the entire sandwich composite structure was reduced. Curves were plotted for the sandwich composites with rectangular, cylindrical and taper inserts. Typical trend curves for all the geometries are shown in the Figure 4.12. All curves predict progressive sandwich stiffness reduction as a function of the crack length. The trend of plotted curves shows better agreement with reference [50] where the plot was shown for the cross ply laminates.

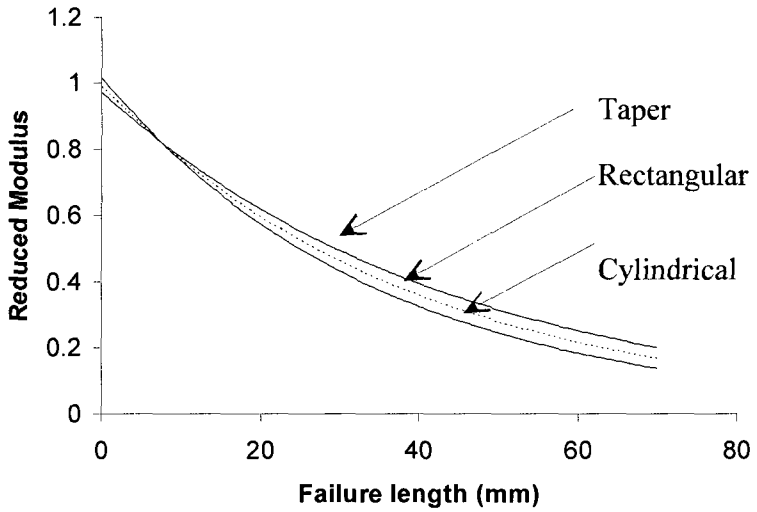

Figure 4.12: Stiffness reduction as a function of failure length

4.5 Finite Element Analysis of the Sandwich Composite

Sandwich models matching the experimental specimen were developed in ANSYS 11. One element is used to model each layer, i.e., 3 layers through the thickness. Because of the symmetry along the length, only half of the beam was modeled with appropriate boundary conditions imposed. An eight-node plane 82 element was selected due to its proven better results for sandwich composite modeling [43]. Plane 82 is a higher order 2D element. It provides more accurate results for mixed (quadrilateral-triangular) automatic meshes and can tolerate irregular shapes easily. The 8-node elements have compatible displacement shapes and are well suited to model curved boundaries. The

8-node element is defined by eight nodes having two degrees of freedom at each node, translations in the nodal x and y directions. This element also has options for the plane stress and plane strain conditions. Due to these options, the 2D element practically behaves as a 3D element, because it takes into account the third dimension and eventually calculates all the nodal element stresses and displacements of a 3D model with much geometrically simpler model and fewer boundary conditions. For the current model, the plane strain condition was used.

Modulus properties of the PU were obtained from the experimental results and are shown in the Table 3(b). For the fiber glass, manufacturers' provided properties were used. Finally for the aluminum, standard documented properties were used. Rigid flexible contact scenarios between the metal inserts and a sandwich foam core were used. Contact between the metal and foam was modeled by the compatible elements (TARGET 169 and CONTACT 172). Since the sandwich model involved three different materials, glass fiber, aluminum and PU, therefore both geometric and material non-linearities were considered. For geometric non-linearity, which was based on the concept that if a structure experiences large deformation, its changing geometric configuration can cause the structure to respond non-linearly. For this non-linearity, the large strain analysis option was used for running the simulation. This option accounts for stiffness changes that result from changes in an element's shape and orientation. It places no theoretical limit on the total rotation or strain experienced by the element. In order to account for the material non-linearity, the automatic time stepping option was used. This option responds to plasticity by reducing the load step after a load step in which a larger plastic strain increment was encountered. If too large a step was taken, the program will bisect and resolve to use a smaller step size.

To observe the failure pattern of inserts of rectangular, cylindrical and taper geometries inside the sandwich composite, simulations were run in ANSYS. Facing bending stress σ_{xx} and the foam core shear stress τ_{xy} were plotted with respect to the relevant axial strain ε_{xx} and shear strain γ_{xy}. The Figure 4.13 shows ANSYS facing stresses for sandwich composite whereas the shear stresses graphs from ANSYS are shown in the Figure 4.14. The figures exhibit that for different insert lengths, shape of the ANSYS stress -strain curves and the magnitude coincided with those obtained experimentally. Taper inserts showed the highest failure stress value as compared to rectangular and cylindrical inserts, a trend that is similar to the experimental results.

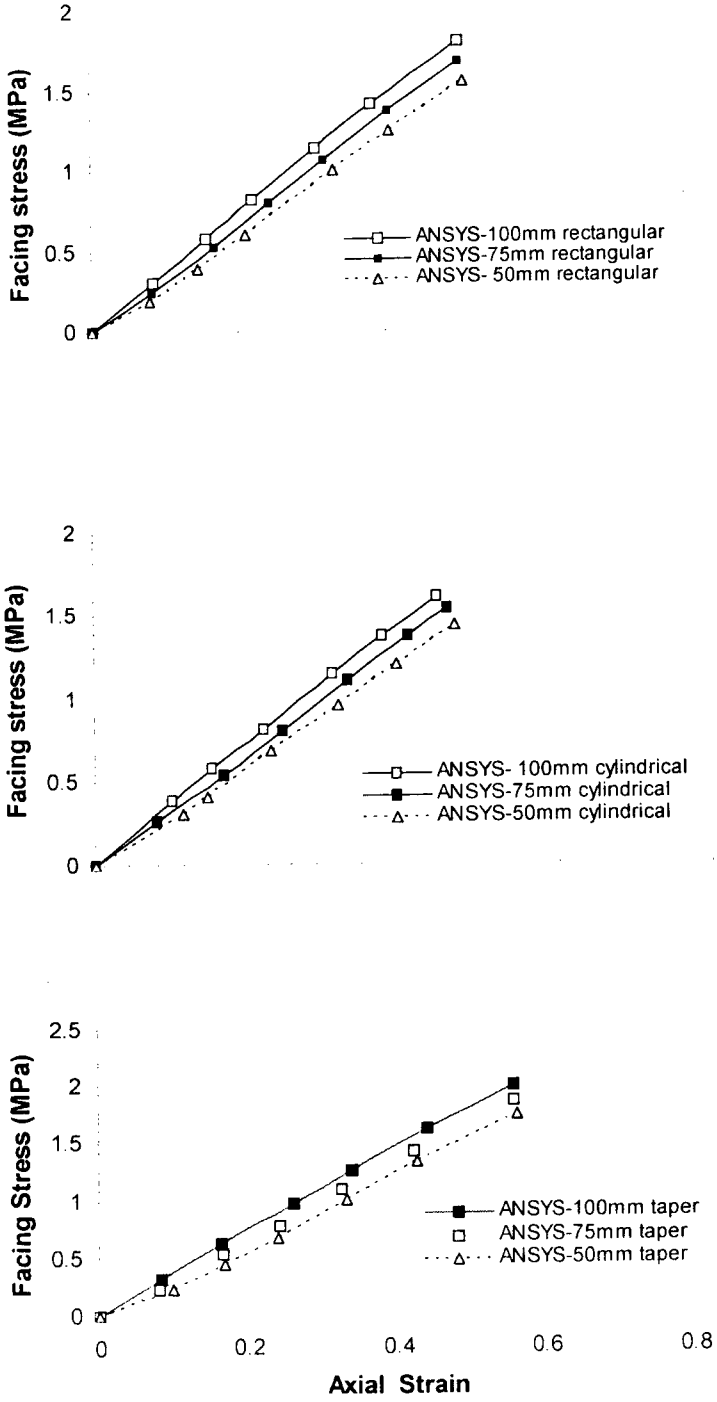

Figure 4.13: ANSYS-Facing stress strain curves for all geometries

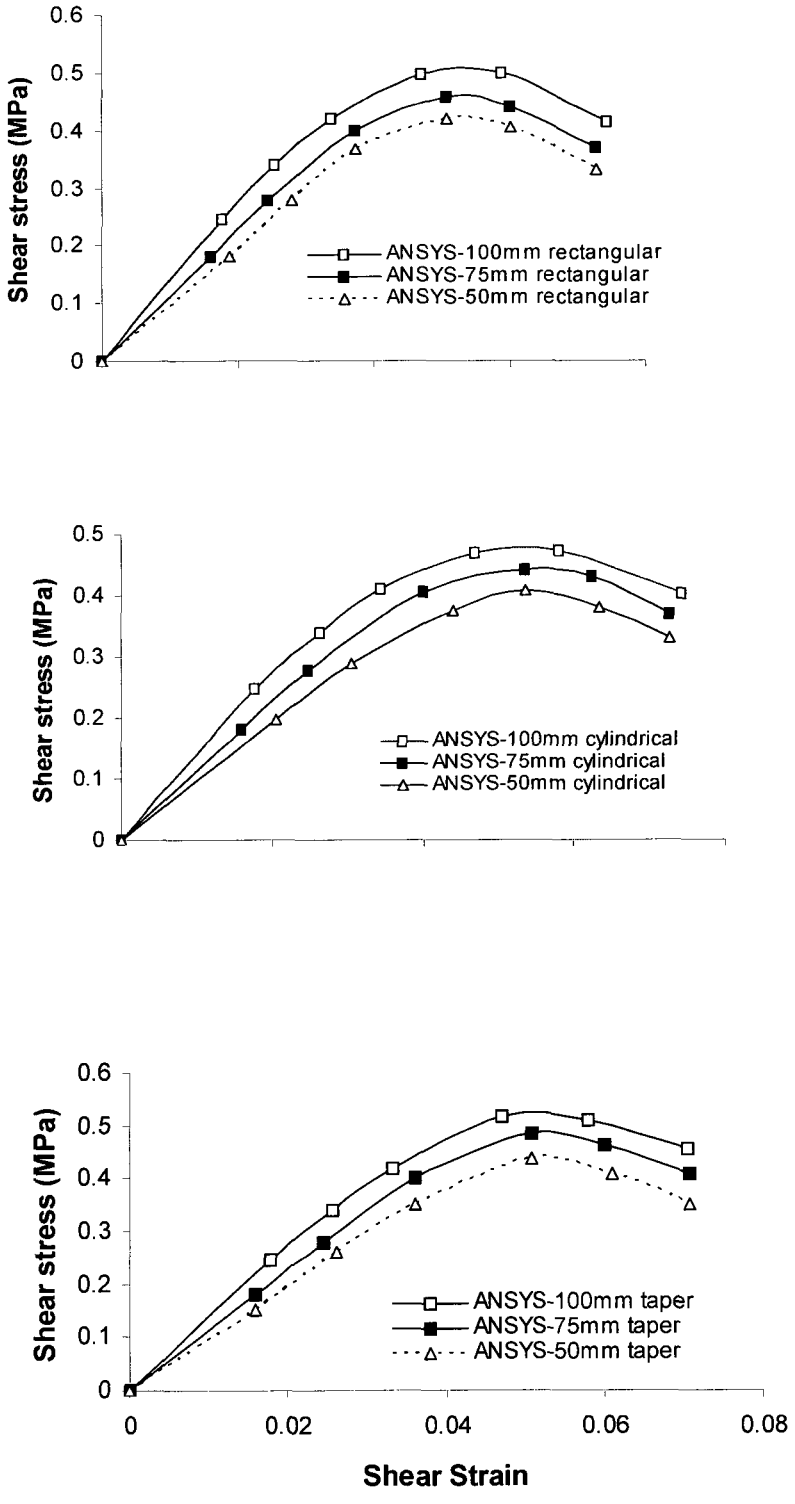

Figure 4.14: ANSYS-Shear stress strain curves for all geometries

4.6 Summary

Adhesion properties of inserts in sandwich composites were studied under flexural loading. Rectangular, cylindrical and (wedge) taper inserts with different lengths were used. Experimental results were obtained and stress-strain curves were plotted for the different combinations. The results showed that the failure stress and the adhesion properties were dependent on the insert embedded length. Failure model to estimate sandwich stiffness was presented. It was shown that the mathematical relations for cross ply laminate failure under an axial load can be used for the sandwich composite with proper assumptions. Results show the reduction in stiffness as a function of failure length. The study also showed the validity of the FE modeling approach used to simulate the interaction between the flexible sandwich and rigid insert. This is of prime importance, as such a modeling technique can be used for the design of sandwich composite. A novel design of a leaf insert inside foam and sandwich composite will be discussed in Chapter 5.

CHAPTER 5

DESIGN, FABRICATION AND TESTING OF FOAM AND SANDWICH COMPOSITE WITH LEAF INSERTS [3]

5.1 Introduction

The present chapter focuses on developing an effective approach for introducing leaf inserts (modified design of taper inserts) for joining and providing anchor points for the foam structures and sandwich composites. To that end, Polyurethane (PU) was foamed to partially engulf metallic leaf inserts of different length in order to study their effect on strength and load carrying capacity.

5.2 Leaf Insert Design and Fabrication

The results in the previous two chapters showed that the taper inserts performed consistently better than the other geometries. Therefore leaf inserts were designed and manufactured. Leaf inserts (modified taper inserts) were manufactured by providing a gradual taper to the shape that ends in as small a thickness as practically possible as shown in the Figure 5.1. Foam structures and

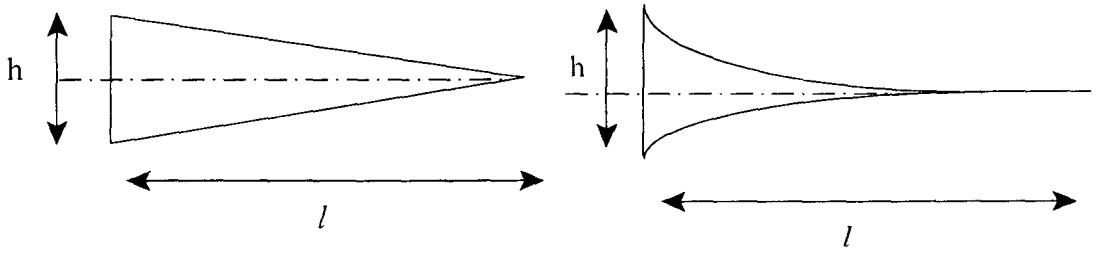

Figure 5.1: Schematic showing the taper and leaf inserts of dimensions: *h=9 - 0.5mm, l=100mm, 75mm, 50mm, w = 50mm.*

[3] Reproduced from: Ahmed, A, Fahim, A and Naguib, H., " Design of New Hybrid Composites Using Metal Embedded in Polymer Foam and Foam Composite. *Journal of Composite Materials,* Volume 43,No.15,July 2009.

foam/fiberglass-clad sandwich composite structures with both tapered and leaf inserts were manufactured for testing purpose. Both types of structures were manufactured from the polyurethane foam with density of 25 kg/m^3, and threefold expansion capabilities. Foaming was carried out inside a rectangular mold with proper provision to attach the inserts. Both the mold and inserts were made of aluminum, however, the mold was treated with an effective mold release compound. In the case of the foam/fiberglass clad sandwich structures, two rectangular fiberglass matts with an approximate thickness of 1 mm were affixed inside the mold before foaming. When foaming occurs, the matts are impregnated with the polyurethane polymer to form the composite cladding. After foaming, the specimen was left in the mold for approximately 24-48 hours to ensure dimensional stability during curing. The dimensions of the sandwich composite structures manufactured in all cases are 300 mm × 120 mm × 52 mm as shown in the Figure 5.2.

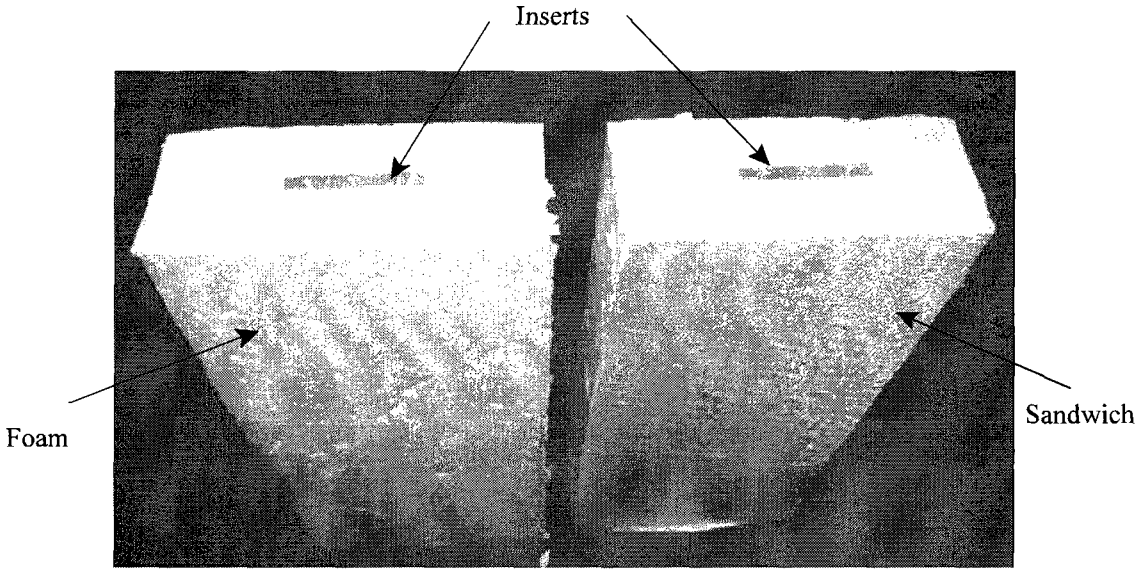

Figure 5.2:Foam and sandwich composite with leaf inserts

Flexure tests on the foam structures were conducted in accordance with the ASTM D790 which outlines the standard flexural testing procedure for plastics. Flexure tests on the foam/fiberglass clad sandwich structures were conducted in accordance with the ASTM C393 which outlines the standard bending testing procedure for sandwich composite. All the tests were conducted at room temperature

on an Instron 4482. The load was applied through the testing machine cross head to the center of the specimen while it was supported by two attachments screwed to the embedded inserts. A slow cross head speed of 5 mm/min was used for all the tests and the load-deflection data were recorded using the Instron data logger. After the final failure, the maximum load was recorded and photographs were taken to document the final state of each specimen. Total of five tests per insert length were conducted as per ASTM standard.

5.3 Results and Discussions

5.3.1 Failure of the Foam Structures with Taper and Leaf inserts

The Figure 5.3 shows the stress-strain plots obtained from the bending tests on the foam structures with leaf inserts respectively. Data for the three lengths of inserts are presented in the figures. The spread of the magnitude of the stress at selected strain values and the average of that stress are indicated on the graphs. A smoothed curve is drawn to join the average stress values.

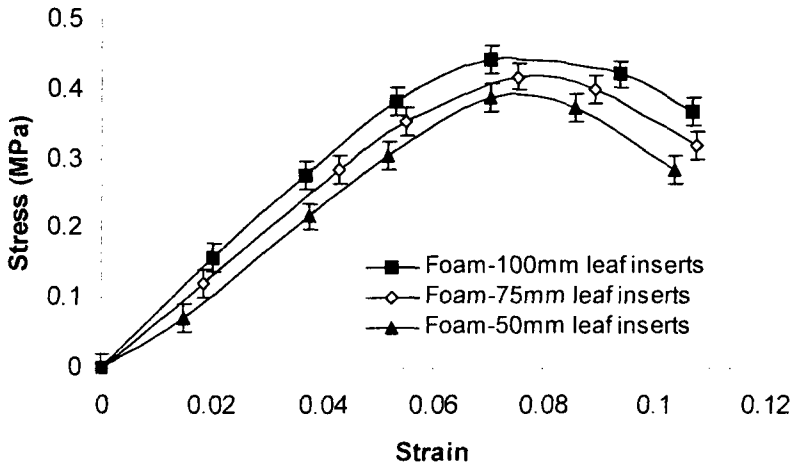

Figure 5.3: Bending stress strain curves for foam with leaf inserts

The average stress strain curves of the Figures 3.10 and 5.3 are plotted in the Figure 5.4 so as to compare the performance of the two insert shapes. The figure shows that for each length, the leaf

inserts perform better than the corresponding taper insert. The Table 5(a) also shows that leaf inserts have consistently higher failure stresses than taper inserts for comparable lengths. The surface areas of the two inserts are very close, therefore the bonding strength for the two cases is close. However the leaf insert tip tapers to a thin edge and is very close to the neutral axis of the slab where the stress is negligible, and hence less prone to result in the initiation of a crack and to propagate if one exists.

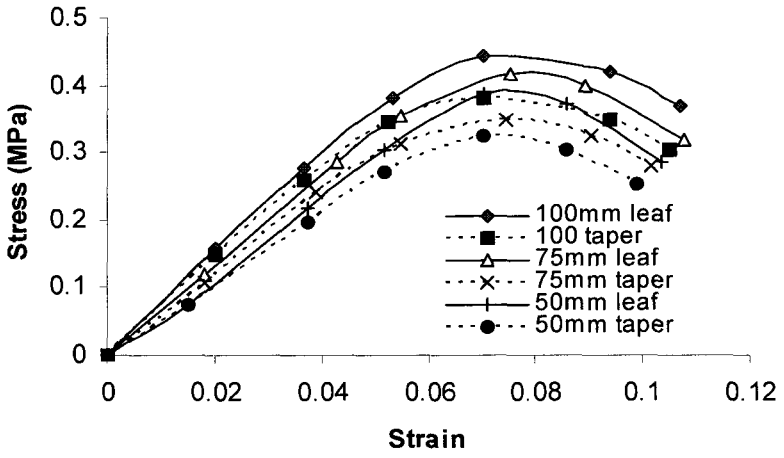

Figure 5.4: Bending stress strain curves for foams with leaf and taper inserts

Table 5(a): Compilation of the failure stresses for the different lengths of taper and leaf inserts

Insert	length (mm)	Failure Stress		Difference %
		Experimental	FE	
Taper	100	0.38	0.37	2.6
	75	0.35	0.34	2.8
	50	0.33	0.32	3.1
Leaf	100	0.43	0.42	2.3
	75	0.4	0.39	2.5
	50	0.38	0.38	2.5

Two modes of failure were observed during the tests. The first was observed for all the cases of the 100 mm and 75 mm inserts for both the taper and the leaf inserts the failure, and was due to the fracture of the foam slab. This is attributed to the fact that the strength of the bond between the foam and the aluminum inserts is higher than the fracture stress of the foam beam. Examination of the nature of the fracture revealed that the foam experience small plastic deformation and the nature of the fracture is ductile. The crack was initiated at the tension side of the slab and propagated along the cross section resulting in complete failure. The second mode of failure was observed in the case of the 50 mm taper and leaf inserts and was due to insert the pullout. This was primarily due to the low bonding strength resulting from the short insert length. The bond strength in this case was less than the fracture strength of the foam. The Figure 5.5 shows a photograph of this type of failure.

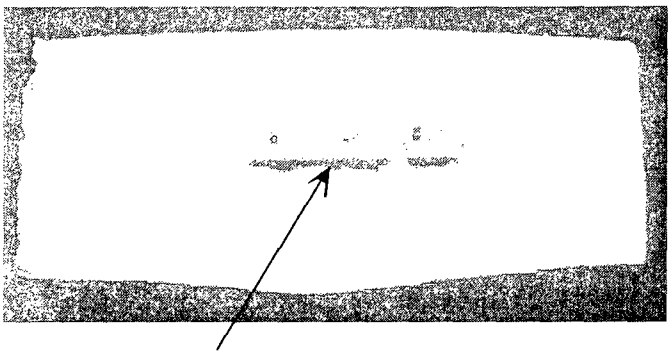

Figure 5.5: Adhesion failure of 50mm leaf insert

5.3.2 Failure of the Sandwich Composite with Taper and Leaf inserts

Results from the bending test results of leaf inserts with 100mm, 75mm and 50mm inserts showed that the adhesion failure occurred in the foam core only. No failure in the facing was observed. Since the flexural modulus of the glass fiber facing was very high and its thickness very small as compared to the PU core, therefore linear stress and strain variation through the facing thickness were documented [27]. Typical sandwich composite facing stress and strain were calculated and plotted as shown in the Figure 5.6. The values of the failure stresses for the tests are given in the Table 5(b).

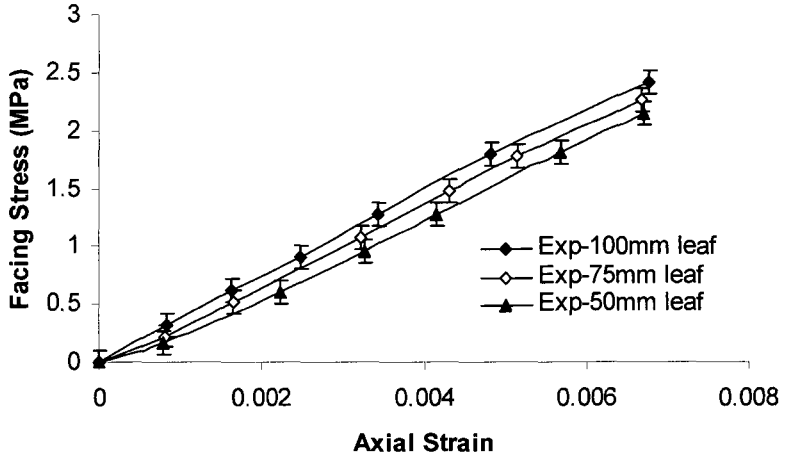

Figure 5.6: Facing stress strain curves for leaf inserts

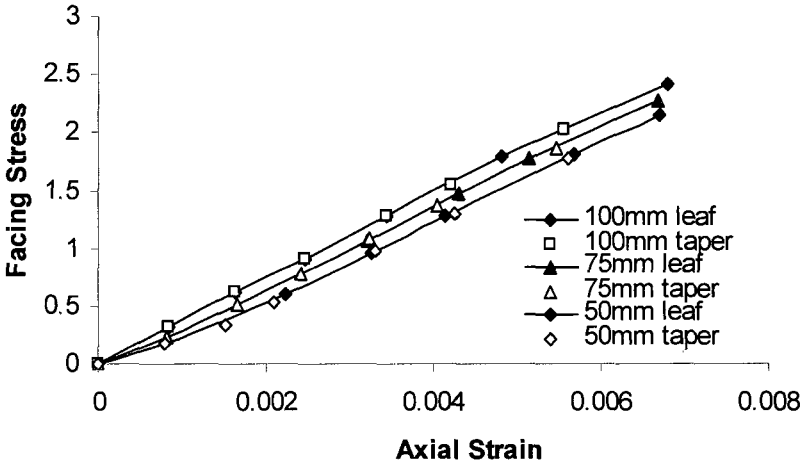

Figure 5.7:Comparison between axial stresses for leaf and taper inserts

The average facing stress strain curves of the Figures 4.9 and 5.6 are plotted in the Figure 5.7 so as to compare the performance of the two insert shapes. The figure shows that for each length the leaf inserts perform better than the corresponding taper insert. Since the sandwich core was in shear due to flexural loading, adhesion failure occurred between the foam core and the insert resulting in the slip of the insert from the sandwich composite. This failure was also due to core smaller stiffness/strength than the fiber glass facing. It was also noted that the length of the insert is directly

related to failure loads of the sandwich structure. Typical shear stress strain were calculated from the Equations 4.1 and 4.2 for the sandwich composite with leaf inserts and are shown in the Figure 5.8. It should be noted that the debonding of the inserts occurs at the root of the insert rather than at the tip as it can be seen in the Figure 5.5. This can be explained by the fact that the tensile force at the tip of the wedge is very small due to its proximity to the neutral axis, and hence the effect of the stress concentration at the tip did not promote early debonding failure. It is also worth mentioning that the integrity of the structure was preserved. No failure in the facings was observed in any of the tests, thus indicating that the bond between the impregnated fiber facing clad and the foam is sufficient for the application.

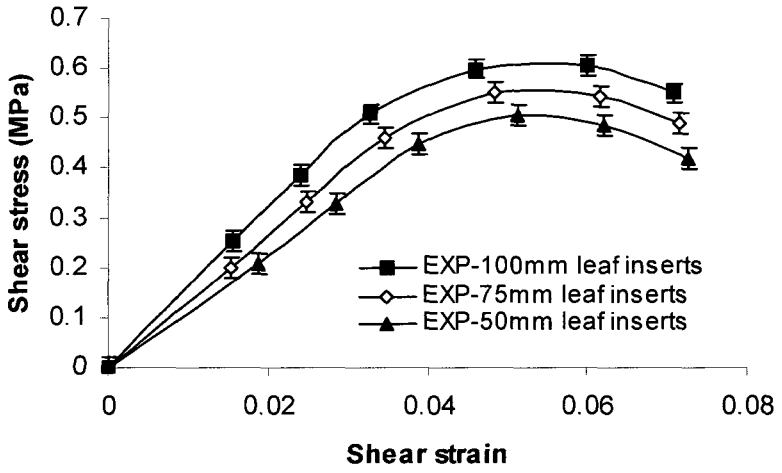

Figure 5.8: Shear stress strain curves for sandwich with leaf inserts

The average shear stress strain curves of the Figures 4.10 and 5.8 are plotted in the Figure 5.9 so as to compare the performance of the two insert shapes. The figure shows that for each length the leaf inserts perform better than the corresponding taper insert. The Table 5(a) also shows that leaf inserts have consistently higher failure stresses than taper inserts for comparable lengths. The figure shows that the stress carrying capacities of the leaf inserts for all lengths are consistently higher than their tapered insert counterparts, and that longer inserts perform better than shorter ones. Unlike the case of foam structures, only one mode of failure is observed here, namely debonding of the inserts.

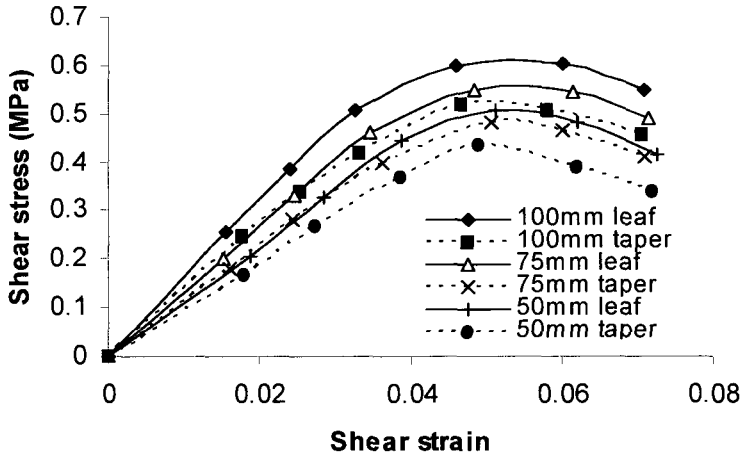

Figure 5.9:Comparison between shear stress for leaf and taper inserts in sandwich specimen

Table 5(b) Fiber and core stress comparison for taper and leaf inserts inside the sandwich structure.

Insert shape	length (mm)	Fiber Stress		Difference %	Shear Stress		Difference %
		Exp	FEA		Exp	FEA	
Taper	100	2.01	2.14	2	0.52	0.51	1.9
	75	1.83	1.85	-1.1	0.48	0.47	2.08
	50	1.72	1.76	2.3	0.44	0.43	2.2
Leaf	100	2.53	2.5	1.1	0.59	0.60	-1.6
	75	2.39	2.44	-2.1	0.55	0.56	-1.81
	50	2.13	2.17	-1.8	0.5	0.49	2

5.4 Analytical Study of the Two Modes of Failure

5.4.1 Fracture Analysis of the Foam Slabs

There are two approaches to the structural design and material selection. One is the traditional approach which is based on the strength of material as compared to the applied stress and the second approach is the fracture mechanics [52]. Two alternative approaches to fracture analysis are in open literature: the energy criterion and the stress intensity approach. The energy approach states that crack extension (fracture) occurs when the energy available for crack growth is sufficient. to overcome the resistance of the material whereas calculation of fracture toughness using stress intensity factor is stated in the latter method. The stress intensity approach based on the Linear Elastic Fracture Mechanics (LEFM) is considered for calculating the fracture toughness of the foam beam under consideration. Most of the available literature on polymer foams use LEFM for calculation of fracture toughness. LEFM is also applicable for cases of moderate plastic deformation in the polymer foams leading to failure [52] The characteristic parameters for LEFM are: applied stress, flaw size, and the fracture toughness. It should be noted that only the foam beam with the long inserts failed due to fracture of the specimen.

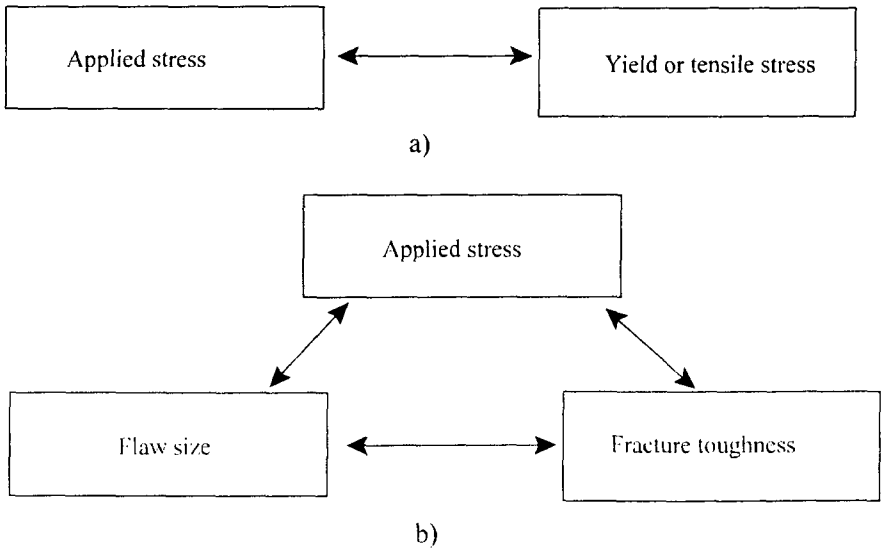

Figure 5.10: Comparison of fracture mechanics and traditional approach
a) Strength of material approach b) Fracture mechanics approach

A single notched foam beam model with a crack length a and a span S is considered as shown in the Figure 5.11. The dimension of the beam used in the analysis matches the experimental samples. Mode-1 loading condition, where the load is normal to the crack plane and tends to further open the

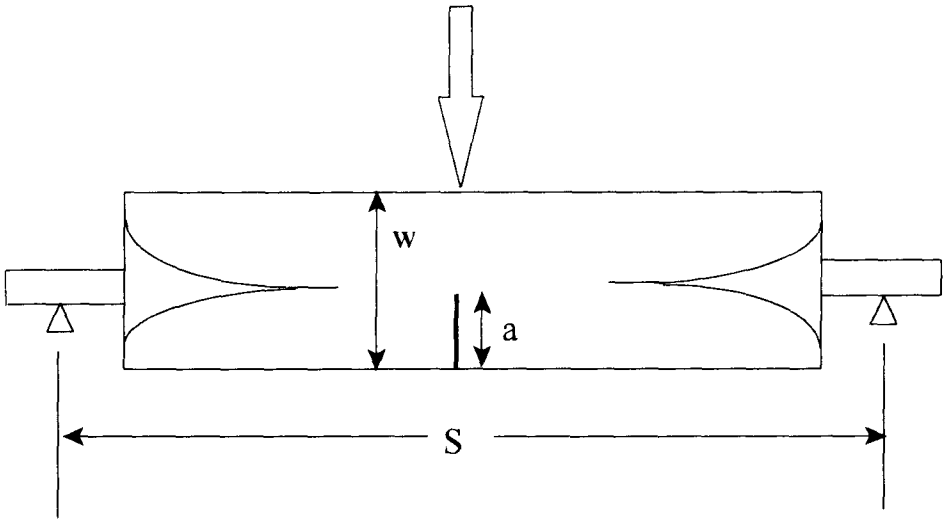

Figure 5.11: Single notched foam beam model

crack, is considered. Mode-1 occurs in the case of the foam slab in bending on the tension side as experienced in the tests conducted. A polar co-ordinate system for describing the stresses in the vicinity of the cracks is shown in the Figure 5.12. Consider an element at coordinates r and θ from the crack leading edge (tip) and in the plane X-Y which is normal to the crack plane aligned with the z-axis. For loading, Mode-1 or tensile mode was studied. It is also known as the opening mode and consists of crack surfaces moving apart. In the case of the foam beam, the crack appeared on the part of the beam where it was under a tensile load, therefore mode-1 was considered. For a Mode-1 loading the normal and shear stresses at the element near the crack tip are functions of the coordinates of the element and are expressed as follows [52,53].

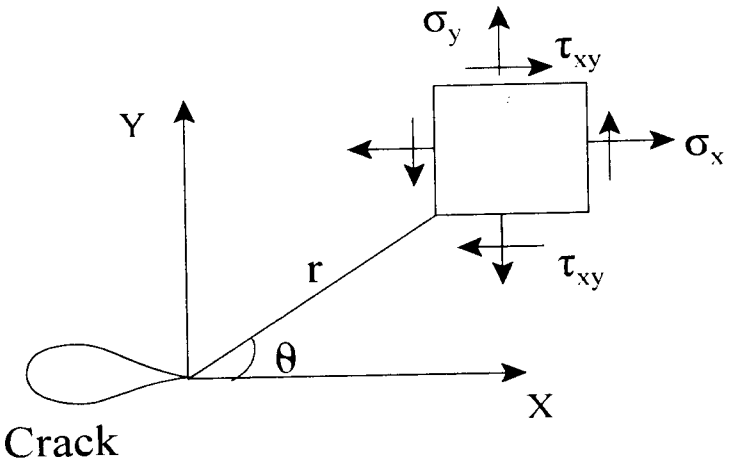

Figure 5.12: Orientation of coordinate axis ahead of crack tip

$$\sigma_x = \frac{K_1}{\sqrt{2\pi r}} Cos\left(\frac{\theta}{2}\right)\left(1+\sin\frac{\theta}{2}\sin(\frac{3\theta}{2})\right) \tag{5.1}$$

$$\sigma_y = \frac{K_1}{\sqrt{2\pi r}} Cos\left(\frac{\theta}{2}\right)\left(1-\sin\frac{\theta}{2}\sin(\frac{3\theta}{2})\right) \tag{5.2}$$

$$\tau_{XY} = \frac{K_1}{\sqrt{2\pi r}} \cos\left(\frac{\theta}{2}\right)\sin\left(\frac{\theta}{2}\right)\cos\left(\frac{3\theta}{2}\right) \tag{5.3}$$

Where $\sigma_x, \sigma_y, \tau_{x,y}$ are normal, shear stresses, and singular field along the crack tip is obtained by substituting $\theta = 0$ in Equations 5.1 to 5.3 and results in:

$$\sigma_x = \sigma_y = \frac{K_I}{\sqrt{2\pi r}} \tag{5.4}$$

$$\tau_{xy} = 0 \tag{5.5}$$

Equation 5.5 shows that at $\theta = 0$ the element has no shear stress component, indicating that it is aligned with the principal axis. The stress components in the Equation 5.4 can be seen to approach infinity as r approaches zero, that is to say as the element approaches the crack tip. At the crack tip, $r = 0$, a mathematical singularity would occur and no value of stress at the crack tip can be inferred from Equation 5.4. The stress intensity factor defines the amplitude of the crack tip singularity. That is, stresses near the crack tip increase in proportion to K. Moreover, the stress intensity factor completely defines the crack tip condition; if K is known, it is possible to solve for all components of stress, strain and displacement as a function of r and θ. This single parameter of crack tip condition turns out to be most important concept in fracture mechanics.

In the above equations K_I is the stress concentration factor, and provides a measure of the severity of the crack.K_I is give by [52] as follows:

$$K_I = \lim_{r,\theta \to 0} (\sigma\sqrt{2\pi r}) \tag{5.6}$$

or in another form as:

$$K_I = f(\frac{a}{w})\sigma\sqrt{\pi a}) \tag{5.7}$$

Where f is a dimension less quantity that depends on the geometry, the loading configuration, and on the ratio of the crack length to other dimensions such as width. In general, f depends on the stress σ. Since the specimens used for the experimental work, were in the form of slabs, it is more appropriate to calculate the stress concentration factor in terms of applied load for rectangular geometries [53] as follows:

$$K_I = \frac{P}{B\sqrt{W}} f(\frac{a}{W}) \tag{5.8}$$

In the Equation 5.8, P is the force, W is the width of the specimen, and B is the specimen thickness. For the critical load P, $K_I = K_{Ic}$ and represents the fracture toughness of the rectangular foam slab [14] given in MPa$\sqrt{m}$. The trace may be non-linear for a variety of reasons; for example due to excessive plasticity occurring at the crack tip, due to inelastic or plastic deformations occurring in the bulk of the specimen, or due to slow crack growth prior to the maximum load being attained. The latter example will obviously also give rise to problems in defining the exact value of the load, P_c, for crack initiation. This is because if slow crack growth occurs before the maximum load is attained, a value of the critical stress-intensity factor for crack initiation based upon the maximum load will be an overestimation of the toughness of the material. These problems may be overcome, at least to a good approximation, by the following the arbitrary rule; The critical load is calculated based on the standard 5% offset method which outlines the fracture toughness calculations for plastics [24]. In this method, a line is constructed from the origin at a 95% slope of the initial linear slope of a load deflection curve as shown in the Figure 5.13.

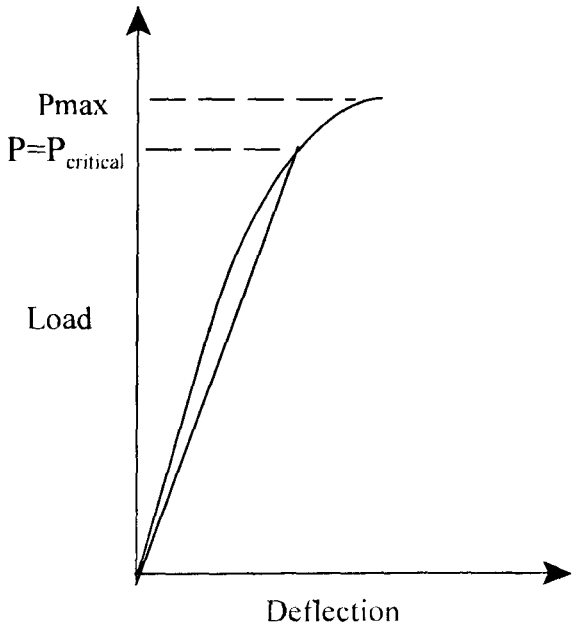

Figure 5.13: Estimation of critical stress

The value of $f(a/W)$ for a single notched beam is given in [52] as:

$$f\left(\frac{a}{W}\right)=\frac{3\frac{S}{W}\sqrt{\frac{a}{W}}}{2\left(1+2\frac{a}{W}\right)\left(1-\frac{a}{W}\right)^{\frac{3}{2}}}\left[1.99-\frac{a}{W}\left(1-\frac{a}{W}\right)\left\{2.15-3.93\left(\frac{a}{W}\right)+2.7\left(\frac{a}{W}\right)^{2}\right\}\right] \quad (5.9)$$

The fracture toughness calculated using Equation 5.9 for the critical load obtained from the load deflection curve of the foam slab with 100 mm leaf insert test data and varying a/W is shown in Figure 5.13. The plot in the figure has the same trend as that reported in [14]. Furthermore it shows that the fracture toughness is constant up to $a/W = 0.07$ and then decreases beyond that point. At $a/W = 0.5$, K_{Ic} is calculated from the experimental data to be 0.27 MPa$\sqrt{m}$. This value compares well with that given in [14] for the same material and $a/W = 0.5$. An edge notched beam model matching the experimental specimen and with $a/W = 0.5$ was developed in ANSYS and subjected to the three point bend loading. The maximum fracture stress of the model was found to be 0.21 MPa. For that stress the fracture toughness was found to be 0.26 as compared to 0.27 found experimentally and 0.3 given in [14]. This study shows that the ability of a foam to resist fracture reduces as the crack size increases.

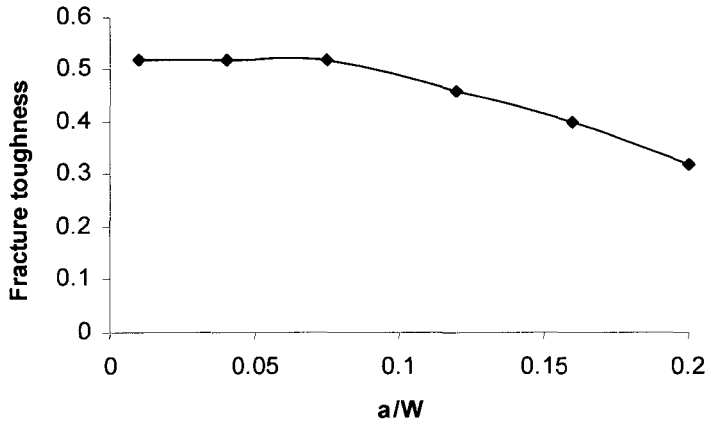

Figure 5.14: Fracture toughness as a function of crack length

5.4.2 Insert Pull-Out Analysis

Failure of foam structures with short inserts and sandwich composite structures with all lengths of inserts tested was due to insert pull-out. This failure occurs when the tensile stress caused by the bending of the specimen exceeds the bond strength between the foam and the insert. Pull-out tests were conducted on an Instron tester 4482 to measure the bond strength between the foam and the insert material. A rectangular insert with an embedded area of 0.01225 m^2 required a force of 260 N to be pulled out of the foam, resulting in an adhesion stress of 0.021 MPa. An insert pull-out will ensue when the condition where the pull-out stress equal to adhesion stress is satisfied.

With reference to the Figure 5.15, at any point on the surface of the insert the bending stress is given by:

$$\sigma_{pull-out} = \frac{Mc}{I} \tag{5.10}$$

Where c is the distance of the point on the surface of the insert from the neutral axis of the structure, I is the moment of inertia of the structure, and M is the bending moment.

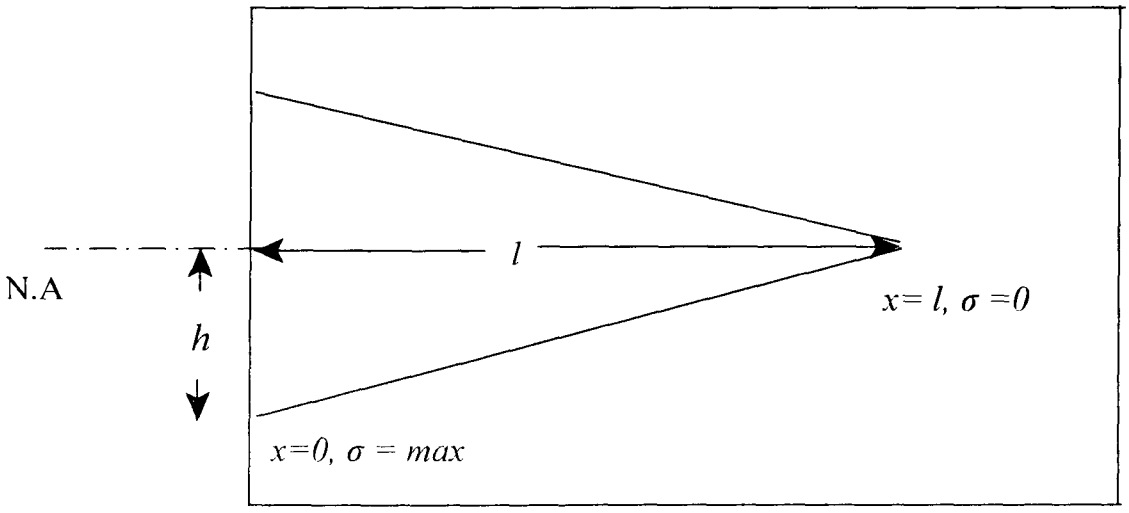

Figure 5.15: Distribution of stresses for taper insert inside sandwich

The integral of $\sigma_{pull\text{-}out}$ over the surface area of the insert results in the pull-out force $F_{pull\text{-}out}$ on the insert. The adhesion force between the foam and the insert material is the product of the experimentally obtained $\sigma_{adhesion}$ and the area of the insert. The Table 5 (c) presents the comparison between $F_{pull\text{-}out}$ obtained using the experimental results on the different inserts and the product of $\sigma_{adhesion}$ and the imbedded surface area of the insert, $F_{adhesion}$. The table shows very good agreement between the prediction, $F_{adhesion}$, and the experimental results, $F_{pull\text{-}out}$. This indicates that the proposed analysis can be used reliably to predict the ensuing of pull-out, and hence failure.

Table 5(c): Comparison between predicted adhesion force and experimental pull-out force

Insert	length (mm)	Adhesion force (N)	Pull-out force (N)
Taper	100	230	240
	75	225	230
	50	220	220
Leaf	100	230	270
	75	225	255
	50	220	245

5.5 Finite Element Analysis of the Test Specimen

Advances in computational features and software have brought the finite element method within reach of both academic research and engineers in practice by means of a general-purpose nonlinear finite element analysis packages, with one of the most used nowadays being ANSYS. The program offers a wide range of options regarding element types, material behavior and numerical solution controls, as well as graphic user interfaces (known as GUIs), auto-meshers, and sophisticated postprocessor and graphics to speed the analyses [50]. In this research, the structural system modeling of polymer structure was carried out using ANSYS version 11. 2D finite foam and sandwich beam models matching the experimental dimensions were developed in a commercial finite element program, ANSYS version 11. The purpose of the exercise was to validate the FE modeling

technique and use that later for the study of sandwich composite with inserts.

An eight-node element (PLANE 82) was selected due to its proven better results for sandwich composite modeling [44]. Plane 82 is a higher order 2-D element. It provides more accurate results than other plane elements for mixed (quadrilateral-triangular) automatic meshes and can tolerate irregular shapes easily. The 8-node elements have compatible displacement shapes and are well suited to model curved boundaries. The 8-node element is defined by eight nodes having two degrees of freedom at each node: translations in the nodal x and y directions. The element may be used as a plane element or as an axis symmetric element. The element has plasticity, creep, swelling, stresses stiffening, large deflection, and large strain capabilities which are required for contact analysis that are non-linear in nature.

For the sandwich composite one element is used to model each layer, i.e., 3 layers through the thickness. Because of the symmetry along the length, only half of the beam was modeled with appropriate symmetry displacement boundary conditions imposed. Nodes at each end of the beam were constrained to simulate a simple supported beam. Modulus properties of the PU were obtained from the experimental results as shown in the Table 3(a). For the fiber glass, manufacturer provided properties were used. Finally for the aluminum, standard documented properties were used. Both the free and mapped meshing was used. Rigid- flexible contact scenarios were used. Contact between the metal and foam was defined by the compatible elements (TARGET 169 and CONTACT 172).

In order to determine the non-linearity of model, both the geometric and material non-linearity was considered. For geometric non-linearity, large strain analysis option was used for running the simulation. This option accounts for stiffness changes that result from changes in an element's shape and orientation. It places no theoretical limit on the total rotation or strain experienced by the element. In order to account for the material non-linearity, automatic time stepping option was used. This option responded to plasticity, by reducing the load step after a load step in which a larger plastic strain increment was encountered. If too large a step was taken, the program will bisect and re-solve to use a smaller step size. The loads were applied using a shorter time step and small load step to facilitate convergence.

5.5.1 Results and Discussions

To observe the failure pattern of inserts of taper and leaf geometries inside the sandwich, simulations were run in ANSYS. The Figure 5.15 shows the stress strain plots for the FE models of the foam structures with the different length of leaf inserts. The plots show the same trends and general values obtained experimentally for the corresponding cases. The failure stresses for the FEA models are provided in the Table 5(b).

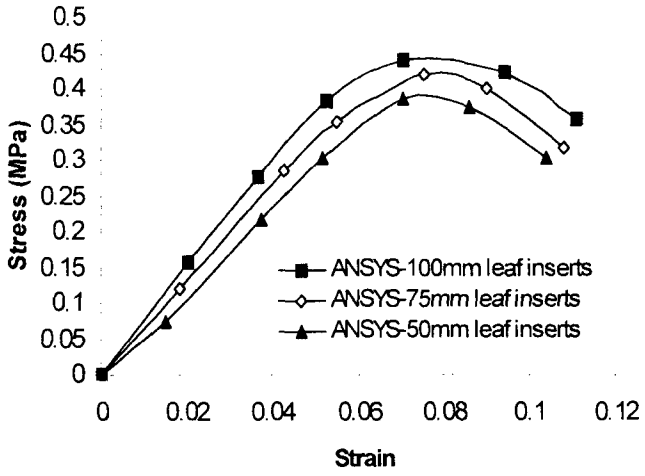

Figure 5.16: Stress strain curves for foams with leaf inserts

The Figures 5.15 show the stress strain plots for the FE models of the foam structures with the different length of the leaf inserts. The plots show the same trends and general values obtained experimentally for the corresponding cases. The failure stresses for the FEA models are provided in the Table 5(b). The table also shows the very good agreement between the experimental and FE models failure stresses. The maximum deviation between the average experimental failure stress and that of the corresponding FE model is 2%.

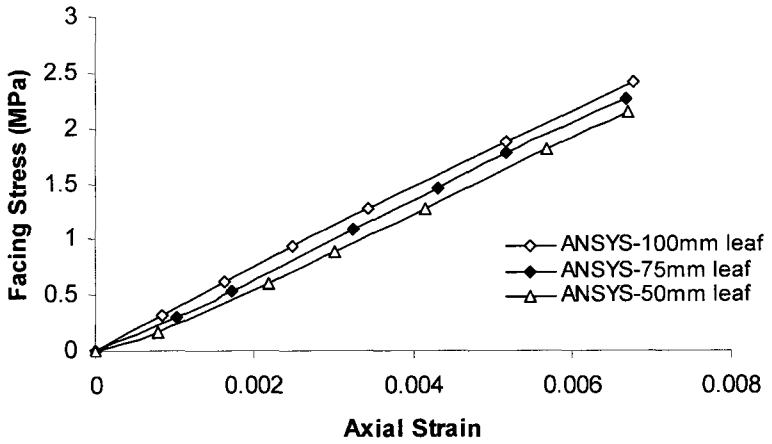

Figure 5.17: Axial stress strain curves for sandwich with leaf inserts

Facing bending stress σ_{xx} and the foam core shear stress τ_{xy} were plotted with respect to the relevant axial strain ε_{xx} and shear strain γ_{xy}. The Figures 5.17 and 5.18 show the comparison of curves for facing stresses and shear stresses for the sandwich with leaf inserts. The figures show that for

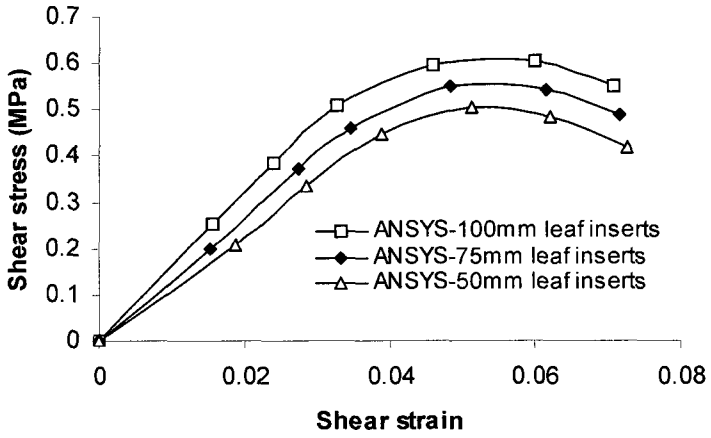

Figure 5.18 :ANSYS-shear stress strain curves for sandwich with leaf inserts

different insert lengths, shape of the ANSYS stress-strain curves and the magnitude coincide with those obtained experimentally. Leaf inserts showed the highest failure stress values as compared to

taper inserts, trend that is similar to experimental values. It has been asserted in [44] that FE analysis can be used to reliably model the non-linear behavior of foams. In this work it is shown that FE can also be used reliably to model the highly non-linear geometrical and material behavior of the rigid-flexible interface between the foam and metal as well to study the failure analysis.

5.6 Summary

Adhesion properties of foam and sandwich composite with taper and leaf inserts were studied under flexural loading. Inserts with different lengths were used. Both the experimental and FE results were obtained and stress strain curves were plotted and compared. The results show that the failure stress and the load carrying capacity were dependent on the insert geometry and embedded length. Two modes of failure were observed. Foam fracture occurs when the adhesion force between the insert and the specimen exceed the strength of the foam on the tension side, and the insert pull-out occurs when pull-out force due to bending exceeds the adhesion force. Analytical treatments of these two modes of failure were conducted, and the results compared well with the experimental ones.

The study show the validity of the FE modeling approach used to simulate the interaction between the flexible foam and sandwich and the rigid insert as well as the analytical failure analysis technique proposed. This is of prime importance, as such techniques can be used for the design of polymer composite structures with metallic inserts. Chapter 6 shall compare the performance of the proposed tapered inserts with those of the standard method of attachment known as the close-out for foam and sandwich composites.

CHAPTER 6

ADHESION PROPERTIES OF FOAMS AND SANDWICH COMPOSITE WITH CLOSE-OUT

6.1 Introduction

This chapter focuses on discussing the placement of close-outs on foam and sandwich composite [55,56]. The close-out is the cap or finished part which covers the exposed edge of the core material. The panel close-outs have several important functions. The first is to close the sandwich to provide protection of the sandwich composite and facing edges from damage and prevent the facing from being peeled off the core. The next are to offer a hard member at which the panel can be attached to the structure or to another panel. Finally, it acts as a moisture and water seal for the panel edges. Typical close-out arrangement is shown in Figure 6.1.

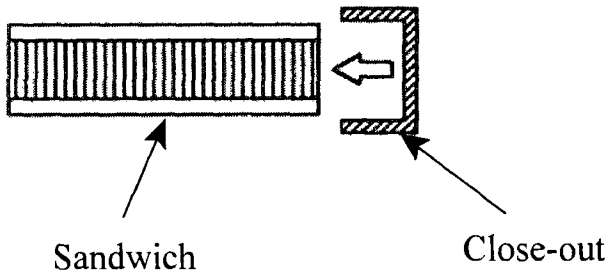

Figure 6.1: Sandwich composite with close-outs.

Close-outs are defined by the fabrication techniques as well as the end use. There are co-fab and post fab close-outs. The co-fab ones are bonded directly into the sandwich when the facings are bonded to the core, while the post-fab close-outs are put on after the panel is fabricated. In addition special tooling and fixtures are often required to align the close-outs and maintain the desired dimensional tolerances. For this reason subsequently assembled or post fab close-outs designs are most commonly used in flat panels. Perhaps the most troublesome and potentially most critical part of the

---

Reproduced from: Ahmed, A, Fahim, A and Naguib, H., "A Study on the Anchoring Orientation of Foam and Sandwich Composite with Inserts. *Journal of Polymer Composites*: Submitted 2010.

sandwich composite is the proper fitting of part and close-out. Since it was reported in previous chapters that the simulation results using ANSYS were in good agreement with the experiment results, therefore this chapter is based on the simulations results of the foam and sandwich composite with close-out and the foam sandwich with inserts. Because of the symmetry, only half of the foam and sandwiches close out models were simulated, with appropriate boundary conditions applied.

6.2 Failure of the Foam with Close-out and Inserts

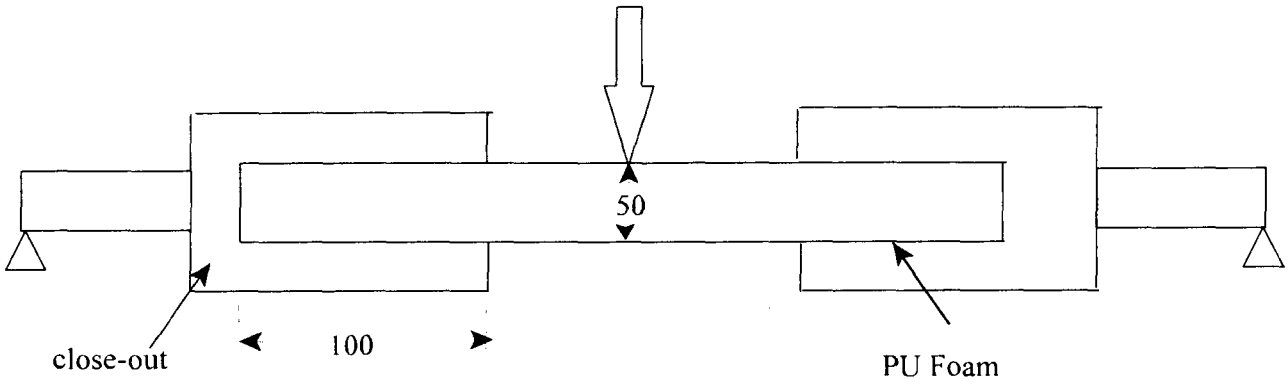

Figure 6.2: Foam with close-out

The first type of simulation was run on the foam-close-out arrangement as shown in the Figure 6.2. Close-outs were modeled in such a way that the contact area of the close-out plates was equivalent to the respective contact area of the rectangular insert embedded in the foam and sandwich composite structures. The length and height of the inner sides of the metallic close-outs which were in contact with the foam, and sandwich composite structures are as follows: l = 50 mm, 75 mm and 100 mm, h = 50 mm. Models were developed for each length, simulated, and compared with the foam sandwich structure with inserts.

In the first case, results for simulations for the foam-close out arrangement were compared with the foam-50mm inserts of leaf, taper, rectangular and cylindrical geometries. Results were compared and are shown in the Figure 6.3. It was observed that fracture stress values for all the foam composite structures with inserts are higher than the fracture stress value for the one with close-out. Since the placement of upper and bottom plates of the close-out were far from the neutral axis of the foam slabs,

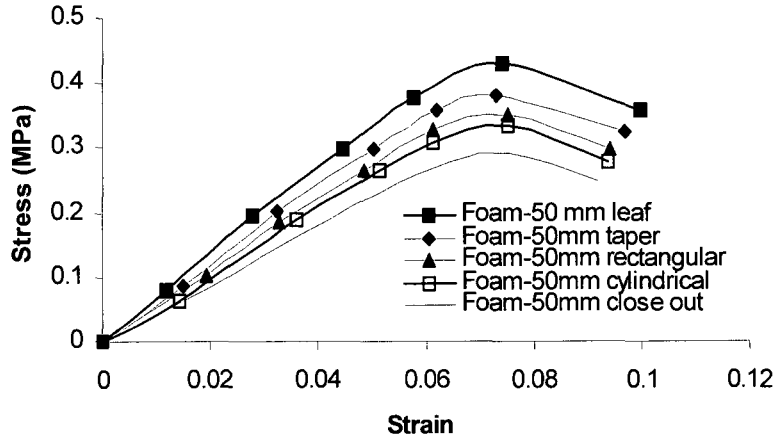

Figure 6.3: Foam-comparison between 50mm inserts and close-outs

therefore the shear stresses were higher on the interfaces between the structure and the close-out

The second simulation case was for a foam sandwich structure with close-out having a surface area matching that of the rectangular insert with 75 mm length. The flexural stress strain curves from the simulation are shown in the Figure 6.4. It can be seen again that the fracture stresses for all the foam sandwich structures with inserts are higher than those of the ones with close-out. The failure was again attributed to the placement of the close-out plates with respect to beam the neutral axis, hence prompting failure at the lower load.

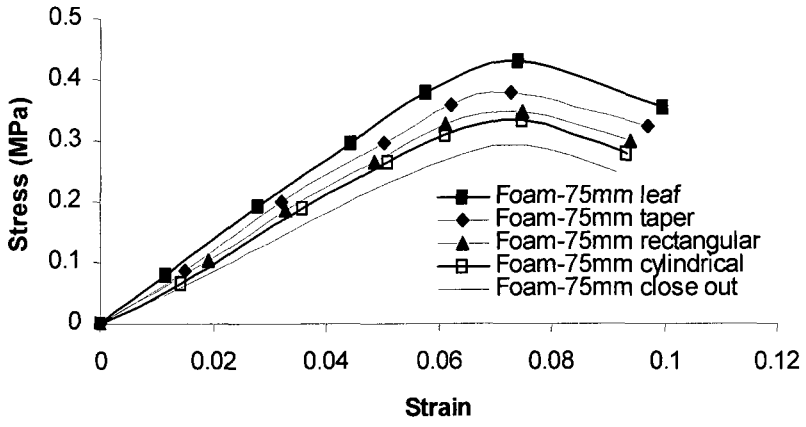

Figure 6.4: Foam-comparison between 75mm inserts and close-outs

Finally, simulations were run on foam sandwich structures with close-out set-up matching the surface area of 100 mm rectangular insert length. Flexural stress strain curves are shown in the Figure 6.5. It was seen that fracture stresses for all the foam-inserts arrangement were higher than the fracture stress value for the foam-close-out set-up. Again, the placement of the close-out plates was not on the neutral axis, therefore the close-out failed at a lower stress value.

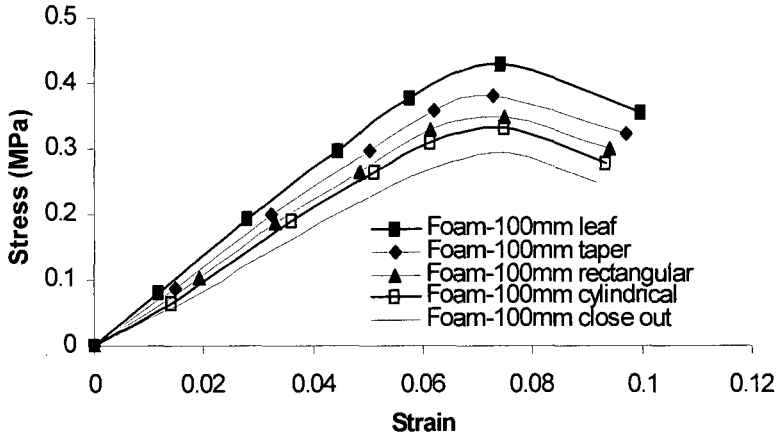

Figure 6.5: Foam-comparison between 100mm inserts and close-outs

6.3 Failure of the Sandwich Composite with Close-out and Inserts

Second types of simulation were run on the sandwich composite-close-out set-up as shown in the Figure 6.6. For simulations, the surface area of the close-out in contact with the sandwich composite structure was exactly the same as that of the imbedded rectangular insert. The analyses were conducted for the 50 mm, 75 mm and 100 mm lengths and the results were compared as shown below.

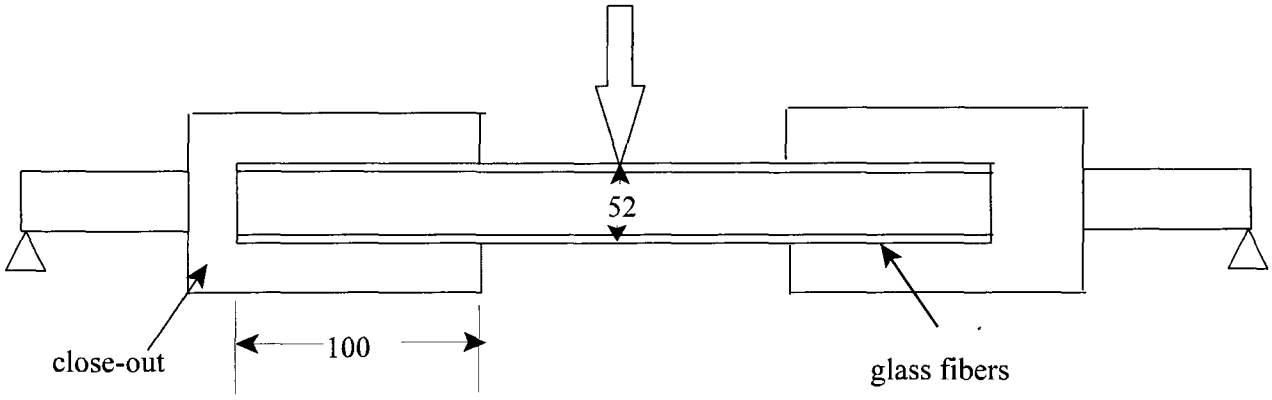

Figure 6.6: Sandwich composite with close-outs

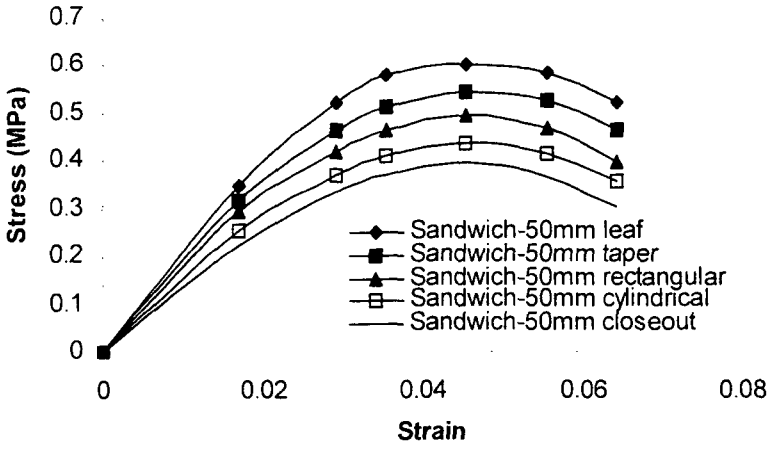

Figure 6.7: Sandwich-comparison between 50mm inserts and close-outs

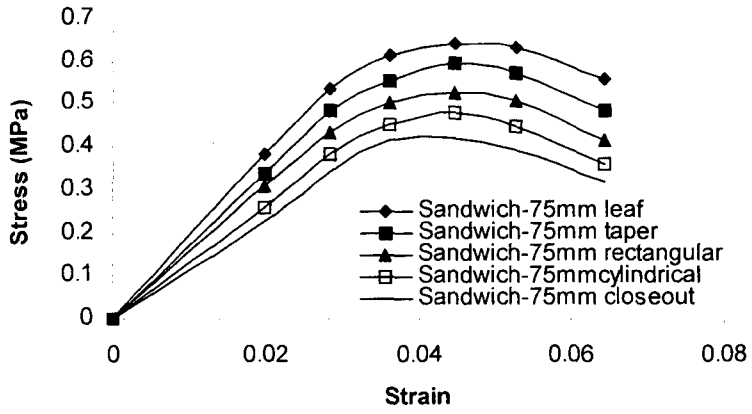

Figure 6.8: Sandwich-comparison between 75mm inserts and close-outs

In the first case, results of simulations for the sandwich structure with the close-out were compared with those with 50 mm inserts of leaf, taper, rectangular and cylindrical geometries. Results were compared and are shown in the Figure 6.7. The figure shows that the fracture stress values for all the cases with inserts are higher than the value for the sandwich structure with close-out. Since for the placement of close-out plates was not on the neutral axis, therefore the close-out failed at a lower stress value.

In the second case, results of simulations for the sandwich structure with the close-out were

compared with those of the 75 mm length leaf, taper, rectangular, and cylindrical inserts. The surface areas for both the configurations were matched. Plots of the results are shown in the Figure 6.8. The figure shows that the fracture stresses for all the sandwich structures with inserts are higher than those for the case of the close-out. This is again for the same reason where the close-out plates were far from the neutral axis.

In the third case, results of simulations for the sandwich structure with the close-out were

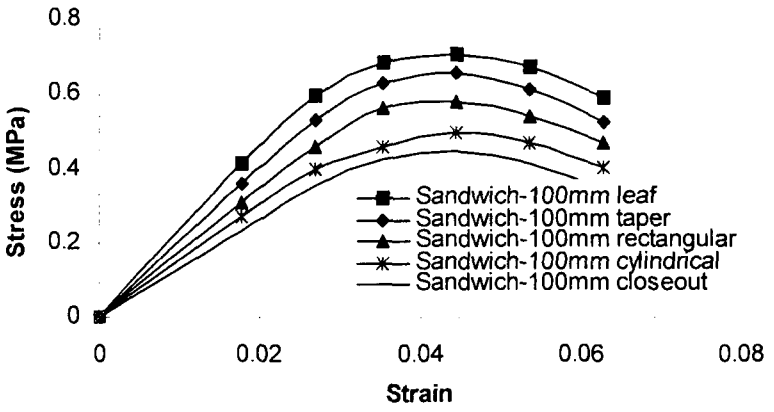

Figure 6.9: Sandwich-comparison between 100mm inserts and close-outs

compared with those for the 100 mm inserts of leaf, taper, rectangular and cylindrical geometries. The surface areas of contact between the metal and the structure for all the cases were again matched. The results are plotted in the Figure 6.9.

The plot show that the fracture stress values for all the cases with inserts are higher than those for the close-out. The reason is again attributed to the distance between the close-out structure interface from the neutral axis causing the arrangement to fail at a lower stress value. The salient results from the plots in the Figures 6.3 to 6.9 are shown in the Table 6(a). All the results obtained so far from the simulations show that placement of a metallic insert inside a foam sandwich composite structure as means of anchoring is more favorable than the standard industrial practice of using close-out anchors. The primary reason for that is attributed to the proximity of the interface surfaces of inserts to the neutral axis when compared with the cases of close-outs. Furthermore, for the cases of inserts, five sides are in effect interface surfaces as compared to three sides for close-outs.

Table 6(a): Comparison between foam-close out and sandwich close-out results

Type	Insert (mm)	Failure Stresses (MPa)				
		Leaf	Taper	Rectangular	Cylindrical	Close-out
Foam	50	0.38	0.33	0.31	0.29	0.26
	75	0.4	0.35	0.33	0.32	0.28
	100	0.43	0.38	0.35	0.34	0.29
Sandwich	50	0.59	0.55	0.49	0.43	0.39
	75	0.63	0.59	0.52	0.47	0.41
	100	0.69	0.64	0.56	0.49	0.45

6.4 Mapping of Foams and Sandwich Composite with Close-out Results

In the cases of inserts, inspection after the experiments were conducted showed that voids were present on the interface surfaces. These voids reduce the bonding area when compared to that for the case of close-outs, where the close-out interface surface is bonded to a consistent skin with no voids. In order to investigate this difference, a foam specimen was sliced and a microscopic analysis of its cell structure was carried out. The results showed that the average cell size is 250 micrometers and the cell population density is 5.5×10^4 cells/cm^3. Using these data, the void fraction in the area was calculated. Using this void fraction, the theoretical area reduction factor was calculated as 0.33. In order to use this reduction in an area factor to map the difference in stress values for the case of insert and close-out with the foam and the sandwich composite, the flexural equation was used. For the foam with close out, the bending equation is written below with subscript "1":

$$\sigma_1 = \frac{3P_1 L_1}{2b_1 d_1^{\,2}} \tag{6.1}$$

Where P is the applied load, L is the span length, b is the width and d is the depth of the specimen. Similarly, for the sandwich composite with close out, the flexural equation with subscript 2 is written below:

$$\sigma_2 = \frac{3P_2 L_2}{2b_2 d_2^2} \tag{6.2}$$

Re-arranging the Equations 6.1 and 6.2 to relate σ_1 in term of σ_2

$$\sigma_1 = \frac{P_1 A_1}{P_2 A_2}\sigma_2 \tag{6.3}$$

The value of failure stress for the sandwich structure with 100 mm close-out obtained from the FE analysis was, $\sigma_2 = 0.45$ MPa as shown before in the Table 6(a). Using this value of stress in the Equation 6.3 and substituting the area reduction factor of 0.33, the failure stress value for the foam with 100 mm close out was calculated and the value obtained was, $\sigma_1 = 0.31$ MPa. This value was very close to the FE failure stress value of 0.29 MPa for foam with 100 mm close out as shown before in the Table 6(a). This validates the observation that voids caused the foam close-out structures to fail at a lower stress value as compared to the sandwich close-out structures. Furthermore, this equation can also be used to map the relationship between the stress values of foam and sandwich with close out of different lengths as well as the stresses of the same structures with inserts.

6.5 Summary

Foam and sandwich composite structures with close-outs were modeled and simulated using ANSYS and compared with those containing inserts. Rectangular, cylindrical, and taper (wedge) inserts with different lengths were used. The results show that the foam and sandwich composite with inserts have higher stress value as compared to same structure with close-outs. Finally mapping of the failure stress using the area reduction factor for the foam and sandwich composite with inserts and close-outs was investigated . It was reported that reduction in area of the foam was responsible for the lower stress values as compared to the sandwich structure.

CHAPTER 7

CONCLUSION AND RECOMMENDATIONS

The modulus of elasticity and adhesion properties of foam structures in the form of slabs with inserts were studied under flexural loading. Rectangular, cylindrical, and the wedge (tapered) inserts with different lengths were used. Experimental results were obtained and the load-deflection curves were plotted for the different combinations. The results showed that the stiffness, adhesion properties, and mode of failure were dependent on the insert embedded length. In general, longer inserts lead to higher moduli. Two modes of failure were observed. For the cases of long inserts, foam fracture tends to occur, while for short inserts, de-bonding tends to occur. The study also showed the validity of the FE modeling approach used to simulate the interaction between the flexible foam slab and the rigid insert. This is of prime importance; as such a modeling technique can be used for the design of such composite structures.

Furthermore, load-bearing properties of sandwich composites with inserts were studied under flexural loading. Rectangular, cylindrical and (wedge) taper inserts with different lengths were used. Experimental results were obtained and stress-strain curves were plotted for the different combinations. The results showed that the failure stress and the adhesion properties were dependent on the insert embedded length. Stiffness model to estimate sandwich failure were presented. It was observed that the mathematical relations for cross ply laminate failure under an axial load can be used for the sandwich composite with proper assumptions. Results showed the reduction in stiffness as a function of crack density. The study also showed the validity of the FE modeling approach used to simulate the interaction between the flexible sandwich and rigid insert. This is of prime importance, as such a modeling technique can be used for the design of sandwich composite structures.

Leaf inserts were also introduced. Leaf inserts showed better adhesion properties as compared to other geometries. The study also showed the validity of the FE modeling approach used to simulate the interaction between the flexible sandwich and rigid insert. Fracture toughness of foam beam and pull-out force for sandwich insert failure was also calculated.

Finally, adhesion properties of the polymer metal foam and composites with close-outs and

different lengths were used. Simulation results were obtained and stress-strain curves were plotted for the different combinations. The results showed that the sandwich composites with inserts have higher failure stress values as compared to foams with inserts. Furthermore, it was also observed that foams and the sandwich composites with inserts performed better in terms of failure stress values as compared to foams, and the sandwich composite with close-outs. Finally, mapping of the failure stress values for the foam and sandwich was done. It was reported that reduction in area of the foam was responsible for lower stress values.

For future study, effect of imbedded inserts on different densities of the polyurethane foams can be considered. Also, the flexural testing of the polyurethane foams and the sandwich composite under the four points bending will also be a good prospect. Furthermore, polyurethane and sandwich composite properties can also be studied using inserts of different metals such as steel of various grades, brass etc. to study the adhesion properties of different metals with foam based composite.

REFERENCES

1. Gibson. J. L., and Ashby, M. F., 1997, Cellular Solids-Structure and Properties, Cambridge University Press, Cambridge, UK.
2. Callister, W .J.,2003, "Material Science and Engineering",John Wiley.
3. Mahfuz, H, Rangari, K, V., Islam, S, M,.and Jeelani, S.,2003, "Fabrication, Synthesis and Mechanical Characterization of Nanoinfused Polyurethane Foams"Composite Part A,35, pp.453-460.
4. Hawkins, M. C, and Toole, B.,and Jackovic D., 2005, "Cell Morphology and Mechanical Properties of Rigid Polyurethane Foams", Journal of Cellular Plastics,41,pp.267-285.H
5. Xiong J, Zhou D., Zheng Z., and Wang X., 2006, "Fabrication and Distribution Characteristics of Polyurethane/single-walled Carbon Nanotube Composite with Anisotropic Structure" Polymer, 47.pp.1763-1766.-
6. Iliev, R, P,. Lee, K, H,.and Park, C, B,.2006, "Manufacture of Integral Skin PP Foam Composites in Rotational Molding",Journal of Cellular Plastics,42,139-151.
7. Hosur, M, V., Abdullah, M,. and Jeelani, S.,2004, "Manufacturing and Low Velocity Characterization of Foam Filled 3D Integrated Core Sandwich Composites with Hybrid Sheets"Journal of Composite Structures,69, pp.167-181.
8. Lee, C, S,.Lee, D, G,. and Oh, G, H,.2004, " Co. Cure Bonding Method for foam core composite sandwich manufacturing", Journal of Composite Structures,66,pp.231-238.
9. Sihn, S., and Rice, B, P,. 2003, "Sandwich Construction with Carbon Foam Core Materials",Journal of Composite Materials,37,1319-1316.
10. Bezazi A., and Scarpa F., 2007, "Mechanical Behavior of Conventional and Negative Poisson's Ratio Thermoplastic Polyurethane Foams under Compressive Cyclic Loading". International Journal of Fatigue,29.pp.922-930.
11. Tsai I. J., Lei, C. H., Lee, H.C., and Lin, H. J., 2007., : "Manufacturing Process and Property Analysis of Industrial Flame Retarded PET Fiber and Polyurethane Composite". Journal of Material Processing Technology,192-193.pp.415421
12. Olurin, O. B., Fleck, N. A., and Ashby, M. F., 2000, "Joining of Aluminum Foams with

Fasteners,"Journal of Material Science, 35, pp.1079-1085.

13. Bernard, T., Bergmann, H. W., Haberling, C., and Hladenwanger, H.G., 2002, "Joining Technologies for Al-Foam-Al-Sheet Compound Structures," Advanced Engineering Materials 4(10), pp.798-802.
14. Kabir, M. E., Saha, M. C., and Jeelani, S., 2006, "Tensile and Fracture Behavior of Polymer Foams," Journal of Material Science and Engineering A, 429, pp. 225-235.
15. McIntyre, A., and Anderton, G. E., 1979, "Fracture Properties of a Rigid Polyurethane Foam over a Range of Densities," Journal of Polymer., 20, pp.247-253.
16. Huang, W. H., 2003, "A Simple Approach to Estimate Failure Surface of Polymer and Aluminum Foams under Multi axial Loads," International Journal of Material Sciences, 45, pp.1531-1540.
17. Subhash, G., Liu, Q., and Gao, X. L., 2006, "Quasi static and High Rate Strain Rate Uniaxial Compressive Response of Polymeric Structural Foams," International Journal of Impact Engineering, 32, pp.1113-1126.
18. Zhang, Y., Rodrigue, D., Kadi, A.A., 2003, "High Density Polyethylene Foams. 1V. Flexural and Tensile Moduli of Structural Foams," Journal of Applied Polymer Science, 90, pp.2139-2149.
19. Moosa, A. S .I., Mills, N. J., 1998, "Analysis of Bend Tests on Polystyrene Bead Foams," Journal of Polymer Testing, 17, pp. 357-378.
20. Benderly, D., Rezek, Y., Zafran, J., and Gorni, D., 2004, "Effect of Composition on the Fracture Toughness and Flexural Strength of Syntactic Foams," Journal of Polymer Composites, 25(2), pp.229-236.
21. Wouterson, E. M., Boey, F. Y. C., and Hu, X., 2004, "Fracture and Impact Toughness of Syntactic Foams," Journal of Cellular Plastics, 40, pp.145-154.
22. Kanny, K., Mahfuz, H., Thomas, T., and Jeelani, S., 2004, "Static and Dynamic Characterization of Polymer Foam under Shear Loads," Journal of Composite Materials, 38(8), pp.629-639.
23. Kreter. P. E.,1985. "Polyurethane Foam Physical Properties as a Function of Physical Density" Journal of Cellular Plastics,21,pp.306-310.
24. Davy G.,Hashemi S., and Kinloch A.J., 1989 "The Fracture of a Rubber-modified epoxy

Polymer Containing Through Thickness and Surface Cracks"Int.Journal of Adhesion and Adhesives,9,pp.69-76.

25. Nicholls R, 1976, Composite Construction Material Handbook, Prentice Hall, USA. pp -460-465

26. Bakos, D. J., and Papanicolou, G. C., 1993, "Effect of Skin Treatment and Core Material on the Bending Properties of the Sandwich Composite", 45.pp.35-43.

27. Daniel, M. I.,and Abot,J. L,2000, "Fabricaton, Testing,and Analysis of Sandwich Composite Beams"Composite Science and Technology,60,pp.2453-2463.

28. Bozhevolyna E., and Lyckegaard, A., 2005 "Structurally Grades Core Inserts in Sandwich Composite"Composite Structures,68,pp, 23-29.

29 Xia, M., Takayanagi, H., and Kemmochi, K., 2002, "Bending Behavior of Filament Wound Fiber Reinforced Sandwich Pipes,"Composite structures, 56 ,pp.201-210.

30. C. S. Karthikeyan,C, S., Sankaran,S., and Kishore, 2007, "Investigation of Bending Modulus of Fiber Reinforced Syntactic Foams for Sandwich and Structural Applications," Polym. adv.Techno, 18,254-256.

31. Theulen ,J, C, M., and Peijs,A. A. J., 1991, "Optimization of Bending Stiffness and Strength of Composite Sandwich Panels,"Composite Structures, 17, pp.87-92.

32. Sarzynski, M. D., and Ochoa,O, O., 2004, "Carbon Foam Core Composite Sandwich Beams: Flexure Response,"Journal of Composite Materials, 39(12), pp. 1067-1080.

33 Mouitz ,A,P., and Thomson,R.S., 1999, "Compression, Flexure and Shear Properties of Sandwich Composite Containing Defects,"Composite Structures, 44,263-278.

34 Shafiq B., and Quispitupa, A., 2006, "Fatigue Characteristic of Foam Core Sandwich Composites," International Journal of Fatigue, 28, pp.96-102.

35. Ahmed A., Fahim A., and Naguib, H., 2009, "Design of New Hybrids with Metal Imbedded in Polymer and Polymer Composite," Journal of Composite Material, 42.

36. Kulkarni, N., Mahfuz, H., and Shaik, J , 2004, "Fatigue Failure Mechanism and Crack Growth in Foam Core Sandwich Composites under Flexural Loading," Journal of Reinforced Plastics and Composites, 23(1), pp.83-94.

37. Lee, S. M., and Tsotsis, 2002, "Indentation Failure Behavior of Honey Comb Sandwich Panels,"Composite Science and Technology, 60, pp.1147-1159.

38. Movsumov, E, A., and Shamiev, F. H., 2005, "Load Carrying Capacity of Circular Plates Made of a Fiber Reinforced Composite,"Mechanics of Composite Materials, 41(2),pp.119-130.

39. Kanny, K.,and Mahfuz, H.,2005, "Flexure Fatigue Characteristics of Sandwich Structures at Different Loading Frequencies,"Composite Structures, 67,pp.403-410.

40. Thomsen ,O, T., and Rits, W.,1998, "Analysis and Design of Sandwich Plates with Inserts-A High Order Sandwich Plate Theory Approach,"Composites: Part B, 29B,795-807

41. Bunyawanichakul, P Castanie, B., and Barrau, J. J.,2005, "Experimental and Numerical Analysis of Inserts in Sandwich Structures,"Applied Composite Materials, 12,pp.171-191.

42. Rice, M.C., Fleischer C.A., and Zupan M., 2006,"Study on the Collapse of Pin Reinforced Foam Sandwich Panel Cores"Experimental Mechanics,46,pp.197-204.

43. Steeves A.C., and Fleck, A.K.,2004 "Collapse Mechanism of Sandwich Beams with Composite Faces",46, Mechanical Sciences, pp.561-583.

44. Manet, V., 1998, "The Use of ANSYS to Calculate the Behavior of Sandwich Structures," Composite Science and Technology, 58, pp.1899-1905

45. Lin, H., Bull. S.J., and Taylor, P.M., 2005, "Simulation of the Deformation and Stress Distribution within a Flexible Material Pressed by a Pinch Gripper," Journal of Material Processing Technology, 169, pp.357-363..

46. Queiroz, F.D., Vellasco, P. C. G. S., and Nethercot, D.A., 2006, "Finite Element Analysis of Composite Beams with Full and Partial Shear Connections"Journal of Constructional SteelResearch,63, pp.505-521

47. Kolakwoski, Z., and Kubaik, T., 2005, " Load Carrying Capacity of Thin Walled Composite Structures",Journal of Composite Structures,67, pp.417-426.

48. Kramer, R,. and Roth, M, A., 2007, " Experimental and Numerical Analysis of Hollow and Foam Filled A-stringers", Journal of Sandwich Structures and Materials, 9, pp.197-208.

49. Richardson M. O. W., 1977. Polymer Engineering Composites,"Applied Science Publisher Ltd ,London, pp.198-209.Chap-4.

50. Daniel, M. I., and Ishai, O.,1994, "Engineering Mechanics of Composite Materials," Oxford University Press,New York, pp.245-265. Chap-7.

51. ANSYS User Manual, Release -11, ANSYS, INC, Canonsburg, PA.

52. Anderson, T, L,.2005, "Fracture Mechanics", Taylor and Francis, Chap-2,pp.25-53.

53. Dowling, E, N., 2007, "Mechanical Behavior of Materials", Pearson Prentice Hall, Chap-8.pp.312-337.

54. Kabir, M. E., Saha, M.C., and Jeelani, S., 2006, "Tensile and Fracture Behavior of Polymer Foams," Journal of Material Science and Engineering A, 429, pp. 225-235.

55. The Basics on Bonded Sandwich Constructions.TSB-124" ,Hexcel S.A, Belgium.

56. Honeycomb technology: materials, design, manufacturing, applications and testing By Tom Bitzer Edition: by Springer, 1997 ISBN 0412540509

57. Gere, J, M., and Timoshenko, S.P., 1997, Mechanics of Materials, PWS Pub, co, Boston, pp.391-397.

58 .Carlsson, L. A., Matteson, R.C., Aviles, F., and Loup, D.C., 2005, "Crack Path in Foam Cored DCB Sandwich Fracture Specimens," Journal of Composite Science and Technology, 65, pp.2612-2621.

59. Dementev, A. G., and Tarakanov, O. G., 1982, "A Statistical Study of the Fracture of Foamed Elastic Polyurethanes under Short Term Loading" Journal of Polymer Science, USSR, 24(7), pp.1585-1596.

60. Roberts, A.P., and Knackstedt, M.. A., 1995, "Mechanical and Transport Properties of Model Foamed Solids," Journal of Material Science Letters, 14, pp.1357-1359.

61. Gere, J, M., and Timoshenko, S. P., 1997, Mechanics of Materials, PWS Pub, co, Boston, pp.311-376, Chap.5.

62. Stegniy, A. I., Zabashta, Y. F., and Fridman, A. Y., 1995, "Internal Friction Of Composite Polymer Materials-Plastic Foams," Int. Journal of Hydrogen Energy, 20 (5), pp.401-403.

63. Zenkert, D.,1990, "Strength of Sandwich Beams with Midplane Debonding in the Core,"Composite Structures, 15,279-299.

64. Cui, W, C., and Wisnom,M. R,1991, "Contact Finite Element Analysis of Three and Four Point Short Beam Bending of Unidirectional Composites" Composite Science and Technology,45, pp.323-334.

65. Davalos, J. F.,Kim, Y., and Barbero, E. J.,1995, "A Layer Wise Beam Element for Analysis of Frames with Laminated Sections and Flexible Joint", Journal of Finite elements in analysis and design, 19, pp.181-194.

66. Vaidya A. S and Vaidya U.K, " Impact response of three dimensional multi functional

sandwich composites", Material Science and Engineering A,472. pp.52.58.

67. Silva Rodrigo and Haskell Adam, "Experimental and theoretical elastic analysis of sandwich composite plates", 52. 2008.

68. Zheng Xi, Yang Fen and Li, Ye, "Experimental and analytical study on the mechanical behavior of stitched sandwich composite panel with a foam core", Advanced Material Research,33, pp.447-482.

69. Rizov V and Mladensky A, "Influence of the foam core material on the indentation behavior of sandwich composite panels",26.pp.117-131.

70. Kumar G, Ramani K and Chong Xu, " Development and Characterization of thermoplastic composite system", Polymer-composite, 23. pp.647-57.

71. Tarlochan F, Mahdi, E and Sahiri, B,B, "Composite sandwich structure for crash worthiness application", Journal of Materials: Design and Application, 221, pp.121-130.

72. Haung, Jong-Shin and Gibson Lorna Jane, "Creep of sandwich beams with foam core", Journal of Materials in Civil Engineering,2.pp.171-182.

73. Mamalis A.G.,and Monakolis.A.J., "On the Crushing Response of Composite Sandwich Subjected to Bending Loads",Journal of Composite Structure,2, pp. 171-182.

74. Altdalst V, Lenz T and Jarnot D., "Polymer Foams as Core Materials in Sandwich-Comparison with Honey Comb", Polymer and Polymer Composites,1998, 6.pp.295-304.

75. Assarar M., E.I Mahi, and Berthelot ,J.E " Mecanique and Industries",2005,6,pp.589-593.

76. Tae Siong, Sup Lee and Dai Gil Lee, "Failure modes of Foam Core Sandwich Beams Under Static and Dynamic Loads",Journal of Composite Materials, 2004,38, pp.1639-1692.

77. Daniel M. .I., and Luo.J..J., "Impact and Post Impact Behavior of Composite Sandwich Panels",Composites: Part A.,2007, 21, pp.1051-1057.

78. Yuon Y and Shutov F.,, "Foamed Polymer Sandwich Composites with Three Dimensional Filler", Journal of Reinforced Plastics and Composites, 2002, 21, pp.653-661.

79. Zabihpur M and Abedian A, " Mechanism of Fatigue Damage in Foam Core With Unsymmetrical Carbon glass Face Sheets", 2007, Journal of Reinforced Plastics and Composites,26,pp. 1831-1842.

80. Du..L, and Tao Huang, " Z-pin Reinforcement on the Core Shear Properties of Polymer Foam Sandwich Composite"2009, Journal of Composite Materials,43, pp.289-300.

81. Shiva Kumar KN, and Smith S.A., " In situ Fracture Toughness of Core Materials in Sandwich Composites.38.pp.655-68.

82. S.C. Sharma, Krishna M., and Bhattacharya D., " Fatigue Properties of Sandwich Composites" 2004, Journal of Material Science and Performance.13.pp.637-41.

83. Bull, P.H., and Edgren F., " Compressive Strength of Foam Core Sandwich in Marine Applications", 2004, Composite Part B, 35B, pp. 535-541.

84. Papa, E, and Rizzi E, "Mechanical properties of Fiberglass Composite Structure: Experimental Results",2001, Structural Engineering and Mechanics,12,pp. 168-188.

85. Woo-Young Jung and Aref A.J., "Analytical and Numerical Studies of Polymer Composite Sandwich", 2005. Composite Structure,2005,68,pp.359-370.

86. Bazant Z P, Z.Yong and Quiang Yu, " Size Effect on Strength of Laminate Faom Sandwich Plates", 2006, ASME-Journal of Engineering Materials,128, pp.366-374.

87. Mines R.A. W and Alias A., "Numerical Simulation of Progressive Collapse of Polymer Composite Sandwich Composite Under Static Loading",Composites A: Applied Science and Engineering",2002,33.pp.11-26.

88. Dvorak G. J, and Suvorov AP., "Enhancement of Low Velocity Damage Resistance of Sandwich Plates",2005, Journal of Solid and Structures,42,pp.2323-2344.

89. Siriruk A, Weistman,J., and Dayakar,P., "Polymeric Foams and Sandwich Composites: Material Properties, Environmental Factors and Shear Lag Modeling",2009, Composites Science and Technology,69, pp.814-820.

90. Mizapur,A, Mohammed H., and Vayafan, M., "The Response of Sandwich Panels with Rigid Polyurethane Core Under Flexural Loading"2006, , Iranian Polymer Journal, pp.1082-1088.

91. Hughes M. L., and Sierakowski, R. L, "Force Protection Under Composite Sandwich Composites",2006, Polymer Science and Technology,66, pp.2500-2505.

92. Shenoi, R. A., Clark SD., and Allen H. G., " Fatigue Behavior of Polymer Foam Composite Beams", 1995,Journal of Composite Materials, 29, pp.2423-2445.

93. Tagarielli, V. L.,Fleck N. A.,.and Deshpende, V. S., "Collapse of Clamped and Simply Supported Sandwich Composite Beams in Three Point Bending",2004, Composite: Part B.,358.,PP. 523-534.

94. Sokolinski V. S., Hongbin S., and Nutt, S. R., "Experimental and Analytical Study of Non-

Linear Bending Response of Sandwich Beams",2003, Composite Structure,60, pp.219-229.

95. Deng A., L. Min and C.Yue, "Mechanical Properties of Z-Direction Reinforced Foam Core Sandwich Composite",2007,24, pp.50-54.

96. Burchadart,C., "Fatigue in Sandwich Structure Loaded in Transverse Shear",1997, Composite Structure,40, pp.73-79.

97. Martins,F.,Costa M., and Branco C. M., "Static Behavior of PVC Foam Composite Sandwich",1998, Cellular Polymers,17, pp. 177-192.

98. Mamalis A. G, Spentzas, K. N, and Ionnidis M., "Structural and Impact Behavior of Innovative Low Cost Sandwich Panels",2008, Journal of Crashworthiness,13, pp.231-236.

99. Kardomatoes, GA, and Simites, GJ., "Buckling of Sandwich Shells Under External Pressure",2005, ASME-Journal of Applied Mechanics,72, pp.493-499.

100. Shakwat W., and Fam, A., "Investigation of Novel Composite Cladding Wall Panel in Flexure",2008, Journal of Composite Materials,42, pp. 315-330.

101. Gdoutos,E. E, Daniel IM., and Wang KA., "Compression Facing Wrinkling of Composite Sandwich Structures",2003, Mechanics of Materials, 35,pp.511-522.

103. Mines, R.A.W., "Impact Energy Absorption of Polymer Composite Sandwich Beams",1998, Key Energy Materials,141, pp.553.572.

102. Mamalis A.G., Spentzas, AK., and Ioannidis, MB., "A New Concept for Sandwich Structures", 2008,Composite Structure, pp.335-340.

105. Marsavina L.,S., Tomasz, and N. Redu, "Polyurethane Foam Behavior: Experimental verses Modeling", 2009, Key Engineering Materials,399, pp.123-130.

103. Ashby M. F. and Brechet, Y.M. J., " Designing Hybrid Materials", 2003, Acta Materialia, 51,pp.5801-21.

104. Ogorkiewicz, R. M. and Sayigh, A.A. M., "Deflection of Carob Fiber/ Arcylic Foam Sandwich Beams",Composites, 4,1973, pp.254-257.

105 Campbell. J.E., Hibbard, G.D, and Naguib, H., "Periodic Cellular Metals/Polyurethane Foams Hybrid Materials",2009,Journal of Composite Materials, 43,pp.207-216.

106. Zangani D., Robinson M., and Gibson A.G., "Evaluation of Stiffness terms for Z-Cored Sandwich Panels", 2007, Applied Composite Materials, 14, 159-175.

107. Zeleniakiene D., and Ziliukas, A., " Stress Concentration Factor of Foamed Materials Used for

Core of Sandwich Composites",2006, Aviation, 6, pp3-7+34.

108. Danielsson M, Grenestedt, JL., "Gradient Foam Core Materials for Sandwich Structures, Preparation and Characterization, Polymers, 1998.

109. Sandiford, D. J. H, and Oxley, D.F., "Serving Up a New Plastic Sandwich", SPE Journal,27, pp.38-42.

110. Raju M., A. Ahmed and Cheng, H. D., " Dynamic Response of Nano Particle Enhanced Composites",2009, Composite Science and Technology,69,pp.772-779.

111. Breuer, U, and Neitzel, M., "Manufacture of All Thermoplastic Plastic by One Step Forming Process",Polymer Composites,19, pp.275-279.

115. Reis, E. M and Rizkallah, A. H, "Material Characteristics of 3D-FRP Sandwich Panels ",2008, Construction and Building Materials",22.pp.1009-18.

112. Hodge A.,Kaul R.,and R.Thomas, "Sandwich Composite for Space Applications",2000, International SAMP Symposium and Exhibition",45.

113. Carlson L.A, and Loup DC., "Crack Path in Foam Cored Sandwich Composites"2005, Composite Science and Technology, 65,15.pp.2612-2621.

114 Qiao, P., Y,.Majia and B.Florin, "Impact Mechanics and High Energy Absorbing Materials "2008. Journal of Aerospace Engineering,21,pp.235-248.

115. Fleck , N..A., and Sridhar, I., "End Compression of Sandwich Columns",2002, Composites Part A: Applied Science and Manufacturing,33,pp. 353-359.

116. Mouitz ,A,P., and Thomson,R.S., 1999, "Compression, Flexure and Shear Properties of Sandwich Composite Containing Defects", Composite Structures, 44,263-278.